U.S.NRC
United States Nuclear Regulatory Commission
Protecting People and the Environment

NUREG/CR-7115, Rev. 1

Performance of Metal and Polymeric O-Ring Seals in Beyond-Design-Basis Temperature Excursions

Office of Nuclear Regulatory Research

AVAILABILITY OF REFERENCE MATERIALS IN NRC PUBLICATIONS

NRC Reference Material

As of November 1999, you may electronically access NUREG-series publications and other NRC records at NRC's Library at www.nrc.gov/reading-rm.html. Publicly released records include, to name a few, NUREG-series publications; *Federal Register* notices; applicant, licensee, and vendor documents and correspondence; NRC correspondence and internal memoranda; bulletins and information notices; inspection and investigative reports; licensee event reports; and Commission papers and their attachments.

NRC publications in the NUREG series, NRC regulations, and Title 10, "Energy," in the *Code of Federal Regulations* may also be purchased from one of these two sources.

1. **The Superintendent of Documents**
   U.S. Government Publishing Office
   Mail Stop IDCC
   Washington, DC 20402-0001
   Internet: bookstore.gpo.gov
   Telephone: (202) 512-1800
   Fax: (202) 512-2104

2. **The National Technical Information Service**
   5301 Shawnee Rd., Alexandria, VA 22312-0002
   www.ntis.gov
   1-800-553-6847 or, locally, (703) 605-6000

A single copy of each NRC draft report for comment is available free, to the extent of supply, upon written request as follows:

Address: **U.S. Nuclear Regulatory Commission**
Office of Administration
Publications Branch
Washington, DC 20555-0001
E-mail: distribution.resource@nrc.gov
Facsimile: (301) 415-2289

Some publications in the NUREG series that are posted at NRC's Web site address www.nrc.gov/reading-rm/doc-collections/nuregs are updated periodically and may differ from the last printed version. Although references to material found on a Web site bear the date the material was accessed, the material available on the date cited may subsequently be removed from the site.

Non-NRC Reference Material

Documents available from public and special technical libraries include all open literature items, such as books, journal articles, transactions, *Federal Register* notices, Federal and State legislation, and congressional reports. Such documents as theses, dissertations, foreign reports and translations, and non-NRC conference proceedings may be purchased from their sponsoring organization.

Copies of industry codes and standards used in a substantive manner in the NRC regulatory process are maintained at—

The NRC Technical Library
Two White Flint North
11545 Rockville Pike
Rockville, MD 20852-2738

These standards are available in the library for reference use by the public. Codes and standards are usually copyrighted and may be purchased from the originating organization or, if they are American National Standards, from—

American National Standards Institute
11 West 42nd Street
New York, NY 10036-8002
www.ansi.org
(212) 642-4900

Legally binding regulatory requirements are stated only in laws; NRC regulations; licenses, including technical specifications; or orders, not in NUREG-series publications. The views expressed in contractorprepared publications in this series are not necessarily those of the NRC.

The NUREG series comprises (1) technical and administrative reports and books prepared by the staff (NUREG–XXXX) or agency contractors (NUREG/CR–XXXX), (2) proceedings of conferences (NUREG/CP–XXXX), (3) reports resulting from international agreements (NUREG/IA–XXXX), (4) brochures (NUREG/BR–XXXX), and (5) compilations of legal decisions and orders of the Commission and Atomic and Safety Licensing Boards and of Directors' decisions under Section 2.206 of NRC's regulations (NUREG–0750).

U.S.NRC
United States Nuclear Regulatory Commission
Protecting People and the Environment

NUREG/CR-7115, Rev. 1

Performance of Metal and Polymeric O-Ring Seals in Beyond-Design-Basis Temperature Excursions

Manuscript Completed: September 2015
Date Published: November 2015

Prepared by
Jiann C. Yang
Edward J. Hnetkovsky
Doris Rinehart
Marco Fernandez

National Institute of Standards and Technology
Engineering Laboratory
Gaithersburg, Maryland 20899

Felix Gonzalez, NRC Project Manager

Prepared for:
Division of Risk Analysis
Office of Nuclear Regulatory Research
U.S. Nuclear Regulatory Commission
Washington, DC 20555-0001

NRC Job Code N6550

Office of Nuclear Regulatory Research

ABSTRACT

This report documents the beyond-design-basis thermal exposure test results of the performance of metallic and polymeric seals typically used in radioactive material transportation packages. The overall objective of the project is to provide test data and insights regarding the performance of these O-ring seals (metallic or polymeric) when exposed to beyond-design-basis temperature conditions that could result due to a severe fire. Tests were conducted using a small-scale test package (pressure vessel) made of stainless steel SS 304 filled with helium initially pressurized at either 5 bar or 2 bar at room temperature. The test package was then exposed in an electric furnace to temperatures equal to, or above the specified maximum operating temperatures of these seals (up to 900 °C) for a pre-determined period (typically 8 h to 9 h). These O-ring temperatures and test periods are more severe than the 800°C for 30 minutes hypothetical accident conditions described in 10 CFR Part 71. In addition, the 800°C and 900°C seal temperatures are much higher than would be expected in real world conditions because transportation packages generally are designed with the seals protected by being located within the package and, therefore, not directly exposed to the exterior conditions of the environment. The pressure drop technique was used to determine if leakage occurred during thermal exposure. There are three test phases in this study. Revision 1 adds test results from Phases II and III.

In Phase I, one metallic and two polymeric (ethylene-propylene compound (EPDM) and Teflon (PTFE)) seals were used. A total of fifteen tests were performed: twelve using metallic seals, two using EPDM, and one using Teflon. Leakage was observed in a number of the thermal exposure tests; the time when leakage occurred varied.

In Phase II, additional test data on EPDM, and PTFE O-rings were obtained. For exploratory purposes, three additional polymeric O-rings (butyl, Viton, and silicone) were also tested in this phase for comparisons. For the EPDM, butyl, PTFE, no leak was detected. However, when tested at 900 °C, EPDM and butyl seals leaked before the test fixture reached 900 °C. One test using silicone O-ring did show leakage. For all the tests that used Viton O-rings, the vessel pressure peculiarly increased during the thermal exposure. The reason for the pressure increase remains unclear.

In Phase III, the test series involved the use of a similar test package, but with a double O-ring configuration tested at 800 °C or 900 °C for 9 h. The outer-inner O-ring combinations were metallic-metallic, EPDM-metallic, blank-metallic, EPDM-EPDM, and butyl-butyl. When the same torque for the single metallic O-ring was used to tighten the bolts in the double metallic-metallic or blank-metallic tests, leaks were observed in the metallic-metallic, but not in the blank-metallic, tests. Even when the appropriate torque value was applied for the double O-ring configuration, the metallic-metallic tests leaked, but only after being at a 900°C environment between two and eight hours; there was no leakage prior to that period. For the EPDM-EPDM and butyl-butyl tests, leaks were observed in all cases even before the vessel reached the test temperature. No leaks were observed with the EPDM-metallic double O-ring configuration.

CONTENTS

LIST OF FIGURES

LIST OF TABLES

EXECUTIVE SUMMARY

The objective of this work is to provide experimental seal performance data for metallic and polymeric seals typically used in radioactive material transportation packages for beyond-design-basis temperature excursions. There are three phases in this project. Phases I and II used a single O-ring configuration, whereas Phase III used a double O-ring configuration.

Tests were conducted using a test package (a pressure vessel) made of stainless steel SS 304 filled with helium initially at either 5 bar or 2 bar at room temperature. Since it is difficult to control a real fire environment for testing, a programmable electric furnace was used to provide various controlled thermal environments to heat the vessel to a specified temperature for a pre-determined duration, which varied from several hours to one or two days. The vessel pressure was monitored to determine if a leak occurred at the exposure temperature.

In Phase I, 15 tests including two shakedowns were performed with some at beyond-design-basis thermal exposure conditions. Of the tests conducted, 12 tests used metallic seals, two used ethylene-propylene compound (EPDM) seals, and one used a PTFE (Teflon) seal.

Of the five repeat metallic-seal tests (Tests # Metallic-2, # Metallic-3, # Metallic-4, # Metallic-8, and # Metallic-12), leakage (decreasing vessel pressure) was observed in three of the tests (Tests # Metallic-3, # Metallic-4, and # Metallic-8) during the 9 h 800 °C (1472 °F) exposure. The times when the leakage occurred (the vessel pressure started to decrease) varied in the three tests performed. In Test # Metallic-3, measurable leakage occurred approximately 6.9 h after the test temperature 800 °C (1472 °F) had been reached. In Test # Metallic-4, measurable leakage occurred about 2.8 h into the 800 °C (1472 °F) exposure. In Test # Metallic-8, leakage was observed roughly 3 h into the test. The two shakedown tests (Tests # Metallic-1 and # Metallic-9) were conducted using a 30 min and 4 h exposure to 800 °C (1472 °F), respectively, and the seal appeared to hold vessel pressure. No leakage (unchanged vessel pressure within the pressure measurement uncertainty) was also observed in the two metallic seal tests that used 100 °C (212 °F) incremental heating from 427 °C (800 °F) to 627 °C (1161 °F) and from 427 °C (800 °F) to 727 °C (1341 °F), respectively, with at least 9 h exposure at each temperature increment. Three repeat metallic seal tests were also conducted at the seal maximum operating temperature of 427 °C (800 °F) for 9 h. The seal maintained vessel pressure within the measurement uncertainty of the pressure transducer in all three tests.

No leakage was observed in one EPDM seal tested at 300 °C (572 °F) for more than 20 h (Test # EPDM-a); however, leakage was observed immediately after the vessel had attained the nominal target temperature of 450 °C (842 °F) in another EPDM seal test (Test # EPDM-b). Leakage was also observed in the test (Test # PTFE-a) that used a PTFE seal after it had been subjected to 300 °C (572 °F) exposure for 22 h during the cooling phase.

In Phase II, additional experimental seal performance data for the two polymeric (EPDM and PTFE) O-ring seals were measured. For exploratory purposes, three additional O-ring seals made of other polymeric materials (butyl, Viton, and silicone) were also studied. Leakage rates were measured using the same stainless SS 304 steel pressure vessel sealed with a polymeric O-ring and following the same test procedure in Phase I. The vessel was filled with helium initially at 2 bar at room temperature and then placed and heated in a programmable electric furnace to a nominal temperature of 316 °C (600 °F) for 8 h. The vessel pressure was monitored to determine if a leak occurred as a result of O-ring failure during the thermal exposure.

A total of 18 tests were performed: four tests used EPDM O-rings, four used Viton, four used silicone, three used butyl, and three used PTFE. For the EPDM, butyl, PTFE, and silicone O-rings, the results, except one silicone O-ring test, showed that within the measurement uncertainty of the pressure gauge, there were no discernible decreases in vessel pressure during the thermal exposure and that the initial pressure was restored after cool-down to room temperature, which implied that any leak was undetectable. For all the tests that used Viton O-rings, the vessel pressure peculiarly increased during the thermal exposure, and the reason for the pressure increase remains unresolved. The post-test examinations of the O-rings revealed that all the O-rings (except PTFE) were irreversibly deformed and severely damaged after the extreme thermal exposure, and the seal material was found to be squeezed out of the O-ring groove of the pressure vessel.

In Phase III, leak tests were performed using the same test pressure vessel with a double O-ring configuration. The outer-inner O-ring combinations were metallic-metallic, EPDM-metallic, blank-metallic, EPDM-EPDM, and butyl-butyl. The vessel was filled with helium initially at 5 bar at room temperature and was then thermally exposed at 800 °C (1472 °F) or 900 °C (1652 °F) for 9 h in the electric furnace to determine if a leak occurred. These O-ring temperatures and test periods are more severe than the 800°C for 30 min hypothetical accident conditions described in 10 CFR 71. A total of eleven tests were carried out using a double O-ring configuration: four tests used metallic-metallic, three used EPDM-metallic, one used blank (no O-ring)-metallic, two used EPDM-EPDM, and one used butyl-butyl. For the four metallic-metallic O-ring tests, leaks were observed in the two tests when the same torque for a single metallic O-ring was used. Even when the appropriate torque value was applied for the double O-ring configuration, the other two metallic-metallic tests leaked, but only after being at a 900°C environment between two and eight hours; there was no leakage prior to that period. No leak was observed in the blank-metallic test. Leaks were detected in all the EPDM-EPDM and butyl-butyl tests, even before the test temperature was reached. No leaks were observed with the EPDM-metallic double O-ring configuration.

ACKNOWLEDGMENTS

This work was sponsored by the U.S. Nuclear Regulatory Commission (NRC). The authors would like to thank Felix Gonzalez (Project Manager), Chris Bajwa, Earl Easton, Robert Einziger, Joseph Borowsky, Mark Adams and Shivani Mehta of NRC, Anita Aikins-Afful from the NRC for technical editing the report, Harold Adkins of Pacific Northwest National Laboratory (PNNL), William Luecke and Michael Moldover of NIST for many helpful discussions, and Gary L. Stevens of NRC for checking the pressure vessel design calculations.

DISCLAIMER

Certain commercial entities, equipment, or materials may be identified in this document in order to describe an experimental procedure or concept adequately. Such identification is not intended to imply recommendation or endorsement by the National Institute of Standards and Technology, nor is it intended to imply that the entities, materials, or equipment are necessarily the best available for the purpose.

ABBREVIATIONS

ANSI	American National Standards Institute
ASME	American Society of Mechanical Engineers
CFR	Code of Federal Regulations
CRUD	Chalk River Unidentified Deposits
DAQ	Data Acquisition
EPDM	Ethylene-Propylene Compound (Diene Monomer)
FDS	Fire Dynamics Simulator
HAC	Hypothetical Accident Conditions
ISO	International Organization for Standardization
NIST	National Institute of Standards and Technology
NRC	Nuclear Regulatory Commission
PTFE	Polytetrafluoroethylene (Teflon)
RES	NRC Office of Nuclear Regulatory Research

1 BACKGROUND

1.1 Introduction

The U.S. Nuclear Regulatory Commission (US NRC) is collecting data to better characterize the performance envelope of seals used on radioactive material transportation packages, during fire exposures that exceed the hypothetical accident conditions (HAC) fire (800 °C for 30 min) described in 10 CFR Part 71.73. Examples of an accident that could potentially produce an exposure beyond the HAC fire were the Caldecott Tunnel fire in 1982 (Adkins *et al*., 2007a), the Baltimore Tunnel fire that occurred in 2001 (Adkins *et al.*, 2007b), and the MacArthur Maze fire in 2007 (Dunn *et al*., 2009). The performance of package seals is important for determining the potential for release of radioactive material from a package during a beyond-design-basis accident because the seals, in general, have lower temperature limits than other package components. It should be noted that the regular approach for evaluating seal performance in any HAC or beyond-design-basis fire is to assume that seals fail completely if their normal operating temperature limits are exceeded at any point in the transient thermal evaluation of a given package. Such conservative and bounding approach yields the maximum possible estimates of potential for release of radioactive material from transportation packages in fire exposures.

NUREG/CR-6886, "Spent Fuel Transportation Package Response to the Baltimore Tunnel Fire Scenario," describes in detail an evaluation of the potential release of radioactive materials from three different transportation packages (Adkins *et al.*, 2007b). This evaluation used estimates of temperatures from a simulation of the Baltimore Tunnel fire using the NIST Fire Dynamics Simulator (FDS) (McGrattan and Hamins, 2003) as boundary conditions for numerical models to determine the temperature of various components of the packages, including the seals. For two of the packages evaluated, the model-estimated temperatures of the seals exceeded their continuous-use rated service temperature, meaning a potential release of radioactive material (i.e., CRUD) if one assumed zero effectiveness (complete failure) of the seal. However, for both of those packages, the analysis determined, by a bounding calculation, that the maximum expected release was well below the regulatory limits for the release allowed during the HAC series of events in 10 CFR Part 71.

Previous work reported in the literature has mainly focused on elastomeric seals and temperatures well below 800 °C (1472 °F). The test fixtures in previous work typically consisted of two flanges or two plates with two concentric O-ring grooves, one for the test seal and one for the secondary external seal, and a small cavity for helium tracer gas (e.g., Bronowski, 2000, Marlier, 2010). Testing of package seals to determine their performance in beyond-design-basis fire scenarios can provide physical data needed to understand the likelihood of a release of radioactive materials.

The objective of this work is to provide experimental seal performance data for metallic and polymeric seals for thermal exposures beyond their rated temperatures. Both materials are used in the design of seals, although metallic seals tend to have higher allowable temperatures because of their design and material properties. The data is obtained using a test fixture consisting of a vessel body and flange cap; the scope of the testing does not evaluate the size of the test fixture as a test parameter. The scope of the testing does not evaluate the performance of aged seals under beyond-design-thermal exposure. Since it is difficult to control and replicate a real fire environment for testing, an electric furnace was used to provide various controlled and repeatable thermal environments.

The pressure drop method was used in this study to examine the seal performance at elevated temperatures. The implementation of the pressure drop technique in a harsh thermal environment proved to be less challenging than other more sensitive test methods, as described in ANSI N14.5-1997. The use of any temporal decrease in vessel pressure as a means to detect potential leakage is best applied to isothermal conditions (ANSI N14.5-1997) where for an ideal gas the molar leakage rate is simply proportional to the rate of decrease in pressure. However, under transient heating conditions, even in the absence of a leak, the rate of increase in vessel volume due to thermal expansion could also contribute to the temporal decrease in pressure, which may be construed as a leak. Therefore, all the leak tests were conducted by maintaining the pressure vessel at a constant elevated temperature in the furnace. Although the monitoring of pressure drop is not the most sensitive way to detect leaks, the sensitivity to detect a small pressure drop could be greatly enhanced if the vessel pressure is monitored over a very long duration. In addition, the sensitivity of the method can further be improved by using a smaller test volume since the sensitivity of a pressure drop is inversely proportional to the test volume (ANSI N14.5-1997). This work make use of these two attributes, long measurement duration and small vessel volume.

The testing was divided into several phases. In Phases I and II, a single O-ring configuration was used. Phase I focused on the thermal performances of a metallic and two polymeric (EPDM and PTFE) O-rings. In Phase II, the focus was solely on polymeric O-rings, and the test series was expanded to include butyl, silicone, and Viton O-rings. In Phase III, a double O-ring configuration was used. The outer-inner O-ring combinations were metallic-metallic, EPDM-metallic, blank-metallic, EPDM-EPDM, and butyl-butyl.

2 TECHNICAL APPROACH

2.1 Experimental Apparatus

2.1.1 Phase I

The test fixture consists of a seamless vessel body with a flange machined from a stainless steel (SS 304) cylindrical stock and a removable SS 304 flange (vessel cap) with seal groove machined to O-ring manufacturer specifications. The flange dimensions were made in conformity with the ASME Standard B16.5-2009 [6], Flange Class 2500 with a design pressure rating up to 29.2 bar (424 psi) at 800 °C (1472 °F) (Table 2-2.1, ASME Standard B16.5-2009). The vessel cavity had a nominal internal volume[1] of 100 mL. The design drawings of the test vessel body and the removable flange (vessel cap) are provided in Appendix A. Nine test vessels with the same dimensional tolerances were constructed and used for this test series.

The metallic seal was a Garlock Helicoflex[2] metal O-ring (GHx P/N H-311291) made of Inconel 718 and silver with an outer diameter of 6.35 cm (2.5 in.) and a cross section of 0.32 cm (0.125 in.). The metallic O-ring groove size and flange surface roughness (minimum 0.80 μm and maximum 1.6 μm) were based on the specifications listed in the Garlock Helicoflex technical literature. The polymeric seals were ethylene-propylene compound (EPDM) O-ring (DBR Industries, 2-228 E0740-75, Lot # 2Q060080040952) and PTFE O-ring (DBR Industries, 228 PTFE; Lot # 04/07 12730-1).

The vessel body and the cap were joined together using four bolts (SS 304 1-1/8 in. 7 TPI). Each bolt was tightened using a micrometer torque wrench (KD Tools 2953 ¾ in. drive 100-600 lb ft, 153-830 N·m, with a resolution of 3.4 N·m). A torque of 416 N·m (307 lb ft) ± 2 N·m (expanded uncertainty with a coverage factor of 2) was used for the metallic seals and 271 N·m (200 lb ft) for the EPDM and PTFE O-rings.[3] In addition, a silicone-base O-ring lubricant (Parker Super O-Lube® from Parker Seal, Lexington, Kentucky) was applied to the EPDM O-ring before the two flanges were bolted together. A 24 cm long stainless steel tubing with an inside diameter of 0.48 cm (0.189 in.) and an outside diameter of 0.953 cm (0.375 in.) was inserted into the bottom of the vessel body flush through a straight-hole with a bevel-groove and was all-around fillet welded to the vessel.[4] The exposed end of the tubing was connected to one arm of a union cross (Swagelok SS-400-4) via a reducing union (Swagelok SS-600-6-4) and a port connector (Swagelok SS-401-PC). Two needle valves (Swagelok SS-1RS4) or bellow valves (Swagelok SS-4BK)[5] for filling and evacuating the test vessel were mounted on the other two respective arms of the union cross using two port connectors (Swagelok SS-401-PC). A union tee (Swagelok SS-400-3) was connected to the fourth arm of the union cross via a port

---

[1] Actual internal volume (see Appendix B) was measured using an internal micrometer with a resolution of 0.005 mm).

[2] The seal material and manufacturer were selected and specified by the U.S. NRC.

[3] The torque requirement for the polymeric O-ring (used as a face seal) was recommended by the manufacturer to be metal-to-metal fit.

[4] Three vessels (Vessels #1, #6, and #7) were tested for surface flaws in the welds using the ASME liquid penetration test (ASME, BVPC-VIII-1-2007) by a local testing laboratory. Vessels #6 and #7 were tested brand new while Vessel #1 was tested after two thermal exposures, one at 800 °C (1472 °F) for 0.5 h and one at 427 °C (800 °F) for 9 h. The test results showed no surface flaws in the welds in all three vessels. Note that performing x-ray of this type weld is difficult at best and with the tube passing through it makes obtaining a good x-ray of the entire weld impossible.

[5] For the first three tests, needle valves were used.

connector (Swagelok SS-401-PC). A pressure transducer (Omegadyne, PX01C1-500A5T)[6] was attached to one arm of the union tee via a tube adapter (Swagelok SS-4-TA-7-4) to measure the vessel pressure. A grounded thermocouple (Omega K-type CAIN-18G-24)[6] to monitor the vessel internal temperature was inserted into the vessel interior through a reducing union (Swagelok SS-400-6-2) which was connected to the other arm of the union tee via a port connector (Swagelok SS-401-PC), the union cross, and the stainless steel tubing.

Due to the large mass and thermal inertia of the test vessel, it was anticipated that the vessel temperature might not be completely uniform when the vessel was heated. Two additional thermocouples (Omega K-type CAIN-18G-24)[7] were placed near the O-ring groove to monitor the temperatures experienced by the seal. In order to securely attach the two thermocouples to their desired locations, two divots 1.25 mm deep and 3 mm in diameter were drilled 90 ° apart in the side of the flange that contained the O-ring groove. The thermocouple tips were placed in these divots, and the thermocouples were clamped onto the sides of the vessel.

Figure 2-1 is a schematic illustration of the experimental apparatus, two photographs of which are shown in Figure 2-2. The upper photograph of Figure 2-2 shows the test vessel placed inside the furnace before testing, and the lower photograph shows the furnace opening was covered with a thermal insulation board during testing. Note that all the connection fittings, the two valves, and the pressure transducer were located outside the furnace.

The exposure of the seal to a high temperature environment was achieved using a programmable temperature-controlled electric furnace (Carbolite CWF 1200) with an internal capacity of 25.4 cm × 25.4 cm × 40.64 cm (10 in. × 10 in. × 16 in.). The electric furnace has a maximum operating temperature of 1200 °C (2192 °F). Although the furnace was equipped with a digital temperature display for internal furnace temperature, a grounded thermocouple (Omega K-type CAIN-18G-24) was placed inside the furnace interior to monitor the furnace temperature for crosscheck. The differences between these two readings were less than 10 °C.

[6] See Appendix B for measurement uncertainty discussion.
[7] Omega WTK-10-60 (Inconel cladding) thermocouples were used subsequently to facilitate their mounting onto the two flanges.

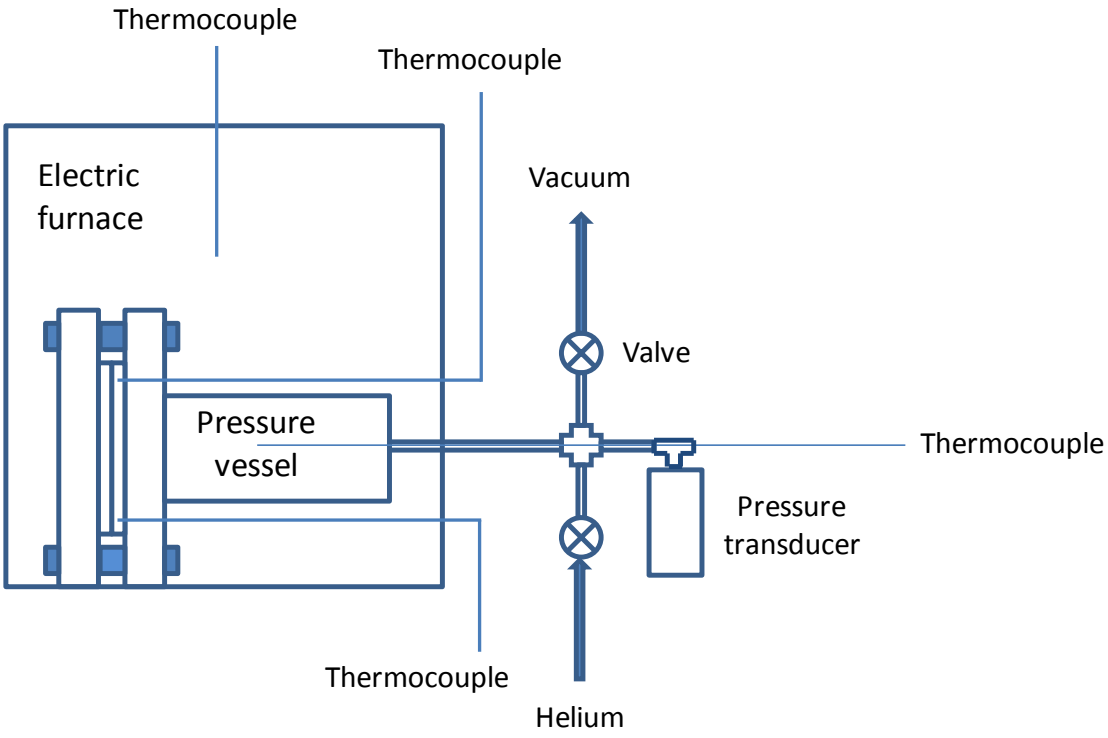

Figure 2-1. A schematic illustration of the experimental apparatus.

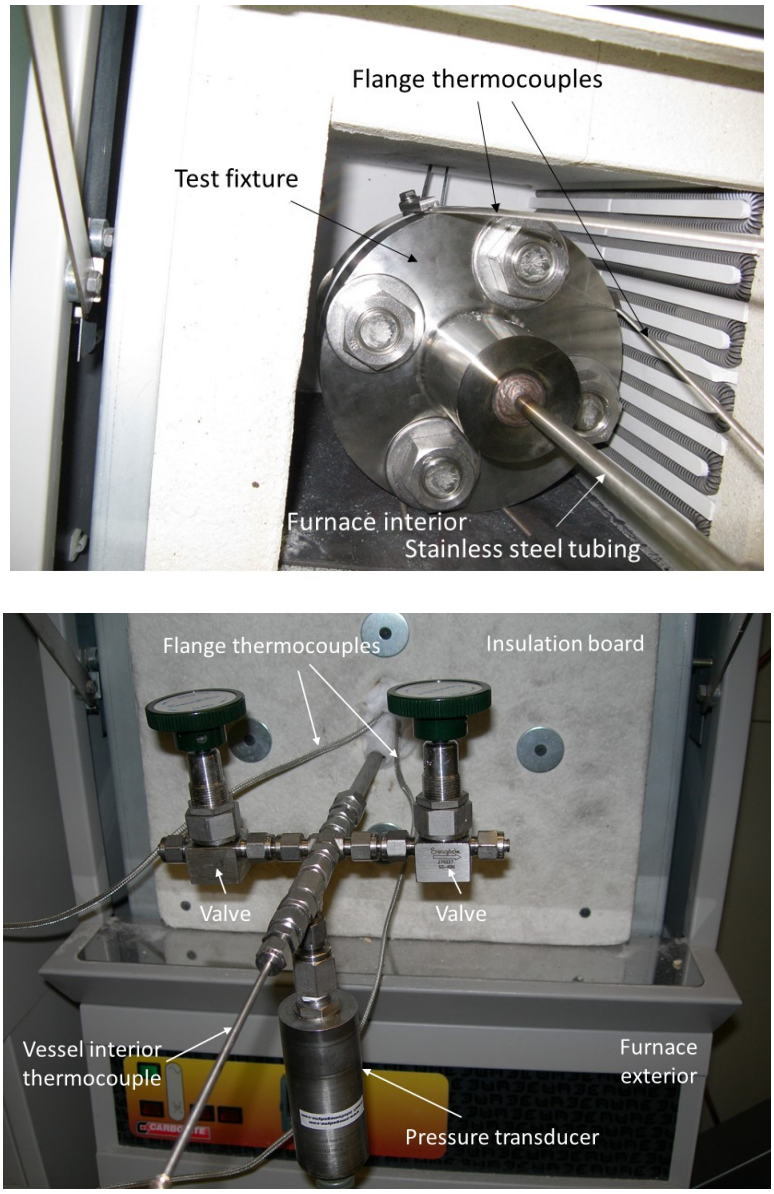

Figure 2-2. Photographs of the experimental apparatus.

2.1.2 Phase II

The experimental apparatus used in this Phase was identical to the one used in Phase I, except a torque of 271 N·m (200 lb ft) was used[8] to tighten the vessel body and cap for *all* the polymeric O-rings tested in this Phase. The five polymeric O-rings used were EPDM, silicone, butyl, Viton, and PTFE. Table 2-1. O-ring seal material information lists the O-ring product descriptions and their maximum operating temperatures. All the O-rings were obtained from DBR Industries.

[8] The original torque wrench used in Phase I was broken, and the wrench manufacturer went out of business; the new replacement wrench can only be set at 6.8 N m (5 lb ft) increments. The applied torque was 414 N m (305 lb ft), not 416 N m (307 lb ft) in Phase I.

Table 2-1. O-ring seal material information

O-ring material	Product information
EPDM	Ethylene-propylene compound (Item ID 2-228 E0740-75, Lot # 2Q06 0080040952); maximum operating temperature: 149 °C (300 °F)
Silicone	Silicone (Item ID 228 S570, Lot # 1Q00 20003195501); maximum operating temperature: 232 °C (450 °F)
Butyl	Butyl 70 (Item ID 228 Butyl 70, Lot # 4Q12 107110/60); maximum operating temperature: 121 °C (250 °F)
Viton	Viton Durometer 75 (Item #83248/1-228, Lot # 3Q09 9206002); maximum operating temperature: 204 °C (400 °F)
PTFE	PTFE (Item ID 228 PTFE, Lot # 04/07 12730-1); maximum operating temperature: 260 °C (500 °F)

2.1.3 Phase III

Five double O-ring configurations were used in this test series: (1) an outer metallic O-ring and an inner metallic O-ring, (2) an outer EPDM O-ring and an inner metallic O-ring (Garlock Helicoflex/Technetics) and (3) an outer blank (no) O-ring and an inner metallic O-ring), (4) an outer EPDM O-ring and an inner EPDM O-ring, and (5) an outer butyl O-ring and an inner butyl O-ring. The outer O-ring material information is provided in Table 2-2. The inner metallic O-ring had the same dimensions as the ones used in the single O-ring configuration test series in Phase I. The inner EPDM and butyl O-rings were the same ones used in the single O-ring configuration test series in Phase II. Other than having a wider boss to accommodate the double O-ring grooves on the vessel cap (see Appendix A), the vessel geometry was identical to that used in Phases I and II. For the metallic-metallic O-ring configuration, two tests used the same torque value of 416 N m (307 lb ft) as was used in the single metallic O-ring tests, and two tests used a torque value of 976 N m (720 lb ft)[9]. For EPDM-metallic O-ring and blank-metallic O-ring configurations, a torque value of 416 N m was used. For EPDM-EPDM and Butyl-Butyl O-ring configurations, a torque value of 637 N m (470 lb ft)[9] was used.

[9] The torque value was calculated based on the proportionality between torque and O-ring diameter. For double O-rings, the sum of the two O-ring diameters was used as the equivalent effective O-ring diameter for torque estimation (per manufacturer's technical information).

Table 2-2. Outer O-ring seal material information

O-ring material	Product information
Metallic	Technetics Group Columbia P/N: H-312522
EPDM	Ethylene-propylene compound (DBR Industries, Item ID 2-235 E0740-75, Lot # 1Q140080218069); maximum operating temperature: 149 °C (300 °F)
Butyl	Butyl 70 (Item ID 2-235-B0612-70, Lot # 3Q140060012619/M0553228); maximum operating temperature: 121 °C (250 °F)

2.2 Experimental Procedure

2.2.1 Phase I

This test series involved the thermal exposure of a test vessel with a metallic or polymeric seal in an electric furnace to determine the seal performance at elevated temperatures. Two nominal temperatures, 800 °C (1472 °F) and 427 °C (800 °F), were selected for thermal exposure testing of the metallic cask seals; 10 CFR Part 71 uses a fire environment thermal exposure temperature of 800 °C (1472 °F) and the published maximum operating temperature of the metallic seal used in this study is 427 °C (800 °F)[10]. For most of the metallic seal tests, the thermal exposure time was 9 h after the flange with the O-ring groove had attained the test temperature. Other thermal exposure protocols were used for some tests (see section 2.3 below). For the polymeric seals, the test seal was exposed to a flange temperature of 150 °C (302 °F) for 1 h, 200 °C (392 °F) for 1 h, 250 °C (482 °F) for 1 h, and 300 °C (572 °F) for 22 h. The maximum operating temperatures of the EPDM and PTFE O-rings are 149 °C (300 °F) and 260 °C (500 °F), respectively.

The assembled test vessel with the test seal installed was placed in the electric furnace, and the tubing system was connected to the vessel. A vacuum line was attached to one valve of the tubing system, and a helium supply line from a 1A cylinder of compressed helium (analytical grade) was connected to the other valve. With the two valves opened and the pressure regulator of the cylinder closed, the entire test system was then evacuated for 60 s using an oil-less rocking piston vacuum pump (GAST Manufacturing Corporation Model 71R645-V110-UAP). The valve that was connected to the vacuum line was closed, separated from the vacuum line, and capped using a plug (Swagelok SS-400-P). The pressure regulator of the compressed helium cylinder was then slowly opened to fill the test vessel with helium at room temperature to a nominal pressure of 5 bar. The helium supply line was disconnected from the fill valve, and the valve was capped using a plug (Swagelok SS-400-P). The tubing connections of the test apparatus were immediately tested for leaks using soapy water. The vessel pressure was then monitored for more than 48 h. If the vessel pressure variations over this period were within the expanded uncertainty of the pressure transducer (0.11 bar)[6], it could be confidently assumed that the vessel pressure was unchanged, and the invariance of vessel pressure was used as an additional “no leak” indicator.

With no leaks detected, the electric furnace was turned on to heat the test vessel from room temperature to the target temperature. Depending on the specific target temperature, the heating process could take more than 4 h. Once the vessel flange temperature reached the target value, the vessel was heated according to the pre-determined exposure duration (see Table 2-3 below). After the thermal exposure, the furnace was turned off, and the vessel was allowed to cool to room temperature inside the furnace. The internal temperature and pressure of the vessel, the furnace temperature, and the flange temperatures were recorded during the entire heat-up and cool-down phases using a LabVIEW-based 16-bit DAQ (Data Acquisition) system (National Instruments NI USB-6251) with an input/output connector block (National Instruments NI SCC-68). The DAQ system sampled at a rate of 100 Hz; however, the data were logged at 1 min intervals.

[10] Generally, in HAC analyses using computer codes, Transportation package design seals do not reach the HAC temperature of 800 °C (1472 °F).

2.2.2 Phase II

The pressure vessel preparation and experimental procedures were identical to those used in Phase I although the test conditions and parameters were different (see Table 2-4). Since the exposed temperature was not high and the tested polymeric O-ring could be easily removed from the O-ring groove, the vessel was *re-used* in this test series, except that brand new bolts were used. Before each test, the O-ring groove and the vessel interior were properly and thoroughly cleaned using acetone and/or vinegar. The vessel used was Vessel #3 from Phase I.

2.2.3 Phase III

Aside from the test conditions and parameters and the double O-ring configuration (see Table 2-5), the test preparation and experimental procedures followed those used in Phases I and II.

2.3 Test Matrix

2.3.1 Phase I

Table 2-3 summarizes the test conditions and parameters used in Phase I. The first column in the table lists the revised test number designations used in this revised NUREC/CR-7115 with their corresponding test numbers in the original NUREC/CR-7115 listed in the second column. The revised test designations provide more clarity, better reflect the test O-ring material, and conform to those used in Phase II and III.

Table 2-3. Nominal test conditions and parameters (Phase I in chronological order)

Test #	Test #	Vessel #	Nominal initial vessel conditions	Exposure duration
Metallic-1	1*	1	24 °C at 5 bar	Heat-up + 30 min at 800 °C + cool-down
Metallic-2	2	2	24 °C at 5 bar	Heat-up + 9 h at 800 °C + cool-down
Metallic-3	3	3	24 °C at 5 bar	Heat-up + 9 h at 800 °C + cool-down
Metallic-4	4	4	24 °C at 5 bar	Heat-up + 9 h at 800 °C + cool-down
Metallic-5	5	5	24 °C at 5 bar	Heat-up + 9 h at 427 °C + cool-down
Metallic-6	6	2**	24 °C at 5 bar	Heat-up + 9 h at 427 °C + cool-down
Metallic-7	7	1**	24 °C at 5 bar	Heat-up + 9 h at 427 °C + cool-down
Metallic-8	8	6	24 °C at 5 bar	Heat-up + 9 h at 800 °C + cool-down
Metallic-9	9	1***	24 °C at 5 bar	Heat-up to 427 °C and then to 800 °C for about 4 h + cool-down
Metallic-10	10	7	24 °C at 5 bar	Incremental heating from 427 °C to 627 ºC with 100 ºC increment§ + cool-down
EPDM-a	11	3**	24 °C at 2 bar	Incremental heating from 150 ºC to 300 °C with 50 ºC increment§§ + cool-down
PTFE-a	12	3**	24 °C at 2 bar	Incremental heating from 150 ºC to 300 °C with 50 ºC increment§§ + cool-down
Metallic-11	13	8	24 °C at 5 bar	Incremental heating from 427 °C to 727 ºC with 100 °C increment§ + cool-down
Metallic-12	14	9	24 °C at 5 bar	Heat-up + 9 h at 800 °C + cool-down
EPDM-b	15	3**	24 °C at 2 bar	Heat-up + more than 24 h at 450 ºC

*Shakedown test; during this test DAQ malfunctioned, and no temporal data was collected.
**Flange and groove surfaces refurbished.
***Flange and groove surfaces refurbished again.
§Vessel was heated at each set temperature for 9 h or more; exact exposure duration for each test is described in Section 3.
§§Vessel was heated at 150 °C (302 °F) for 1 h, 200 °C (392 °F) for 1 h, 250 °C (482 °F) for 1 h, and 300 °C (572 °F) for more than 20 h.

2.3.2 Phase II

Table 2-4 summarizes the test conditions and parameters used in Phase II.

Table 2-4. Nominal test conditions and parameters (Phase II in chronological order)

Test #	Vessel #	Nominal initial vessel conditions	Thermal exposure duration
EPDM-1	3	24 °C at 2 bar	Heat-up + 8 h at 316 °C + cool-down
Silicone-1	3	24 °C at 2 bar	Heat-up + 8 h at 316 °C + cool-down
Silicone-2	3	24 °C at 2 bar	Heat-up + 8 h at 316 °C + cool-down
Silicone-3	3	24 °C at 2 bar	Heat-up + 8 h at 316 °C + cool-down
Silicone-4	3	24 °C at 2 bar	Heat-up + 8 h at 316 °C + cool-down
Butyl-1	3	24 °C at 2 bar	Heat-up + 8 h at 316 °C + cool-down
Butyl-2	3	24 °C at 2 bar	Heat-up + 8 h at 316 °C + cool-down
Butyl-3	3	24 °C at 2 bar	Heat-up + 8 h at 316 °C + cool-down
Viton-1	3	24 °C at 2 bar	Heat-up + 8 h at 316 °C + cool-down
Viton-2	3	24 °C at 2 bar	Heat-up + 8 h at 316 °C + cool-down
Viton-3	3	24 °C at 2 bar	Heat-up + 8 h at 316 °C + cool-down
Viton-4	3	24 °C at 2 bar	Heat-up + 8 h at 316 °C + cool-down
EPDM-2	3	24 °C at 2 bar	Heat-up + 8 h at 316 °C + cool-down
EPDM-3	3	24 °C at 2 bar	Heat-up + 8 h at 316 °C + cool-down
EPDM-4	3	24 °C at 2 bar	Heat-up + 8 h at 316 °C + cool-down
PTFE-1	3	24 °C at 2 bar	Heat-up + 8 h at 316 °C + cool-down
PTFE-2	3	24 °C at 2 bar	Heat-up + 8 h at 316 °C + cool-down
PTFE-3	3	24 °C at 2 bar	Heat-up + 8 h at 316 °C + cool-down
EPDM-5	3	24 °C at 5 bar	Heat-up + 9 h at 900 °C + cool-down
EPDM-6	3	24 °C at 5 bar	Heat-up + 9 h at 900 °C + cool-down

2.3.3 Phase III

Table 2-5 summarizes the test conditions and parameters used in Phase III.

Table 2-5. Nominal test conditions and parameters (Phase III in chronological order)

Test #	Vessel #	Nominal initial vessel conditions	Thermal exposure duration
EPDM-Metallic-1[11]	10	24 °C at 5 bar	Heat-up + 9 h at 800 °C + cool-down
EPDM-Metallic-2	11	24 °C at 5 bar	Heat-up + 9 h at 800 °C + cool-down
Metallic-Metallic-1	See Note 1	24 °C at 5 bar	Heat-up + 9 h at 900 °C + cool-down
Metallic-Metallic-2	See Note 2	24 °C at 5 bar	Heat-up + 9 h at 900 °C + cool-down
EPDM-Metallic-3	See Note 3	24 °C at 5 bar	Heat-up + 9 h at 900 °C + cool-down
Blank-Metallic-1	See Note 4	24 °C at 5 bar	Heat-up + 9 h at 900 °C + cool-down
EPDM-EPDM-1	16	24 °C at 5 bar	Heat-up + 9 h at 900 °C + cool-down
EPDM-EPDM-2	17	24 °C at 5 bar	Heat-up + 9 h at 900 °C + cool-down
Butyl-Butyl-1	16*	24 °C at 5 bar	Heat-up + 9 h at 900 °C + cool-down
Metallic-Metallic-3	18	24 °C at 5 bar	Heat-up + 9 h at 900 °C + cool-down
Metallic-Metallic-4	19	24 °C at 5 bar	Heat-up + 9 h at 900 °C + cool-down

Note 1: Body of Vessel #12 and cap of Vessel #14; body of Vessel #14 was never fabricated.
Note 2: Body of Vessel #13 and cap of Vessel #15; body of Vessel #15 was never fabricated.
Note 3: Body of Vessel #10 (with boss re-furbished) and cap of Vessel #12
Note 4: Body of Vessel #11 (with boss re-furbished) and cap of Vessel #13
*Cleaned and re-used

[11] In the double O-ring Test # designation, the following convention is adopted: the outer O-ring is identified first, and the inner O-ring is identified second. For example, “EPDM-Metallic” represents the outer O-ring as EPDM and the inner O-ring as Metallic.

3 RESULTS AND DISCUSSION

In this section, test results are presented and discussed. It should be noted that only after the vessel had reached the specified test temperature was the pressure drop method applied to determine if a leak had occurred under this isothermal thermal exposure condition. During the transient heat-up phase of the vessel, the temporal variation of vessel pressure could not readily be used to determine if there was a potential leak unless a catastrophic seal failure occurred, causing a significant drop in pressure. As the vessel was heated, the vessel pressure and temperature increased. The temporal volumetric thermal expansion of the pressure vessel also introduced an additional parameter. The interplay among these parameters, vessel temperature, pressure, and volume, precluded the use of the transient pressure data to conclusively determine whether a leak had occurred during the heat-up phase. Another indicator for leak was to determine whether the vessel pressure could be restored to the initial pressure after the thermal exposure and cool-down. The restoration of the initial pre-test charged vessel pressure after cool-down indicated no leak had occurred during a test.

In the following sub-sections, the figures, which show the measured temporal variations of vessel pressure and temperatures in each test, contain five curves, one for vessel pressure and four for temperatures measured at the vessel interior, two locations on the flange where the test O-ring was housed, and the furnace interior. These figures share a common feature; all exhibit three stages in the temperature measurements. The initial rise in temperature is due to the heating of the test vessel from room temperature to the targeted test temperature in the furnace (the heat-up period). The plateau portion of the temperature curve represents the thermal exposure duration at the test temperature (the test period), and the subsequent decrease in temperature indicates the cooling of the test vessel after turning off the electric furnace at the conclusion of the thermal exposure at the test temperature (the cool-down period). In some of the figures, overshooting of the targeted temperature is apparent during the heat-up phase as a result of an initial furnace set-point higher than the targeted temperature. This was in attempt to rapidly ramp up the furnace temperature to shorten the heat-up time.

3.1 Phase I[12]

3.1.1 Metallic O-Rings

3.1.1.1 Test # Metallic-1 (Test #1; Vessel #1)

The thermal exposure test using Vessel #1 was intended to be a shakedown of the experimental apparatus. Four and a-half hours (4.5 h) was required for the flange temperature to reach the equilibrium furnace temperature of 800 °C (1472 °F). The vessel was then maintained at this temperature for an additional 30 min before turning off the electric furnace.

During the heat-up phase, the DAQ readings from the pressure transducer and the thermocouples became erratic due to unknown reasons; the problem was later diagnosed to be improper grounding and connection to the DAQ system. The readings from the pressure transducer and thermocouples were recorded manually using a voltmeter and a thermocouple reader, respectively. At 800 ºC (1472 °F), the vessel pressure reached 14.6 bar and was holding at 14.6 bar for the additional 30 min of heating. After the vessel was cooled to room temperature, the vessel pressure recovered its initial pressure of 5.0 bar at room temperature,

[12] For clarity, the results are presented and grouped based on the O-ring material rather than on the chronological order in the test series for Phases I, II, and III.

which indicated the no leakage.

A post-test inspection of the test vessel revealed that the metallic seal was soldered to the flange of the vessel body and a silver-color coating was imprinted on the surface of the O-ring groove, as shown in Figure 3-1. The high-temperature exposure also discolored the test fixture.

Figure 3-1. Post-test photographs showing silver from the metallic O-ring deposited on the O-ring groove and the O-ring bonded to the test vessel (Vessel #1) body.

3.1.1.2 Test # Metallic-2 (Test #2; Vessel #2)

Before Test # Metallic-2 (Test #2) was conducted, an exploratory test was performed to examine the severity of the leak without using a metallic O-ring. The vessel was charged with helium to 5.62 bar at room temperature, and the vessel pressure was monitored at room

temperature. Figure 3-2 is the test result, which indicates that the vessel pressure began to drop and leakage occurred immediately at the start of the test and continued slowly over the entire experimental run-time (26.43 h). The reference helium leakage rates $L_{R,He}$ (ref·cm^3/s) were estimated based on the method described in Appendix D. The time-averaged leakage rate is estimated to be 2.4 × 10^{-3} ref·cm^3/s.

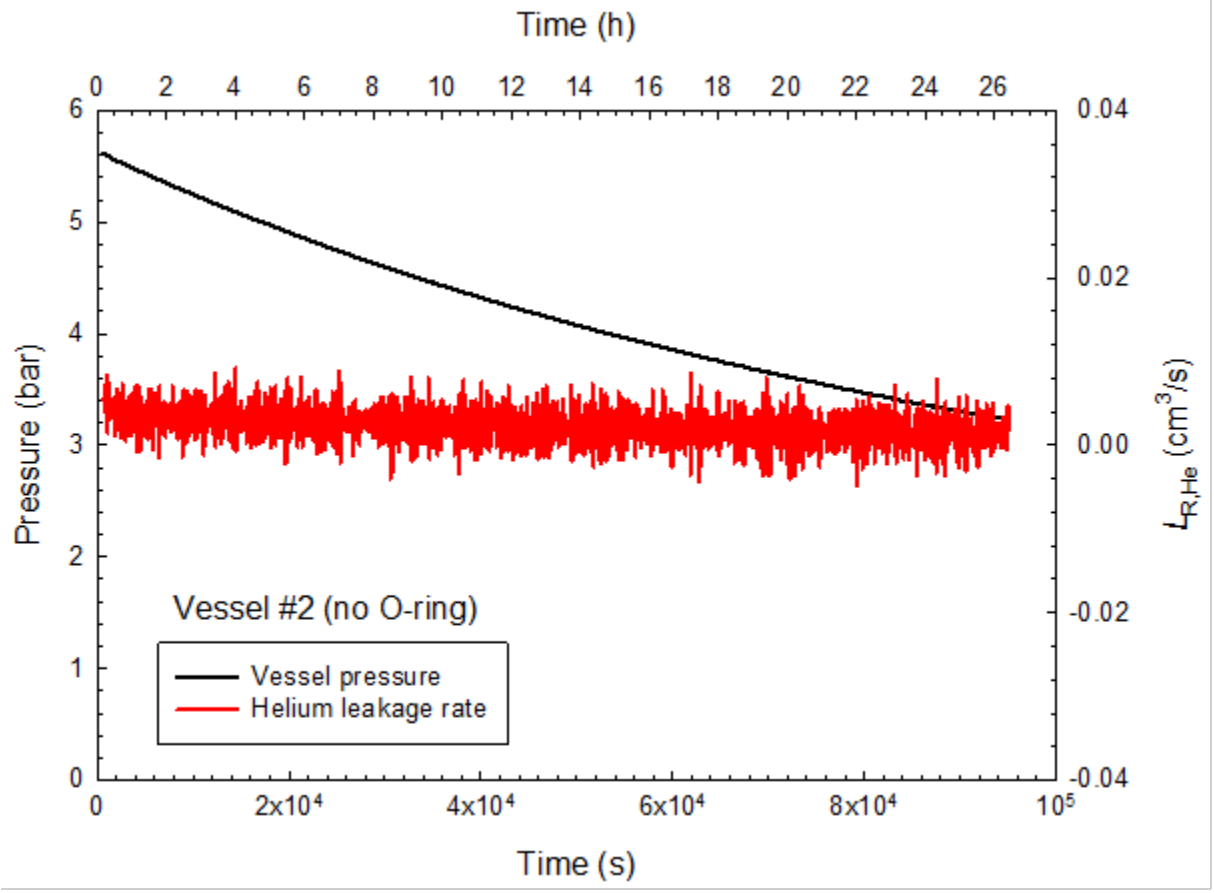

Figure 3-2. Temporal variations of vessel pressure at 24 °C without metallic O-ring.

Figure 3-3 shows the temporal variations of the vessel internal pressure and temperature, two flange temperatures and furnace temperature during the heat-up, the constant-temperature heating (isothermal), and a portion of the cool-down phases for Test # Metallic-2 (Test #2). The rapid decrease in the furnace temperature identifies when the furnace was turned off and the beginning of the cool-down phase. Figure 3-4 shows a re-plot of Figure 3-3 with the time scale extended to include the entire cool-down phase, which normally takes more than several days to naturally cool the test vessel inside the powered-down furnace from 800 °C (1472 °F) to room temperature.

The scale of the ordinate for pressure in Figure 3-3 is magnified to show that the pressure starts to decrease shortly after the vessel temperature has reached 800 °C (1472 °F) and continues to decrease very slowly during the remainder of the 9 h constant-temperature heating phase. Although the continuous downward trend does seem to imply the occurrence of a very tiny leak, the decrease in pressure is within the expanded measurement uncertainty of the pressure

transducer (0.11 bar) and is not considered significant in this test. However, the complete thermal exposure history, shown in Figure 3-4, indicates that the vessel pressure is restored to its original charge pressure (≈ 5 bar) after the thermal exposure, indicating no leakage. For this test, the occurrence of a leak is inconclusive based only on the small pressure drop.

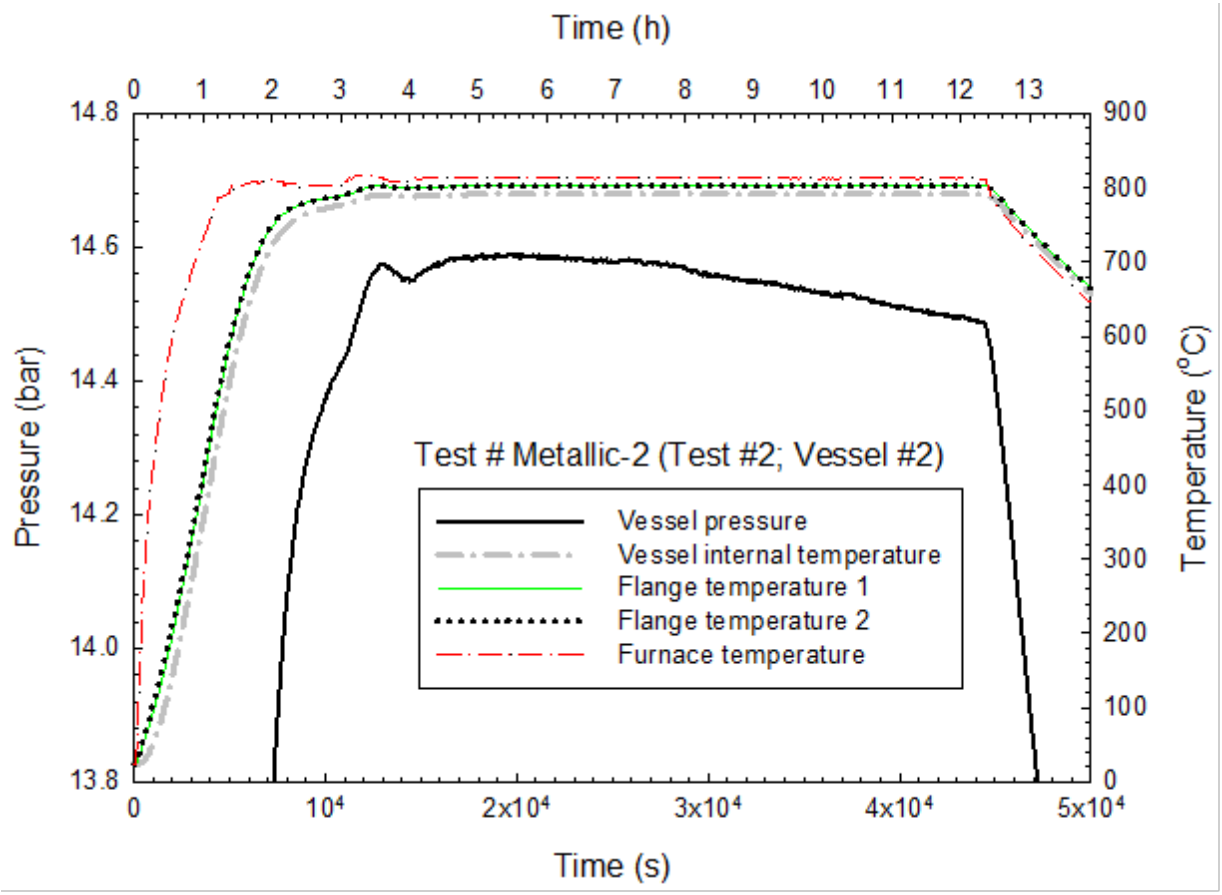

Figure 3-3. Temporal variations of vessel pressure and temperature in Test # Metallic-2 (Test #2).

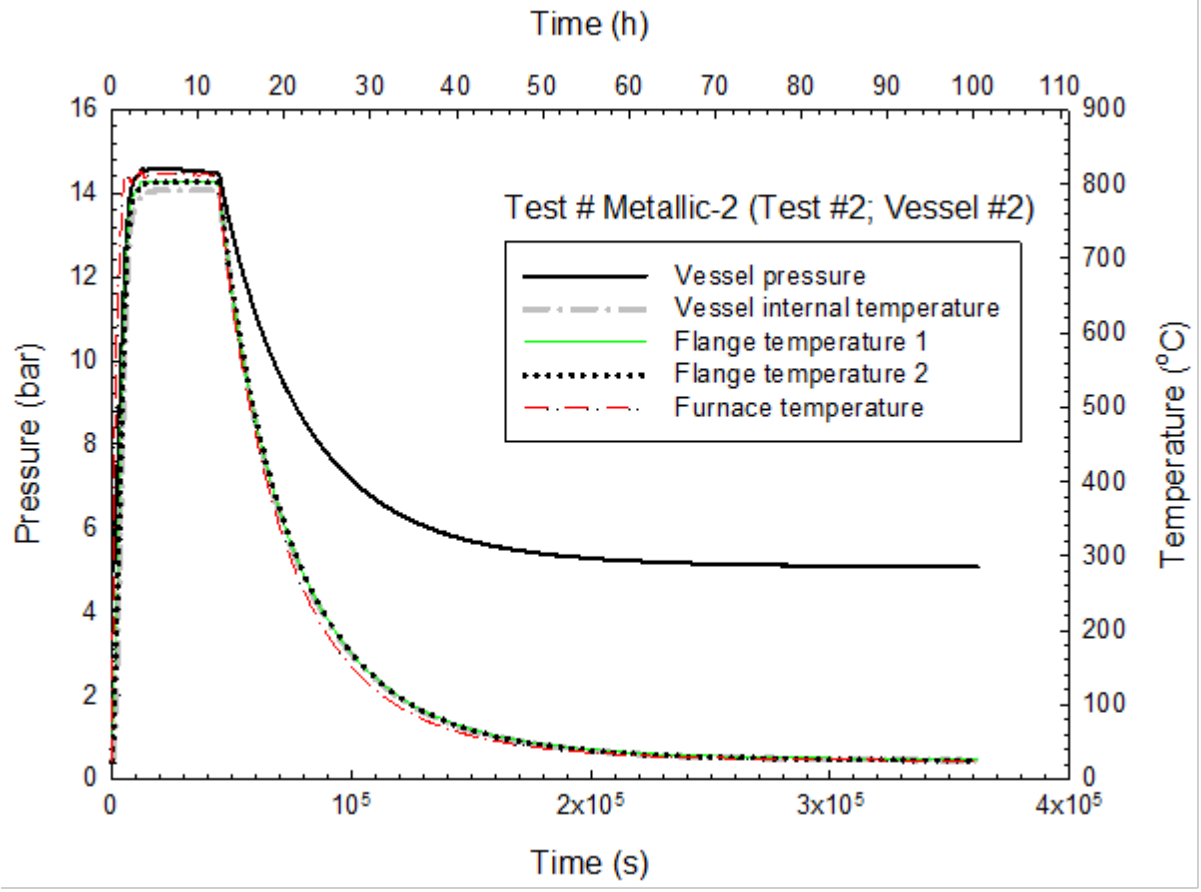

Figure 3-4. Temporal variations of vessel pressure and temperature in Test # Metallic-2 (Test #2) with time scale extended, including the cool-down phase.

3.1.1.3 Test # Metallic-3 (Test #3; Vessel #3)

Test # Metallic-3 (Tests #3) is a repeat of Test # Metallic-2 (Test #2). Figure 3-5 presents the test results which show the occurrence of a leak during the 9 h constant-temperature heating phase at 800 °C (1472 °F). In Test # Metallic-3, the vessel pressure decreases slowly initially and then significantly after about 25,000 s (6.9 h) at 800 °C (1472 °F). Since the leakage rate is directly proportional to the time rate of change of pressure, this two-stage decrease in pressure indicates a slower leak rate (small time derivatives of vessel pressure [dP/dt]) at first and then a faster leak rate (large dP/dt) at the end. Another leak indicator is revealed in Figure 3-6, which shows the entire time history of the test. After cooling to room temperature, the vessel does not recover its initial charge pressure of approximately 5 bar because of the leak. Isothermal reference helium leakage rates ($L_{R,He}$) during the 9 h heating in this test are shown in Figure 3-7.

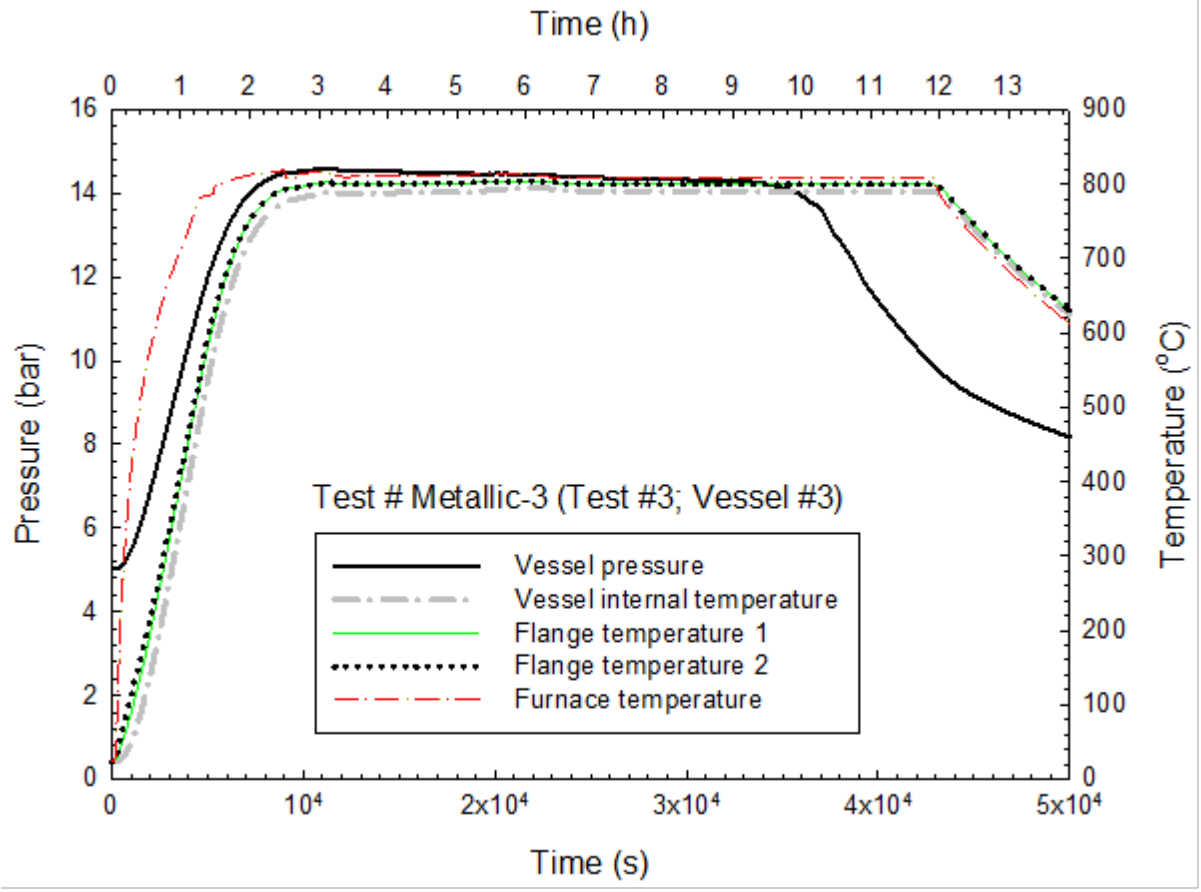

Figure 3-5. Temporal variations of vessel pressure and temperature in Test # Metallic-3 (Test #3).

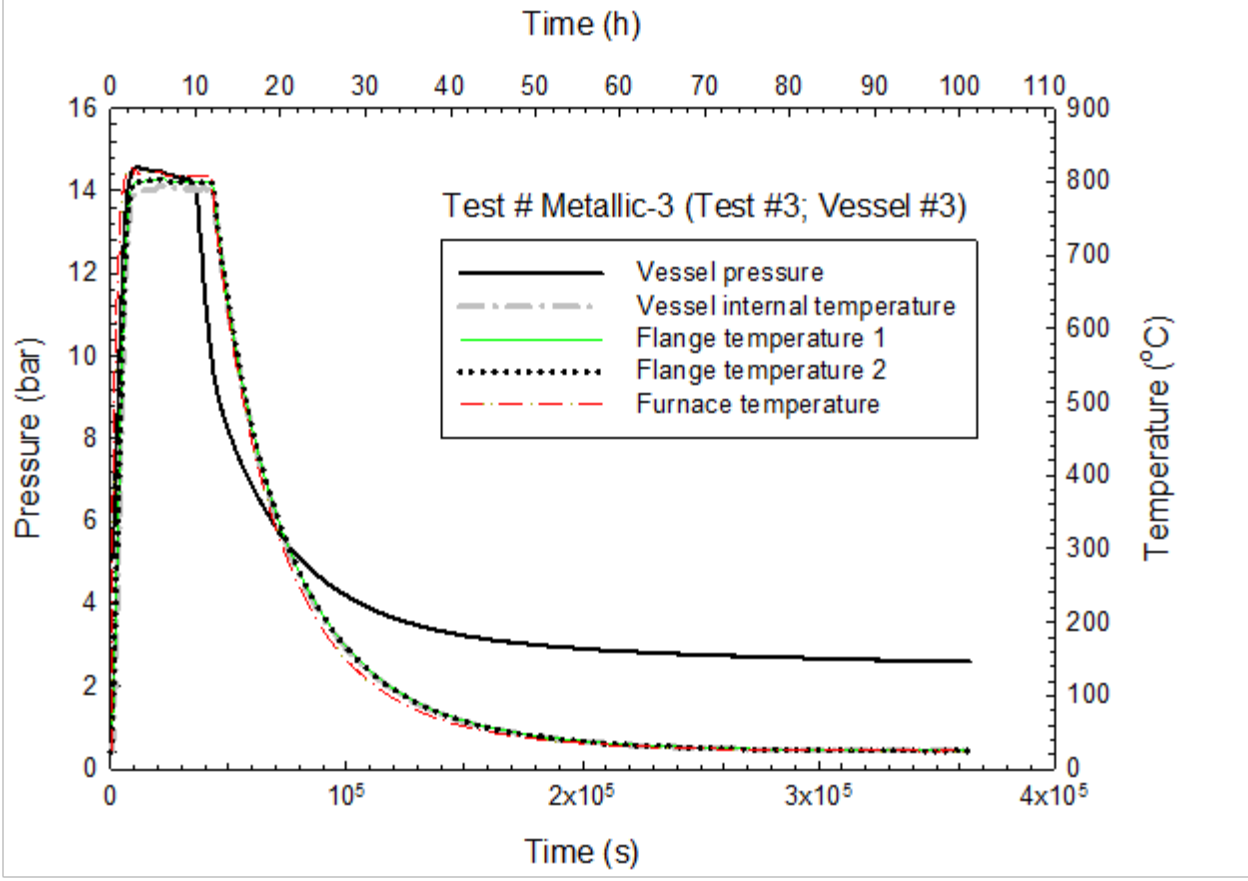

Figure 3-6. Temporal variations of vessel pressure and temperature in Test # Metallic-3 (Test #3) with time scale extended, including the cool-down phase.

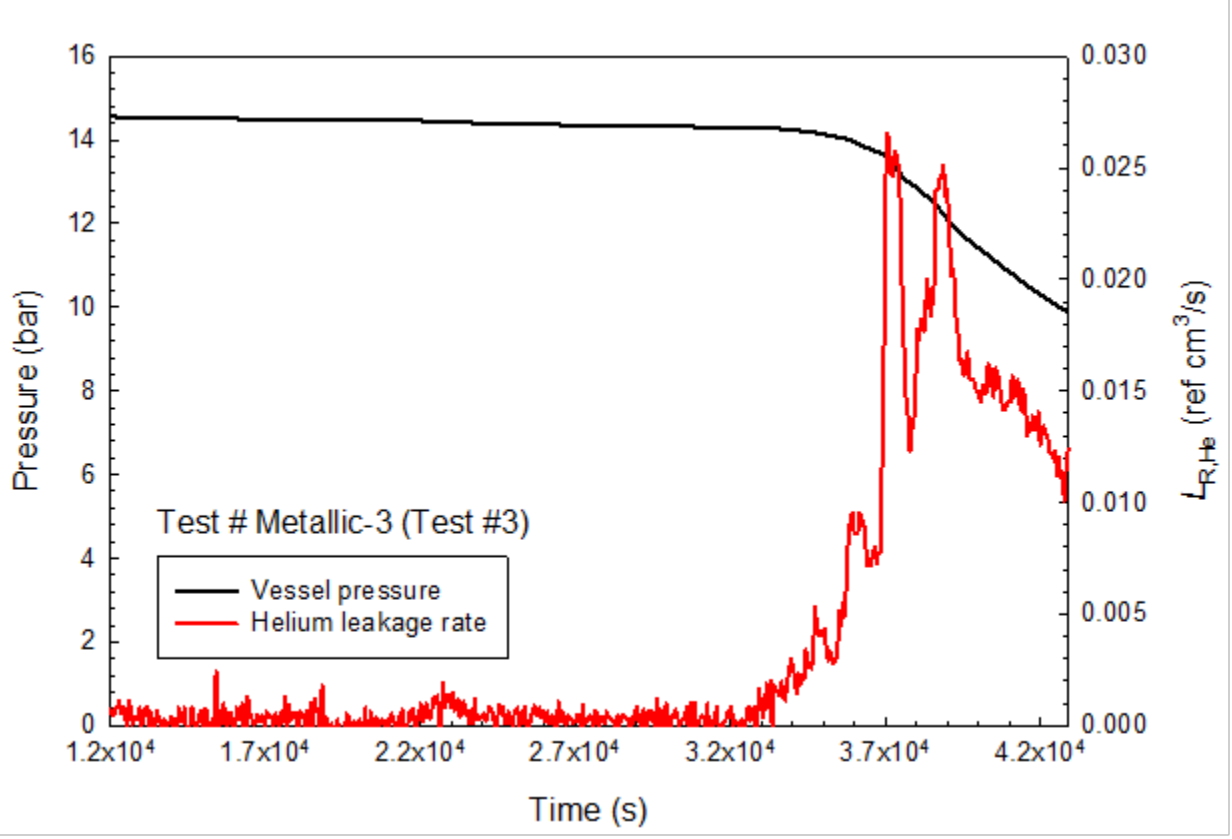

Figure 3-7. Isothermal reference helium leakage rate during the 9 h heating in Test # Metallic-3 (Test #3).

3.1.1.4 Test # Metallic-4 (Test #4; Vessel #4)

Test # Metallic-4 (Test #4) is another repeat of the thermal exposure condition used in Test # Metallic-2 (Test #2). Figure 3-8 shows the test results from Test # Metallic-4. In this test, the pressure remained relatively constant for about 10,000 s (2.8 h) initially during the 9 h constant-temperature heating phase, begins to drop significantly for about 15,000 s (4.2 h) with large *dP*/*dt*, and decreases slowly with small *dP*/*dt* for the remaining duration. Figure 3-9 shows the complete time-pressure and time-temperature histories of the test. The calculated reference helium leakage rates are shown in Figure 3-10.

It is interesting to note that despite the occurrence of a leak in these two tests (Tests # Metallic-3, and # Metallic-4), the vessel pressure did not equilibrate to atmospheric pressure at the end of the cool-down-phase, which took several days. This observation indicated that re-sealing could potentially occur as the vessel was cooled down.

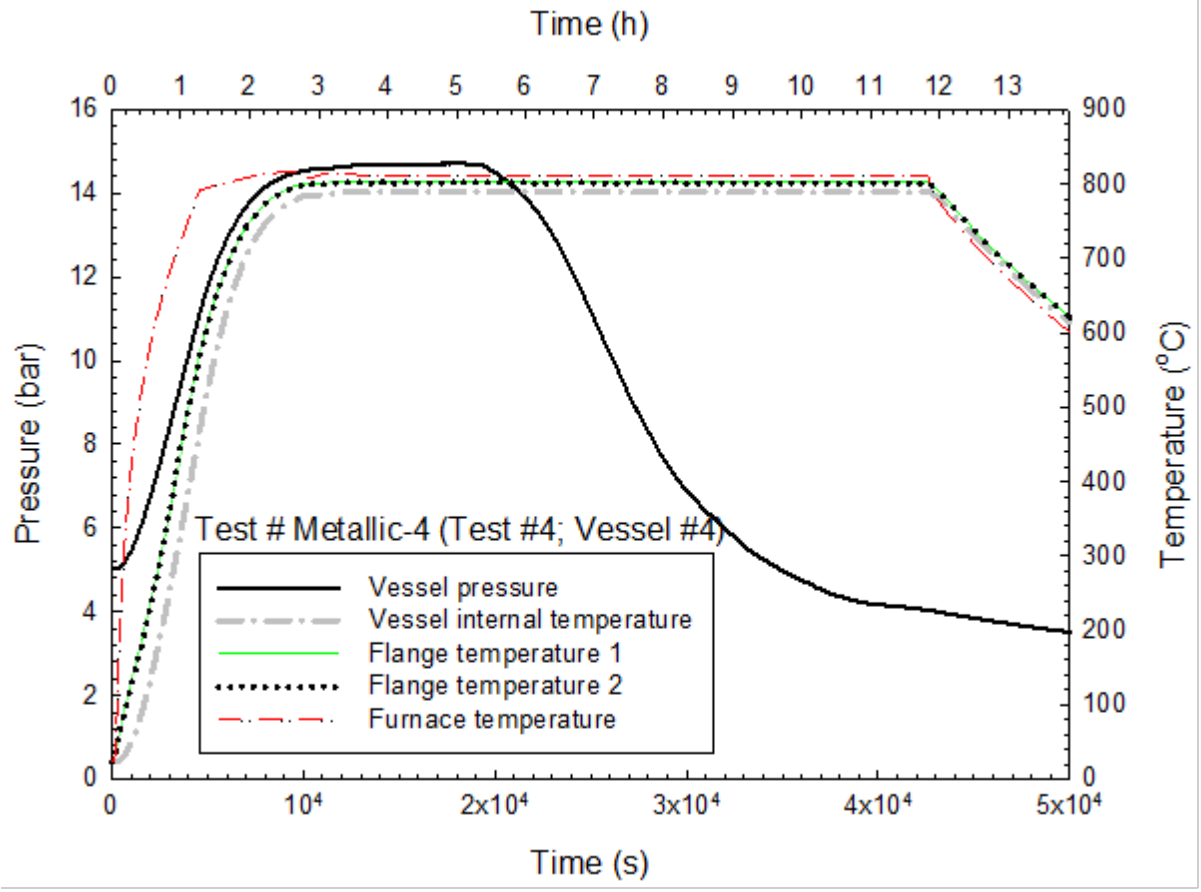

Figure 3-8. Temporal variations of vessel pressure and temperature in Test # Metallic-4 (Test #4).

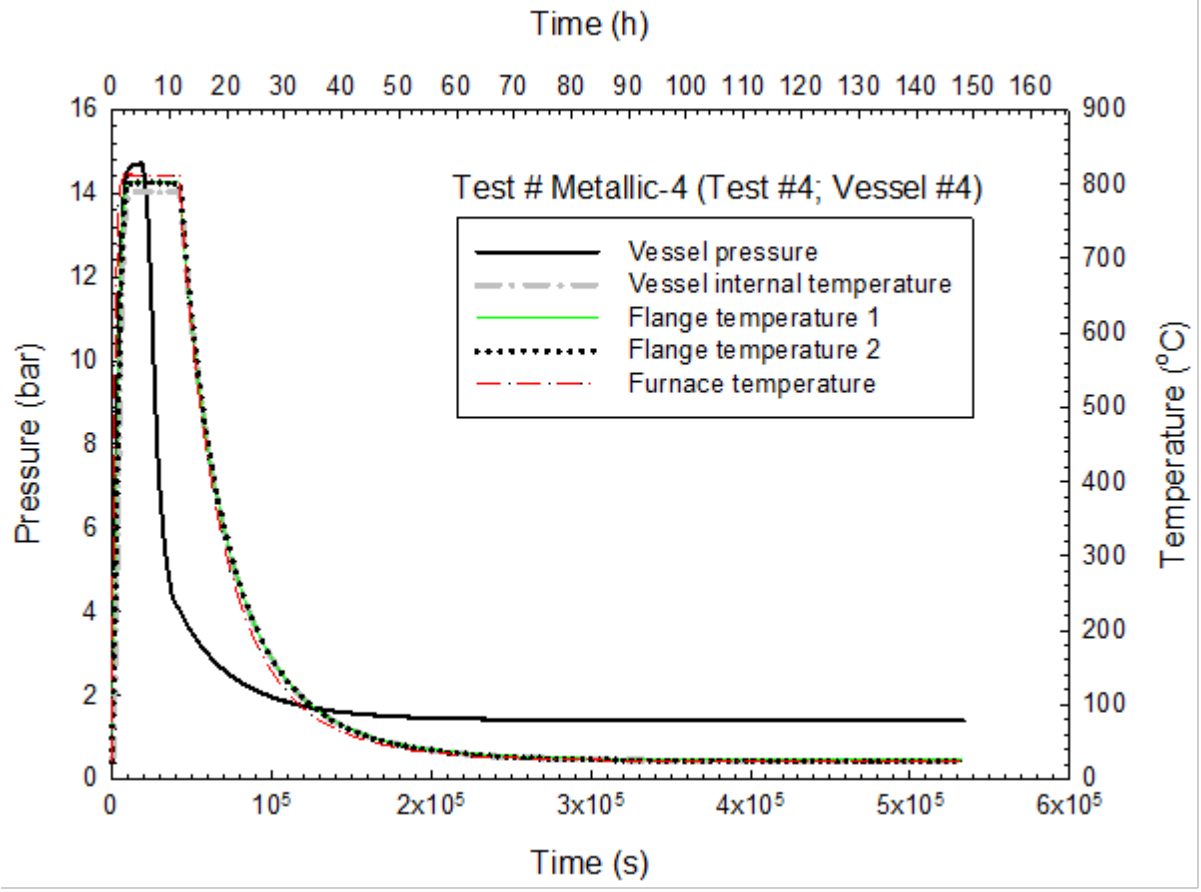

Figure 3-9. Temporal variations of vessel pressure and temperature in Test # Metallic-4 (Test #4) with time scale extended, including the complete cool-down phase.

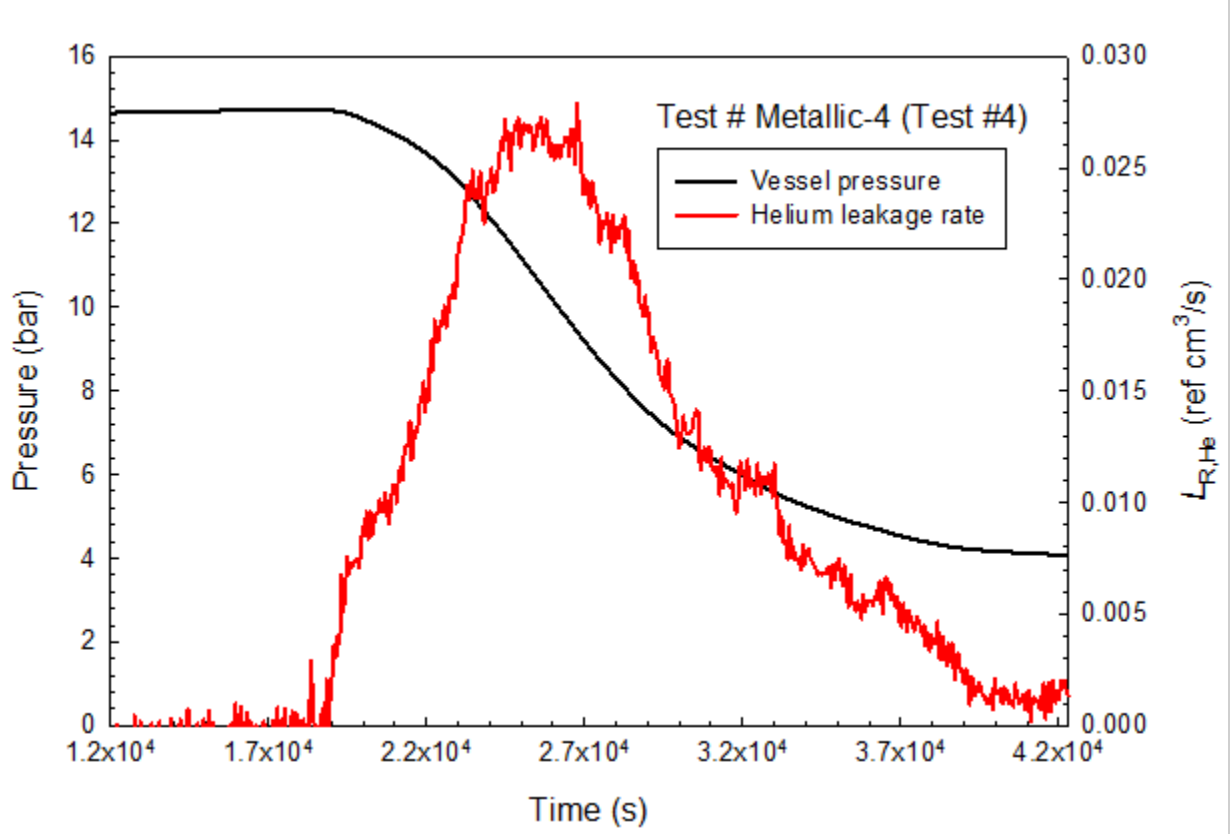

Figure 3-10. Isothermal reference helium leakage rate during the 9 h heating in Test # Metallic-4 (Test #4).

3.1.1.5 Test # Metallic-5 (Test #5; Vessel #5)

The results for Test # Metallic-5 (Test #5) are shown in Figure 3-11. The vessel pressure remained constant during the entire 9 h constant-temperature heating period at 427 °C (800 °F). The seal held vessel pressure. This was confirmed as the initial pressure at room temperature was recovered after the cool-down phase. In addition, the pressure remained unchanged for over 140 h after the cool-down. Figure 3-12 shows the complete thermal exposure cycle of the test.

A photograph of the exposed vessel is shown in Figure 3-13. The extent of discoloration of the vessel depends on the test temperature (Figure 3-1 *vs*. Figure 3-13). A post-test inspection revealed that the metallic O-ring seal was not soldered to either flange surfaces, and no silver coating from the seal was transferred to the O-ring groove.

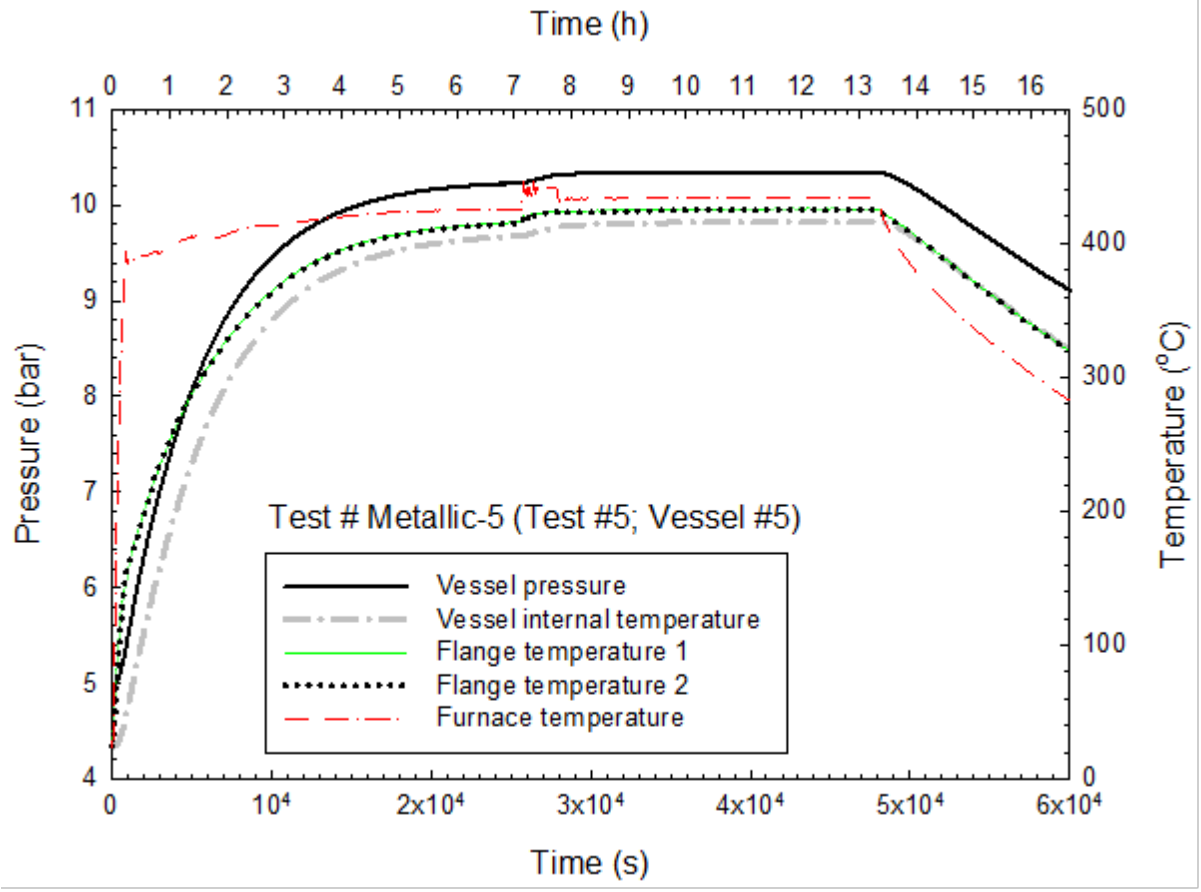

Figure 3-11. Temporal variations of vessel pressure and temperature in Test # Metallic-5 (Test #5).

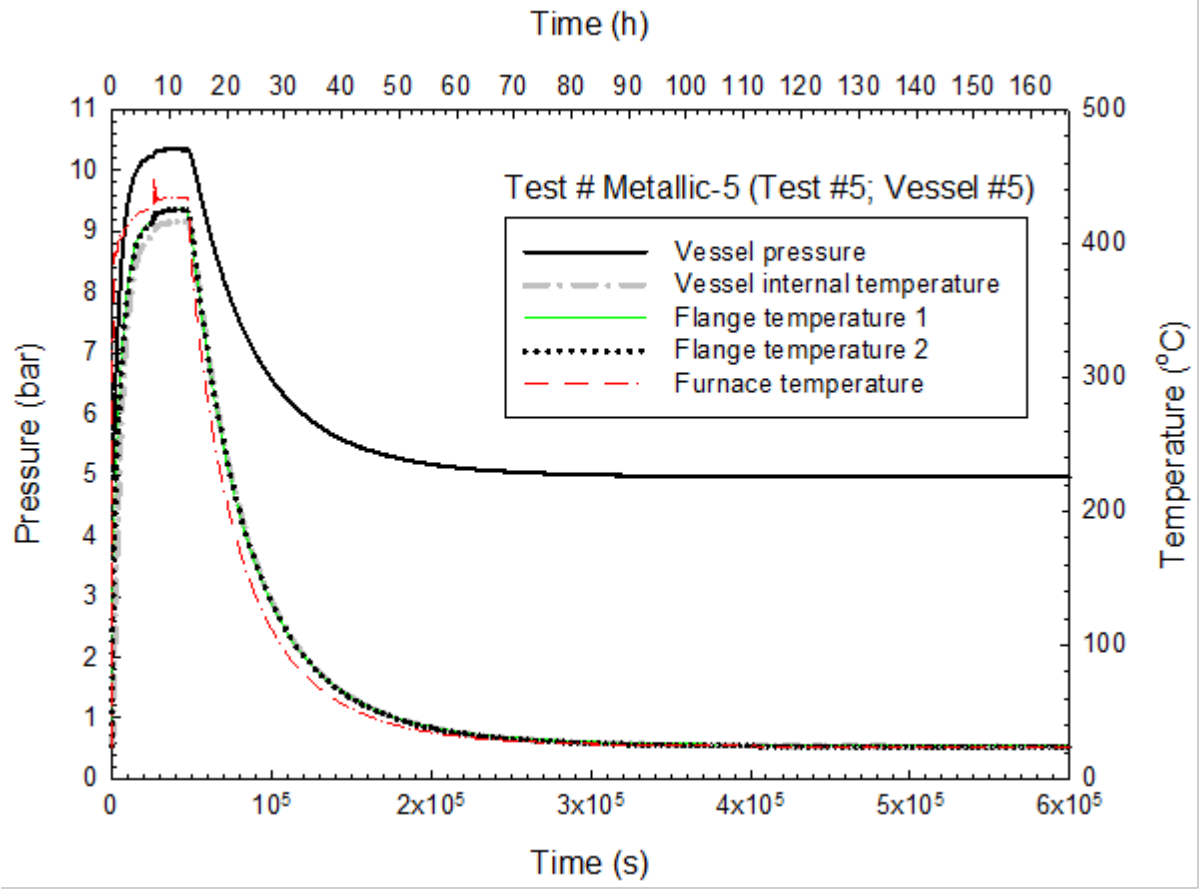

Figure 3-12. Temporal variations of vessel pressure and temperature in Test # Metallic-5 (Test #5) with time scale extended, including the complete cool-down phase.

Figure 3-13. Post-test photograph of Vessel #5 (vessel body with O-ring removed) after exposure at 427 °C (800 °F) for 9 h.

3.1.1.6 Test # Metallic-6 (Test #6; Vessel #2 Refurbished)

The results for Test # Metallic-6 (Test #6) using the refurbished Vessel #2 are shown in Figure 3-14. The refurbishment only involved the re-facing of the surfaces of the flanges and O-ring groove to the specified tolerances. For this test, the vessel pressure started to decrease very slowly during the constant-temperature heating period. The scale of the ordinate is magnified in Figure 3-14 to elucidate the continuous decrease in pressure. However, the small pressure drop is within the pressure measurement uncertainty of 0.11 bar. Although the continuous decrease in pressure does seem to imply that a very small leak might have occurred during the test, the initial charge pressure was restored when the vessel was cooled to room temperature after the thermal exposure (as shown in Figure 3-15), an indication of no leakage.

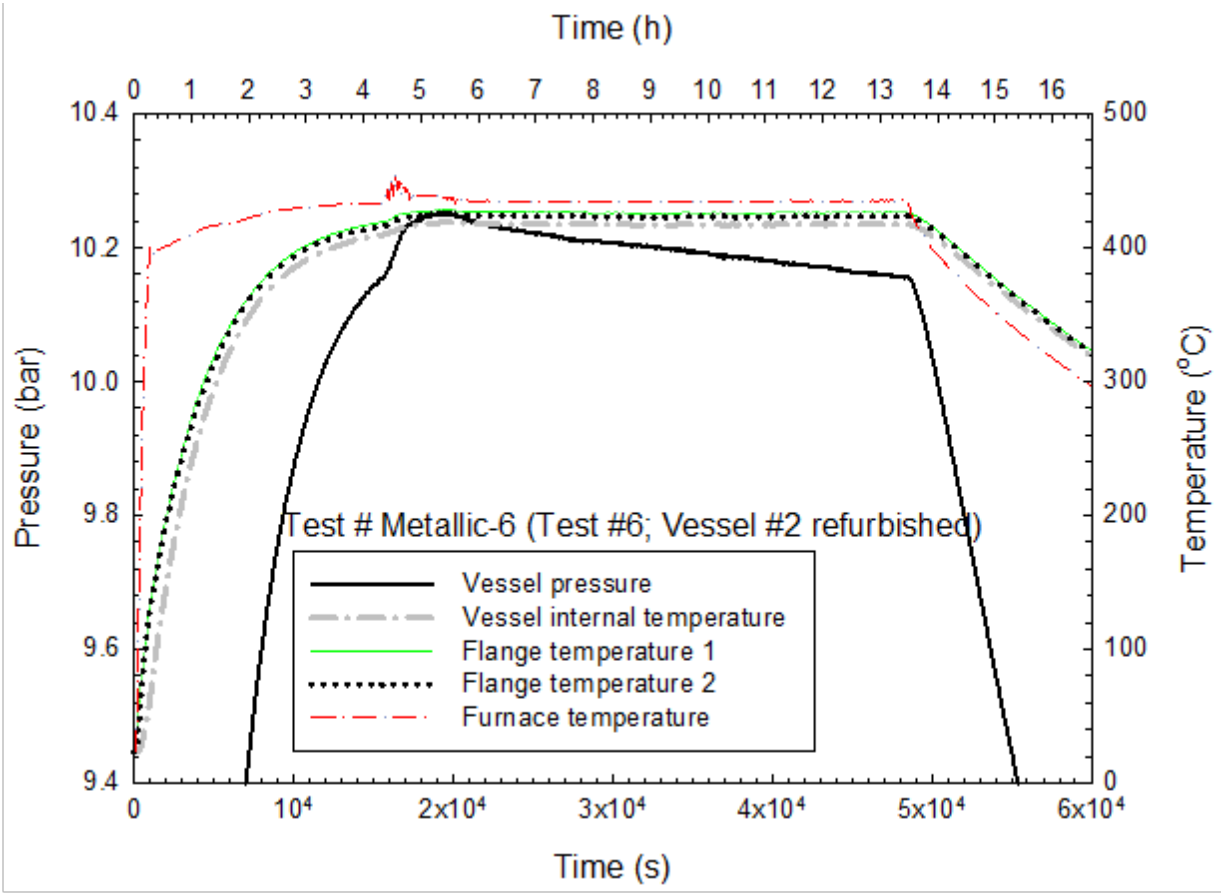

Figure 3-14. Temporal variations of vessel pressure and temperature in Test # Metallic-6 (Test #6).

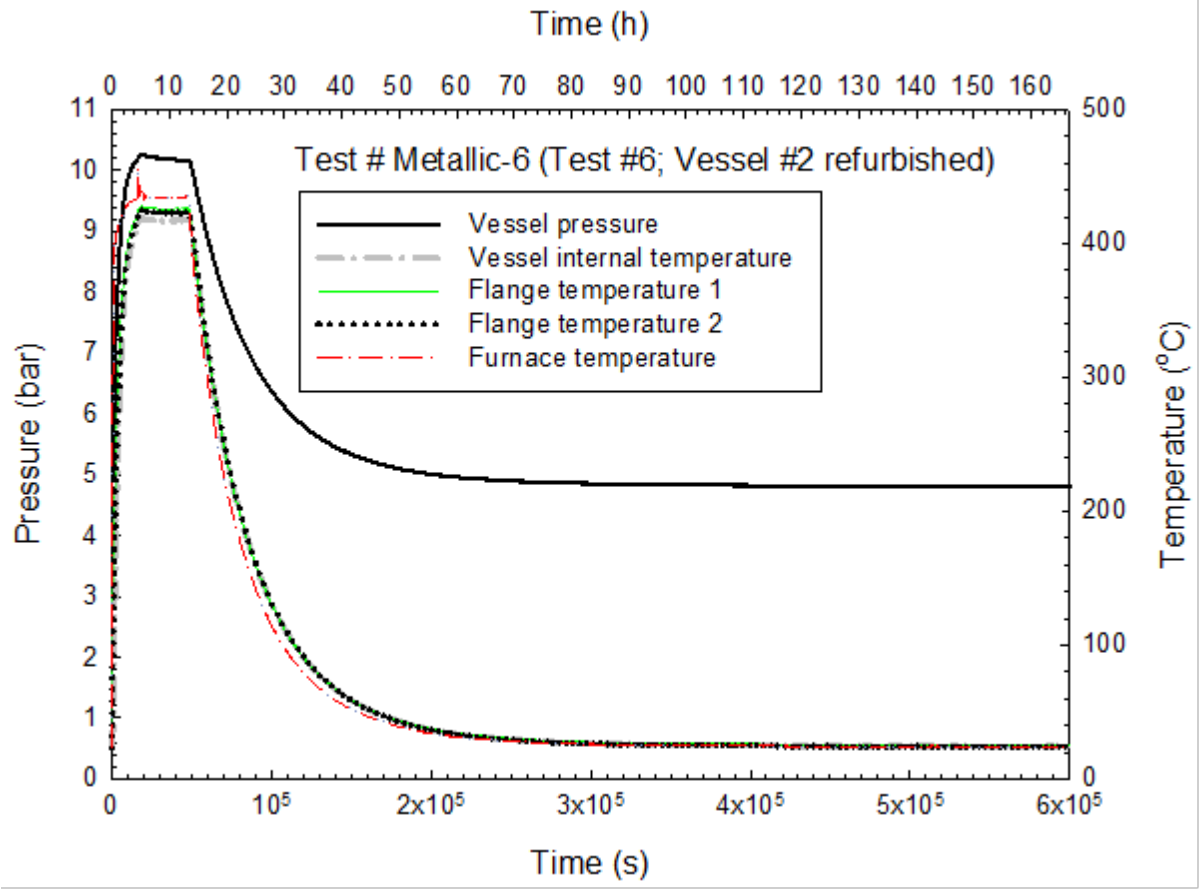

Figure 3-15. Temporal variations of vessel pressure and temperature in Test # Metallic-6 (Test #6) with time scale extended, including the complete cool-down phase.

3.1.1.7 Test # Metallic-7 (Test #7; Vessel #1 Refurbished)

Figure 3-16 shows the results for Test # Metallic-7 (Test #7) using the refurbished Vessel #1. The same refurbishing process used in Vessel #2 was applied to Vessel #1. As indicated in the figure, the vessel pressure remained unchanged during the 9-h constant-temperature heating period. No leakage was observed during Test # Metallic-7. Figure 3-17 is the complete thermal exposure history of Test # Metallic-7.

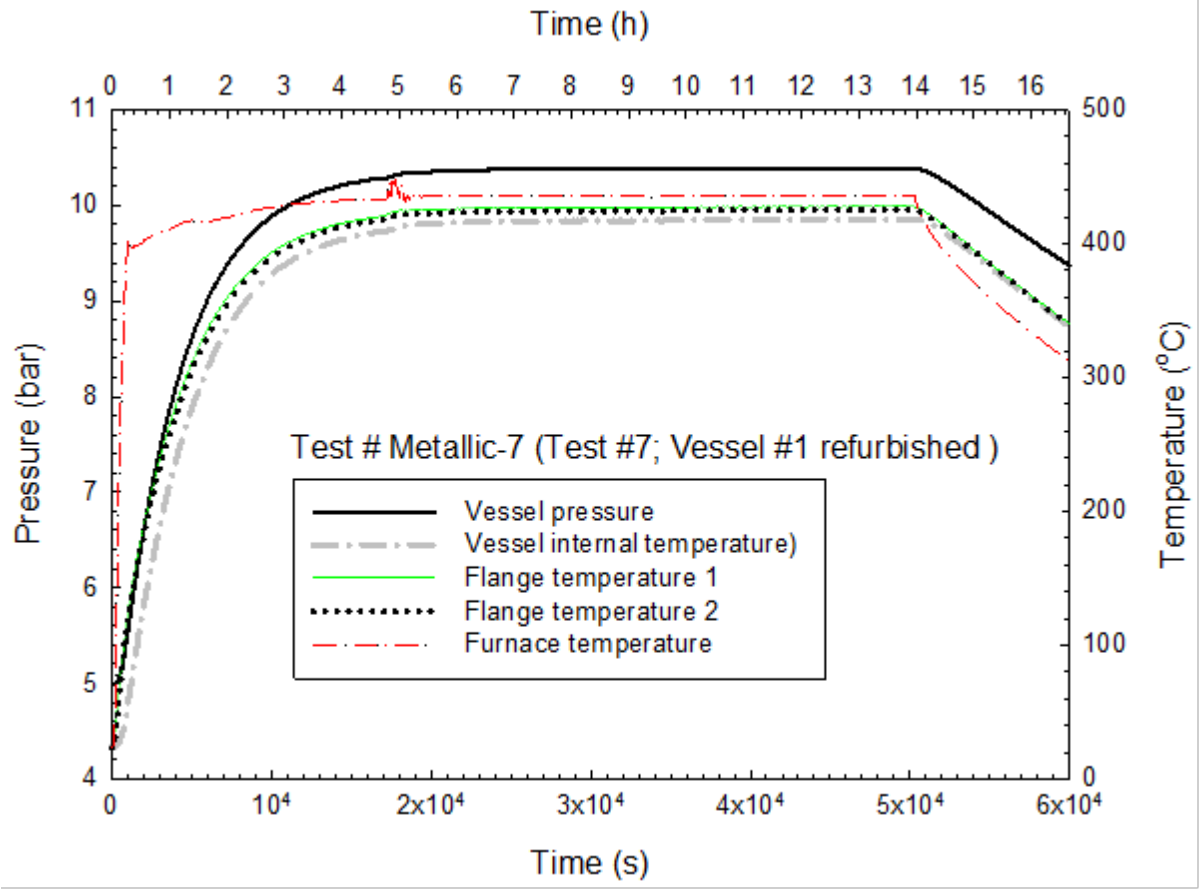

Figure 3-16. Temporal variations of vessel pressure and temperature in Test # Metallic-7 (Test #7).

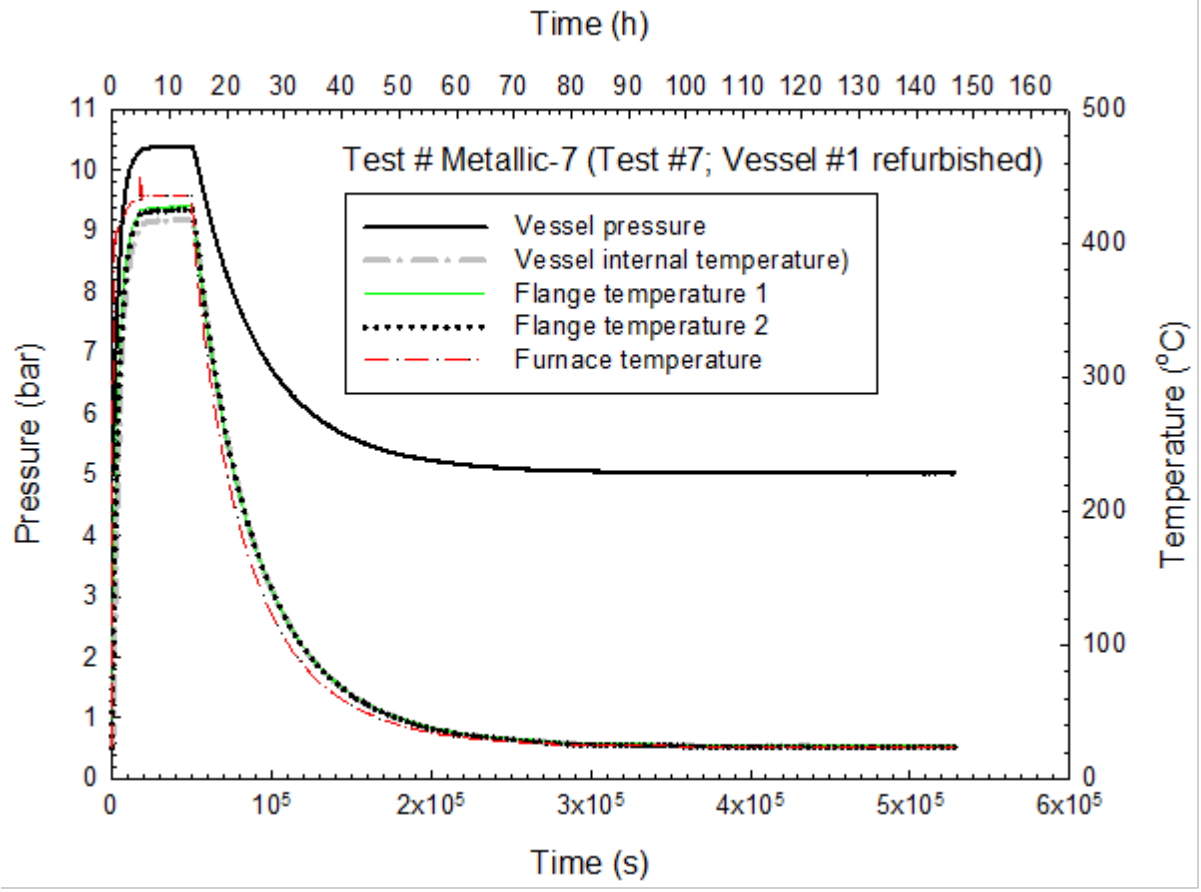

Figure 3-17. Temporal variations of vessel pressure and temperature in Test # Metallic-7 (Test #7) with time scale extended, including the complete cool-down phase.

3.1.1.8 Test # Metallic-8 (Test #8; Vessel #6)

The test conditions were similar to Tests # Metallic-2, Metallic-3, and Metallic-4. Figure 3-18 shows the thermal exposure results for Vessel #6. The pressure trace indicates that leakage occurs after about 3-h exposure to 800 °C (1472 °F). For this test, the pressure initially decreases very rapidly, followed by a gradually decrease in vessel pressure. However, the pressure never dropped below 2 bar, indicating that the seal had some residual sealing capacity. Figure 3-19 is the complete time-pressure and time-temperature histories of Test # Metallic-8 (Test #8). Figure 3-20 shows the calculated isothermal reference helium leakage rates during the 9-h heating.

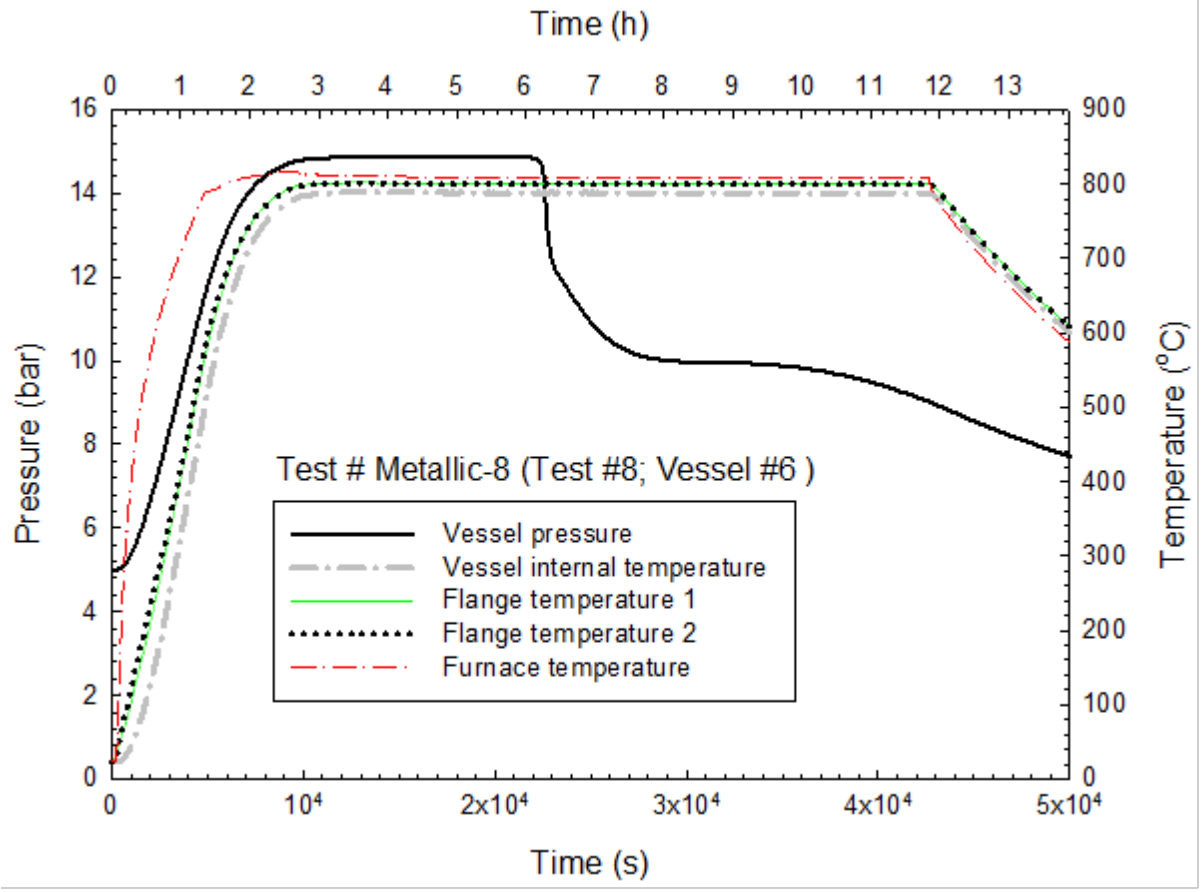

Figure 3-18. Temporal variations of vessel pressure and temperature in Test # Metallic-8 (Test #8).

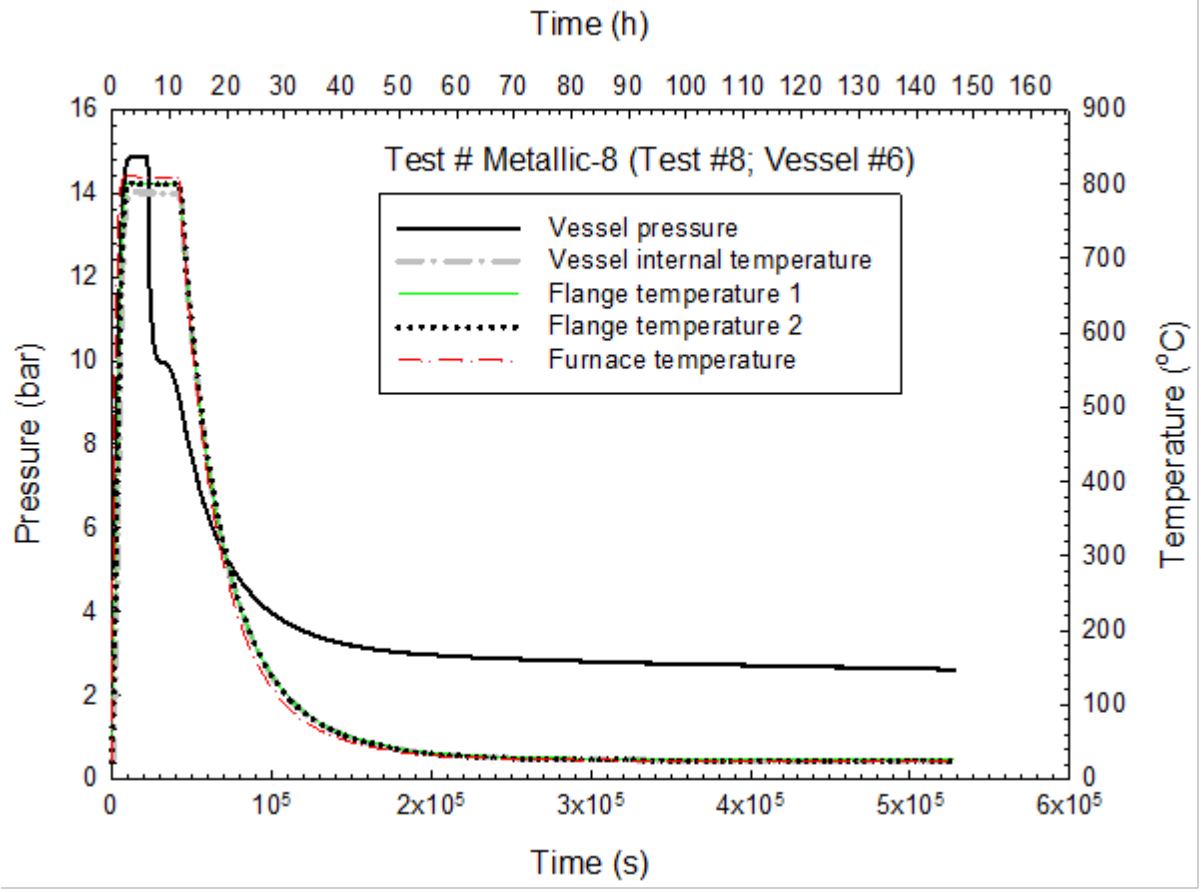

Figure 3-19. Temporal variations of vessel pressure and temperature in Test # Metallic-8 (Test #8) with time scale extended, including the complete cool-down phase.

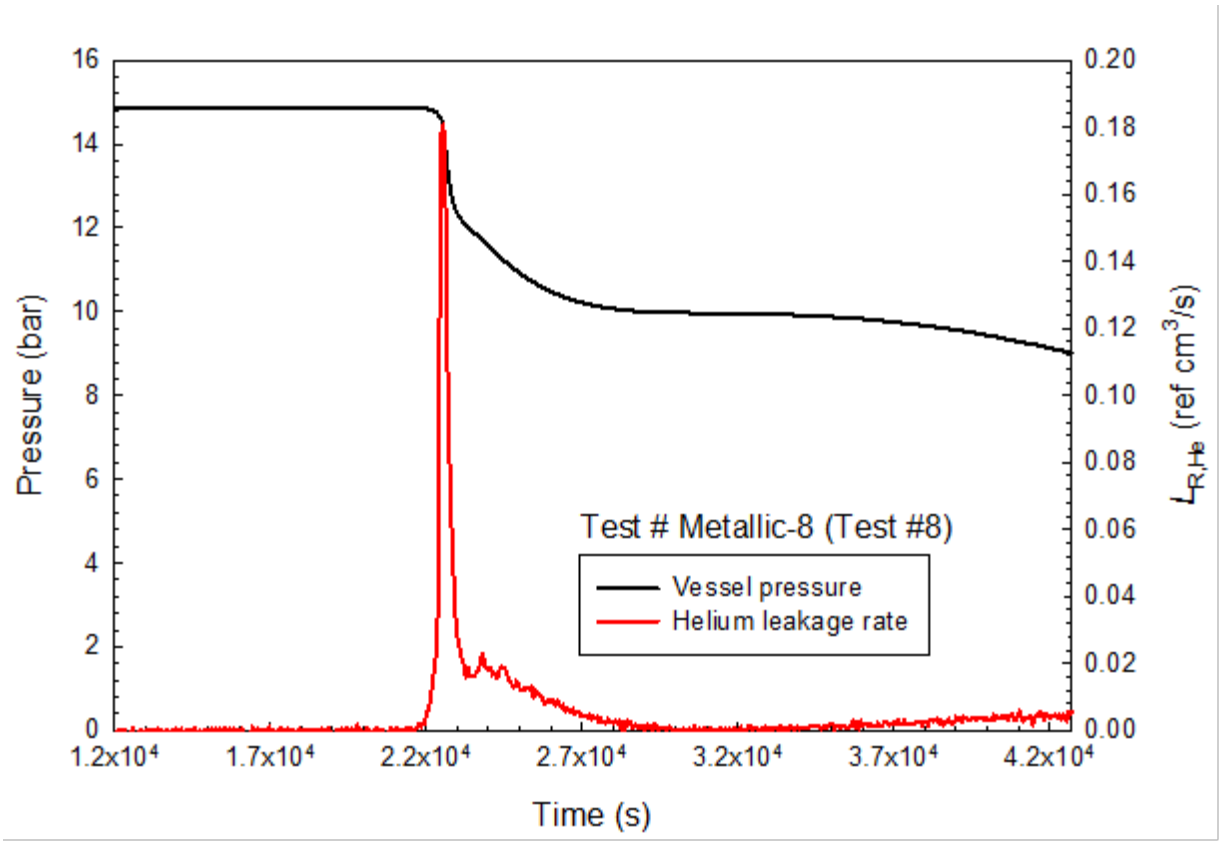

Figure 3-20. Isothermal reference helium leakage rate during the 9 h heating in Test # Metallic-8 (Test #8).

3.1.1.9 Test # Metallic-9 (Test #9; Vessel #1 Re-refurbished)

Test # Metallic-9 (Test #9) was performed using Vessel #1, which had been used once at 800 °C (1472 °F) for 30 min and once at 427 °C (800 °F) for 9 h and refurbished twice. The sole intent of this test was to check the performance of the pressure transducer against a pressure gauge[13] to ensure that the pressure transducer functioned properly. Figure 3-21 shows the set-up used for this comparative test. The only difference between this arrangement and the original was the addition of a pressure gauge.

The test protocol involved the heating of the vessel to 427 °C (800 °F). Once the vessel reached 427 °C (800 °F), the furnace temperature was raised to 800 °C (1472 °F), and the vessel was heated at 800 °C (1472 °F) for a little more than 3 h. Figure 3-22 and Figure 3-23 show the pressure and temperature data using different time scales respectively. No leak is indicated in the figures since the attainable pressure at 800 °C (1472 °F) remained constant. However, the pressure at 800 °C (1472 °F) was lower than those recorded in previous tests under similar conditions (≈ 12 bar *vs.* ≈ 14.5 bar). This is due to the increase of the measurement volume with the addition of the pressure gauge which used a C-shape Bourdon tube with a surprisingly large volume. The gauge was dissembled and the internal volume of the Bourdon tube, which had a nearly elliptical cross section, was estimated to be more than

[13] WIKA model with a range of 0 bar (0 psig) to 13.79 bar (200 psig) and a resolution of 0.14 bar (2 psig).

12 mL. Figure 3-24 correlates the pressure readings from the pressure transducer with those from the pressure gauge at different times during the heating phase. The pressure transducer clearly functioned properly, and the transducer readings correspond, within the measurement uncertainties, to those obtained from the pressure gauge.

Figure 3-21. A photograph showing the pressure gauge used to check the pressure transducer performance.

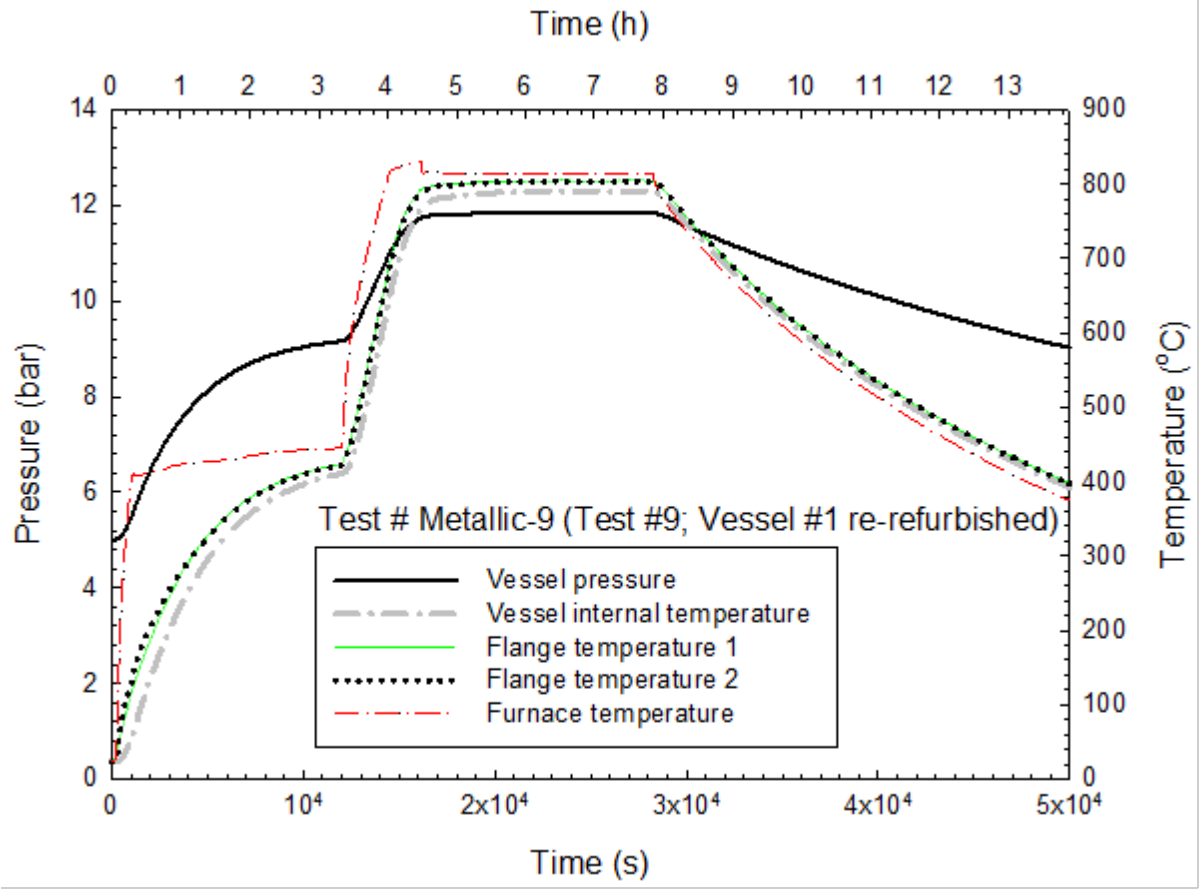

Figure 3-22. Temporal variations of vessel pressure and temperature in Test # Metallic-9 (Test #9).

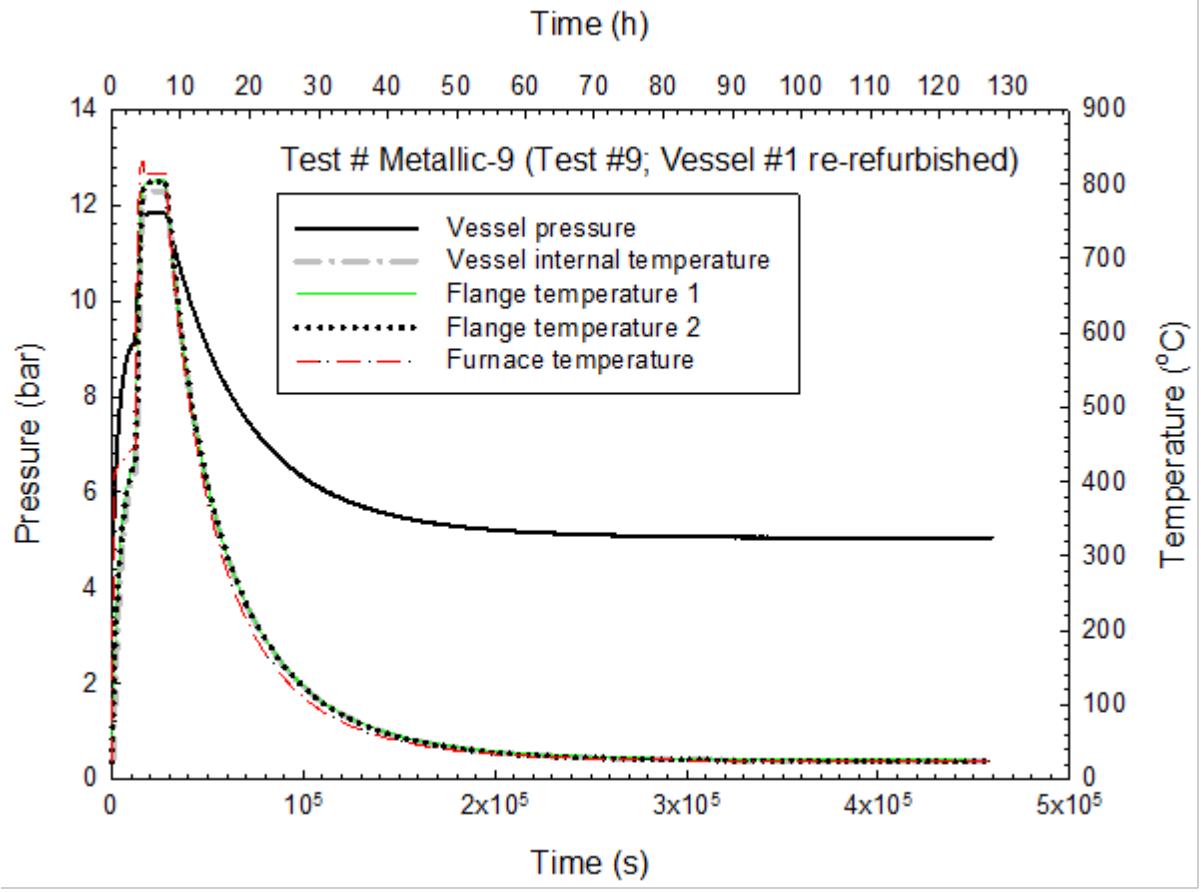

Figure 3-23. Temporal variations of vessel pressure and temperature in Test # Metallic-9 (Test #9) with time scale extended, including the complete cool-down phase.

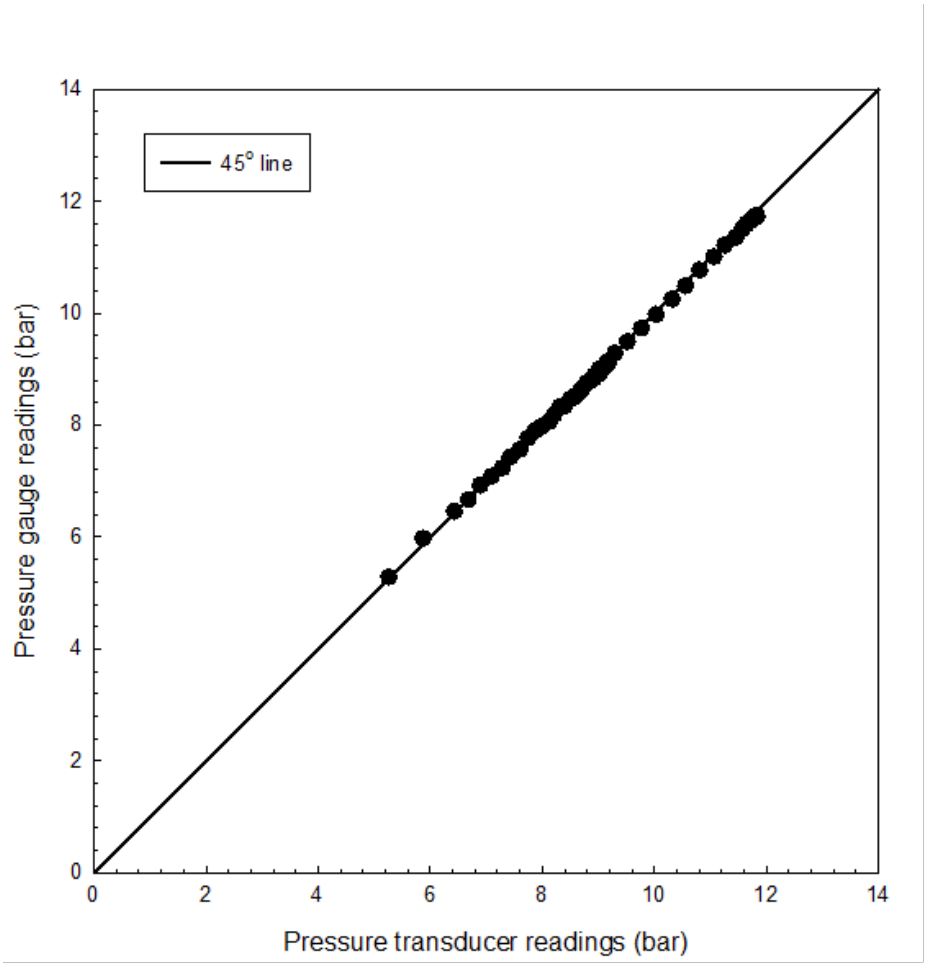

Figure 3-24. Comparison of pressure measurements from pressure transducer and pressure gauge.

3.1.1.10 Test # Metallic-10 (Test #10; Vessel #7)

In Test # Metallic-10 (Test #10), an incremental heating protocol was used to assess the metallic seal performance. The vessel was initially heated to 427 °C (800 °F) and held for 9 h at this temperature. Then, the furnace temperature was raised to 527 °C (981 °F), and the vessel was heated at 527 °C (981 °F) overnight (more than 9 h). The vessel was then heated to 627 °C (1161 °F) for 9 h. Figure 3-25 and Figure 3-26 show the test results. No leak was observed based on the pressure traces at the test temperatures, 427 °C (800 °F), 527 °C (981 °F), and 627 °C (1161 °F), and the recovery of the initial pressure at room temperature. Post-test removal of the O-ring from the groove was very easy. A post-test inspection of the vessel indicated that the metallic seal did not bond onto the O-ring groove.

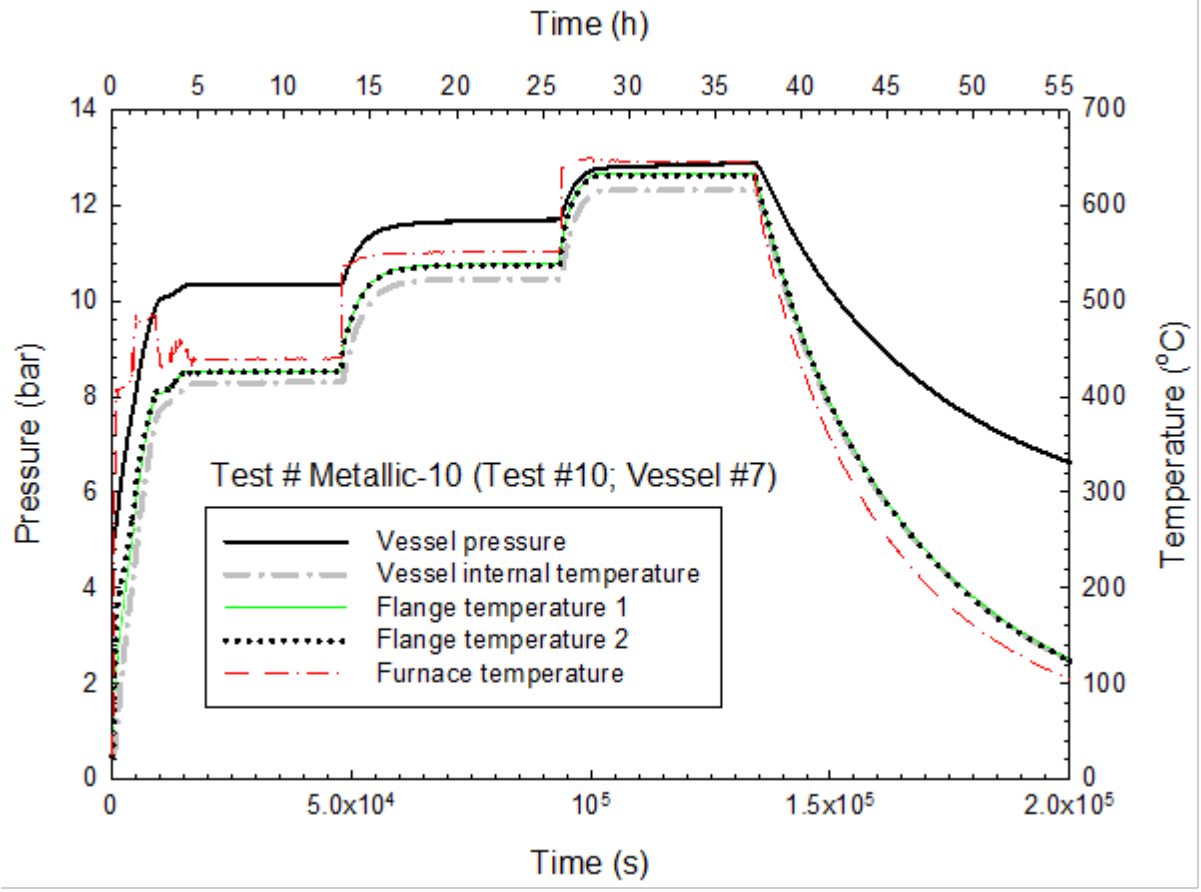

Figure 3-25. Temporal variations of vessel pressure and temperature in Test # Metallic-10 (Test #10).

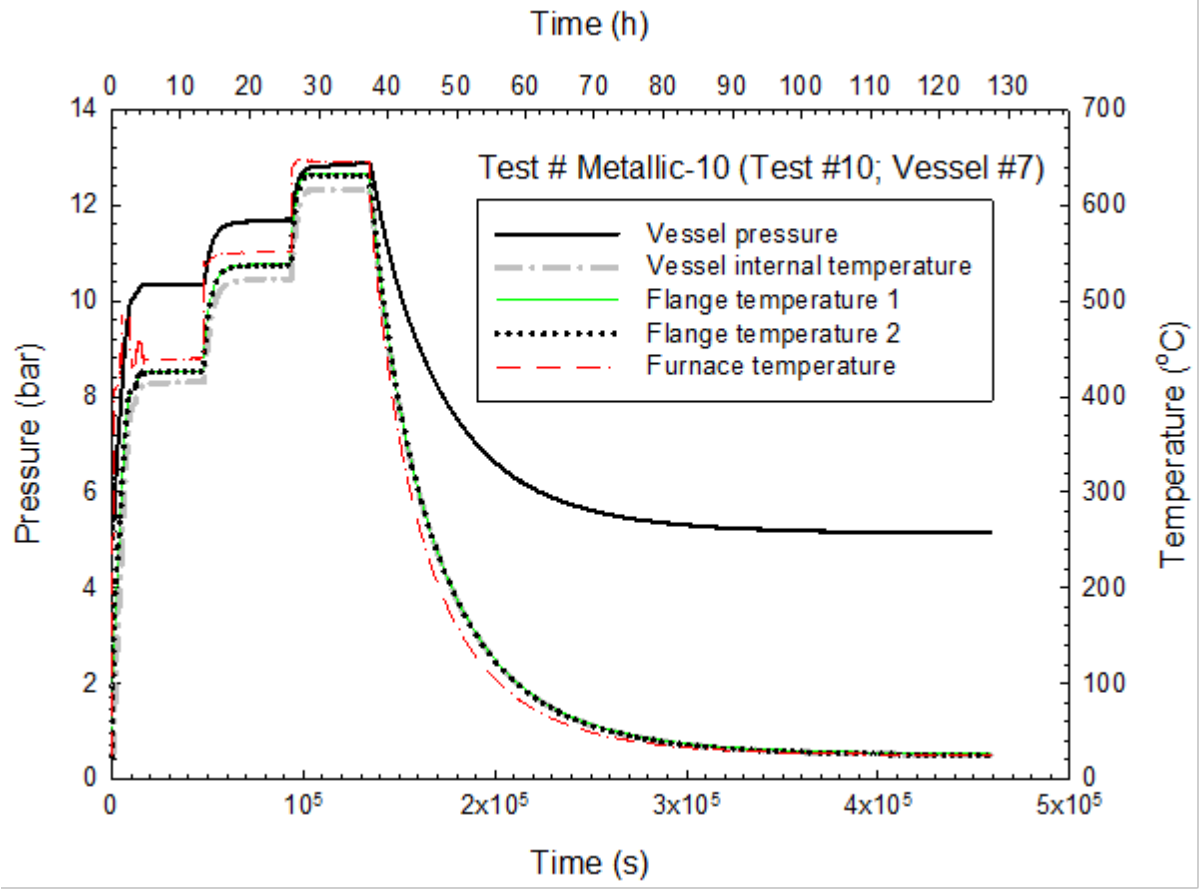

Figure 3-26. Temporal variations of vessel pressure and temperature in Test # Metallic-10 (Test #10) with time scale extended, including the complete cool-down phase.

3.1.1.11 Test # Metallic-11 (Test #13; Vessel #8)

For Test # Metallic-11 (Test #13), a metallic seal and a new vessel were used. The vessel was evacuated (for 1 min) and filled with helium (to 5 bar) and then evacuated and filled again twice. Contrary to the previous vessel filling process used in Tests # Metallic-1 (Test #1) to Test # PTFE-a (Test #12), two additional evacuating and filling cycles were applied in order to determine if the evacuation process had any effect on the results.[14] In this test, an incremental heating protocol was used. The test vessel was first heated at 427 °C for more than 10 h, then at 527 °C for 9 h, then at 627 °C for more than 10 h, and finally at 627 °C for 9 h. Figure 3-27 and Figure 3-28 show the results. No leakage was observed during the entire incremental heating processes. However, after the vessel was cooled down to room temperature, the vessel pressure did not recover to its original (starting) value (≈ 5 bar) but remained at a slightly higher constant value of ≈ 5.2 bar over a duration of more than 50 h, albeit within the uncertainty of the transducer. This was not due to the drift of the pressure transducer because when the vessel content was vented to the atmosphere, the pressure transducer showed an atmospheric

[14] Whether the test vessel was evacuated once or three times, no discernible difference in the final attainable vessel pressure was observed under the same test conditions.

pressure reading.

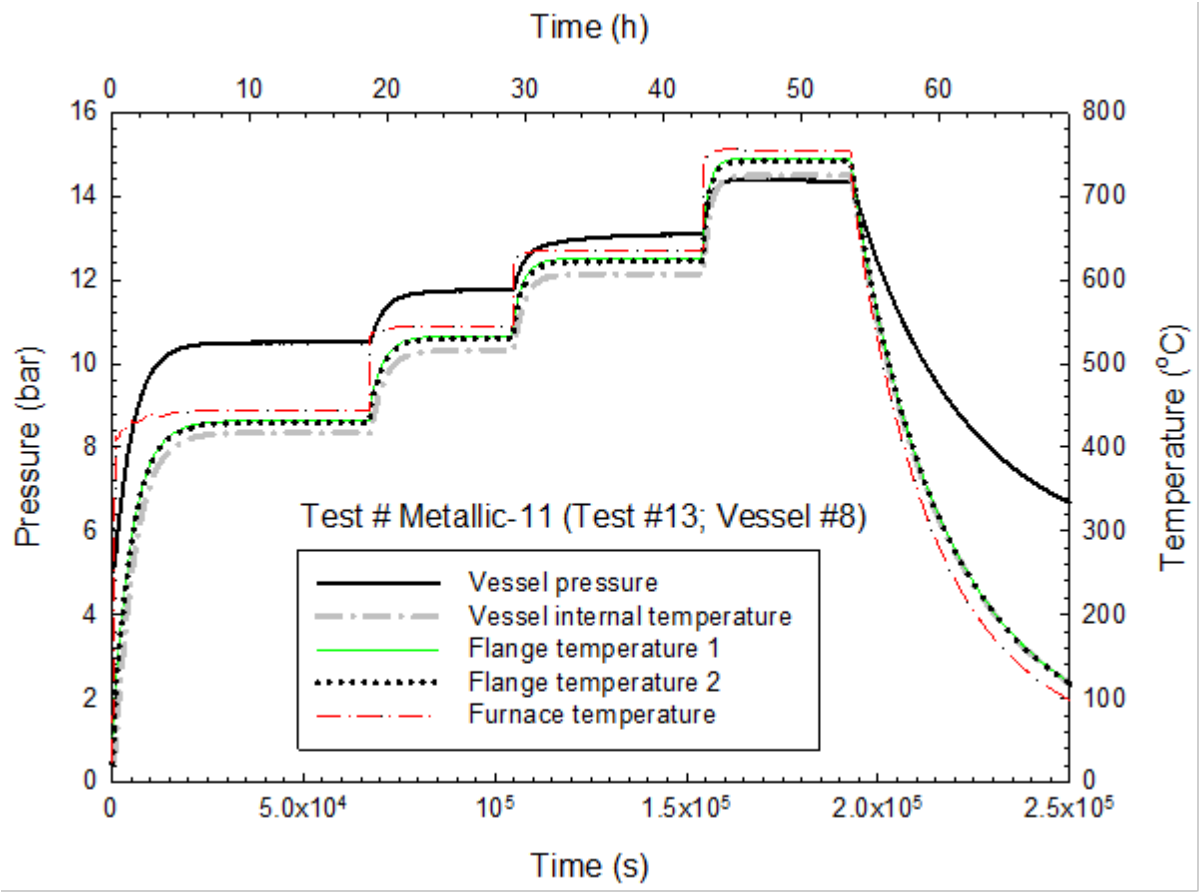

Figure 3-27. Temporal variations of vessel pressure and temperature in Test # Metallic-11 (Test #13).

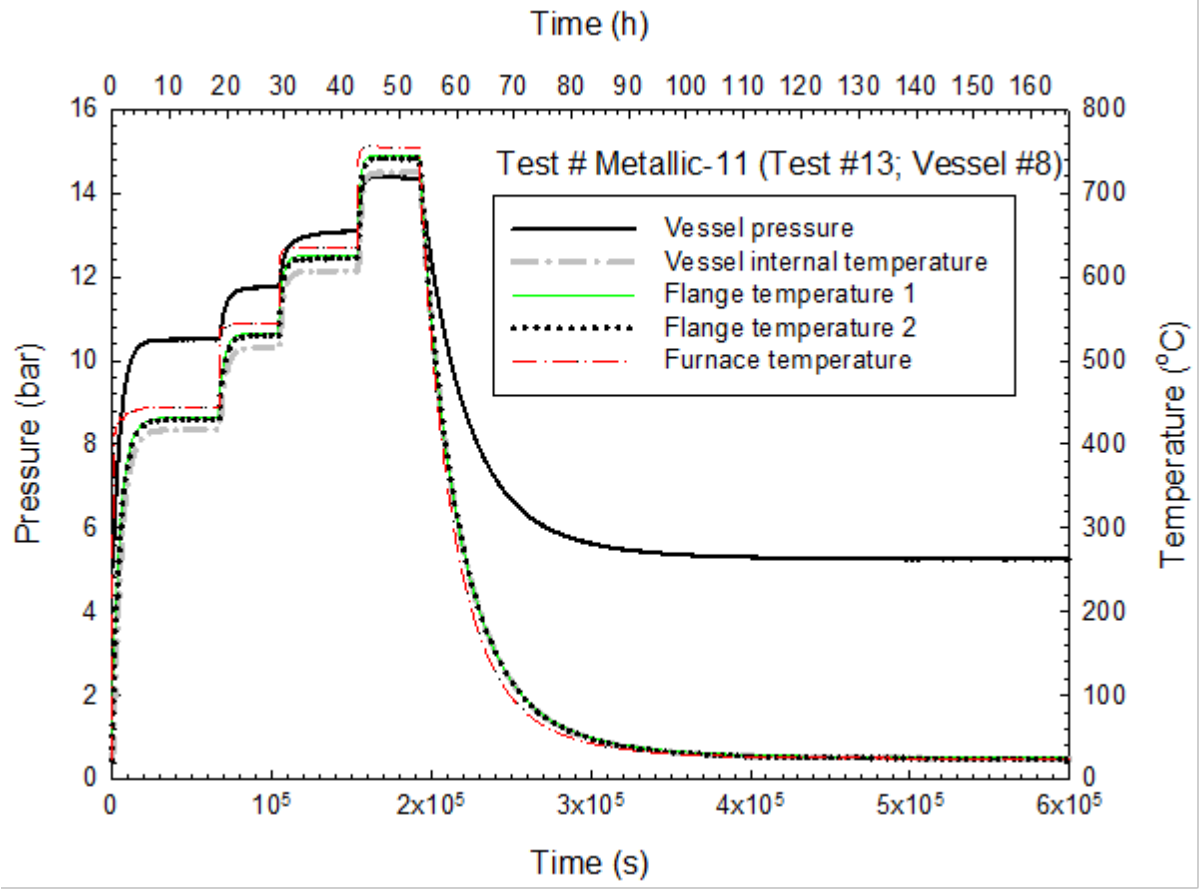

Figure 3-28. Temporal variations of vessel pressure and temperature in Test # Metallic-11 (Test #13) with time scale extended, including the complete cool-down phase.

3.1.1.12 Test # Metallic-12 (Test #14; Vessel #9)

In Test # Metallic-12 (Test #14), a new vessel with a metallic seal was used. The vessel was evacuated and charged with helium three times to prepare for the test. This test was a repeat of Tests # Metallic-2, Metallic-3, and Metallic-4. Figure 3-29 shows the first 50,000 s (≈ 14 h) of the pressure-time and temperature-time histories to illustrate the absence of a leak (constant pressure at constant temperature). The pressure-time and temperature-histories during the complete heating and cooling cycle is shown in Figure 3-30. However, similar to the observation in Test # Metallic-11, after the test vessel was cooled down to room temperature, the vessel pressure did not recover to its starting value (≈ 5 bar) but remained at a slightly higher constant value of ≈ 5.2 bar over a duration of more than 50 h. Again, this was not due to the drift of the pressure transducer because when the vessel content was released to the atmosphere, the pressure transducer gave an atmospheric pressure reading.

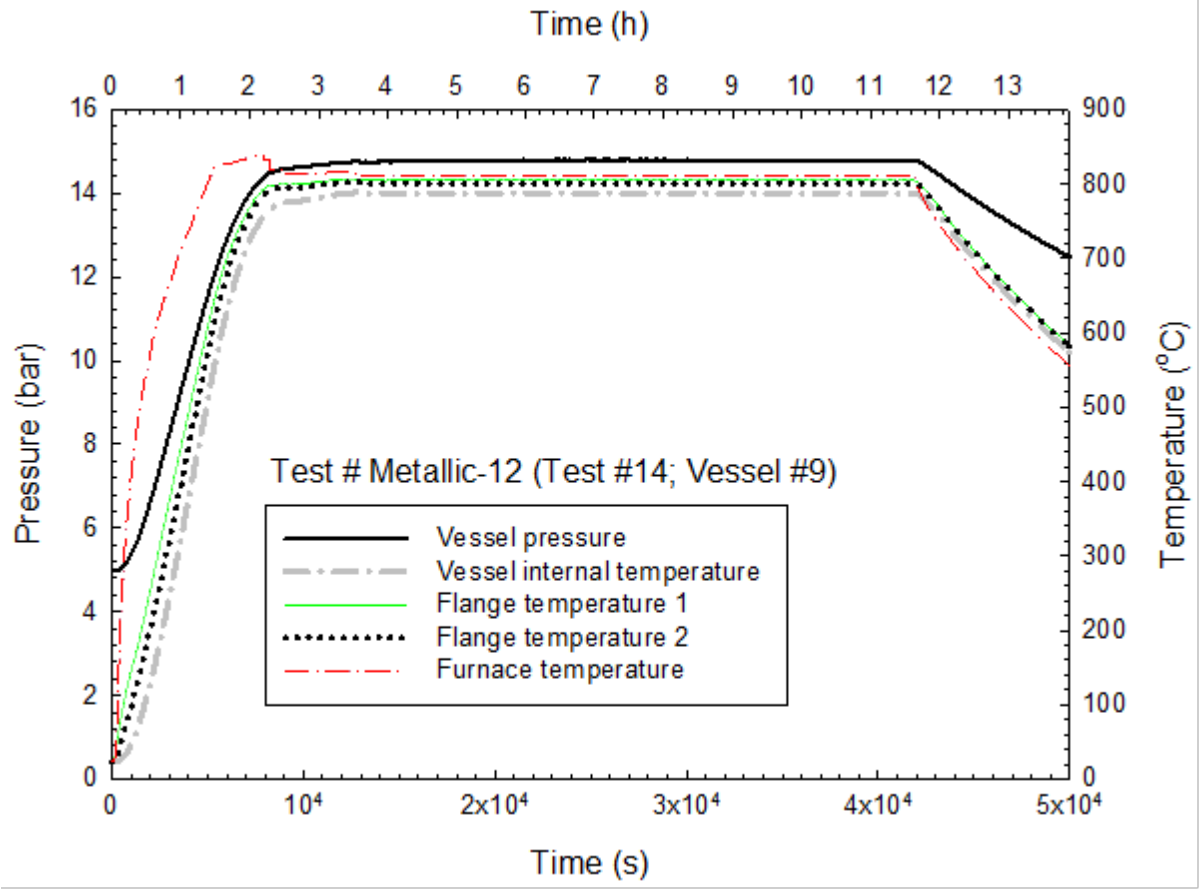

Figure 3-29. Temporal variations of vessel pressure and temperature in Test # Metallic-12 (Test #14).

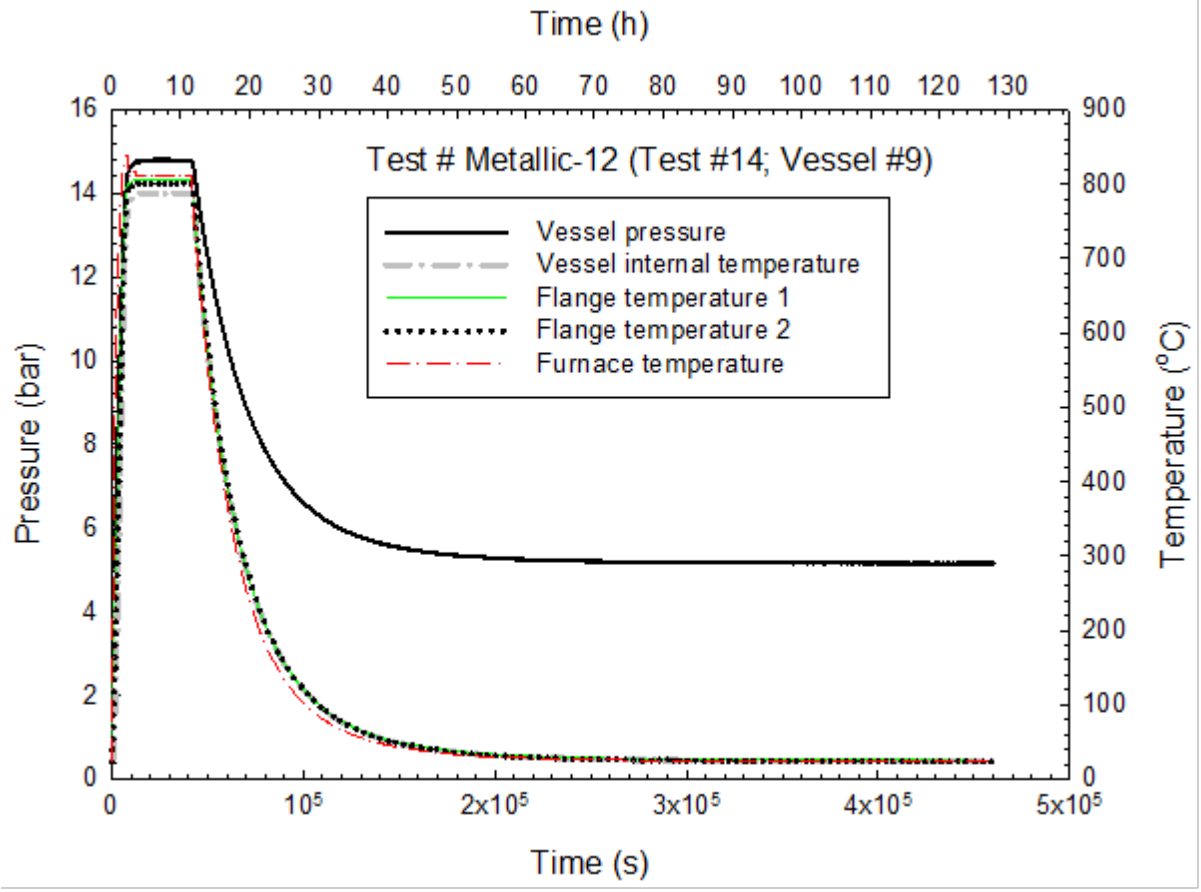

Figure 3-30. Temporal variations of vessel pressure and temperature in Test # Metallic-12 (Test #14) with time scale extended, including the complete cool-down phase.

3.1.2 EPDM O-Rings

3.1.2.1 Test # EDPM-a (Test #11; Vessel #3 Refurbished)

An EPDM O-ring (DBR Industries 2-228 E740-75, Lot # 2Q060080040952) with an outer diameter of 6.35 cm (2.5 in.) and a cross section of 0.32 cm (0.125 in.) and refurbished Vessel #3 were used in this test. Vessel #3 was refurbished by re-facing the flange to remove the O-ring groove originally machined for the metallic seal and re-machining a new O-ring groove for the EPDM O-ring which has different groove dimensions from its metallic counterpart.

Figure 3-31 and Figure 3-32 are the test results plotted using different time scales. The spikes (overshoots) in the furnace temperature measurements reflect the way the furnace temperature was intentionally ramped and manipulated to accelerate the incremental heating of the vessel to the set temperatures. During the first 1 h heating at 150 °C (302 °F), the vessel pressure remained constant. The subsequent 1 h heating at 200 °C (392 °F) and the following 1 h heating at 250 °C (482 °F) also indicated the maintenance of vessel pressure. The final heating at 300 °C (572 °F) for more than 20 h shows a slow decrease in pressure, albeit within the pressure measurement uncertainty. However, the vessel pressure was restored to its initial value after the thermal exposure test, as shown in Figure 3-32. Post-test inspection of the exposed vessel revealed that the O-ring was still pliable and could be easily removed from the

O-ring groove.

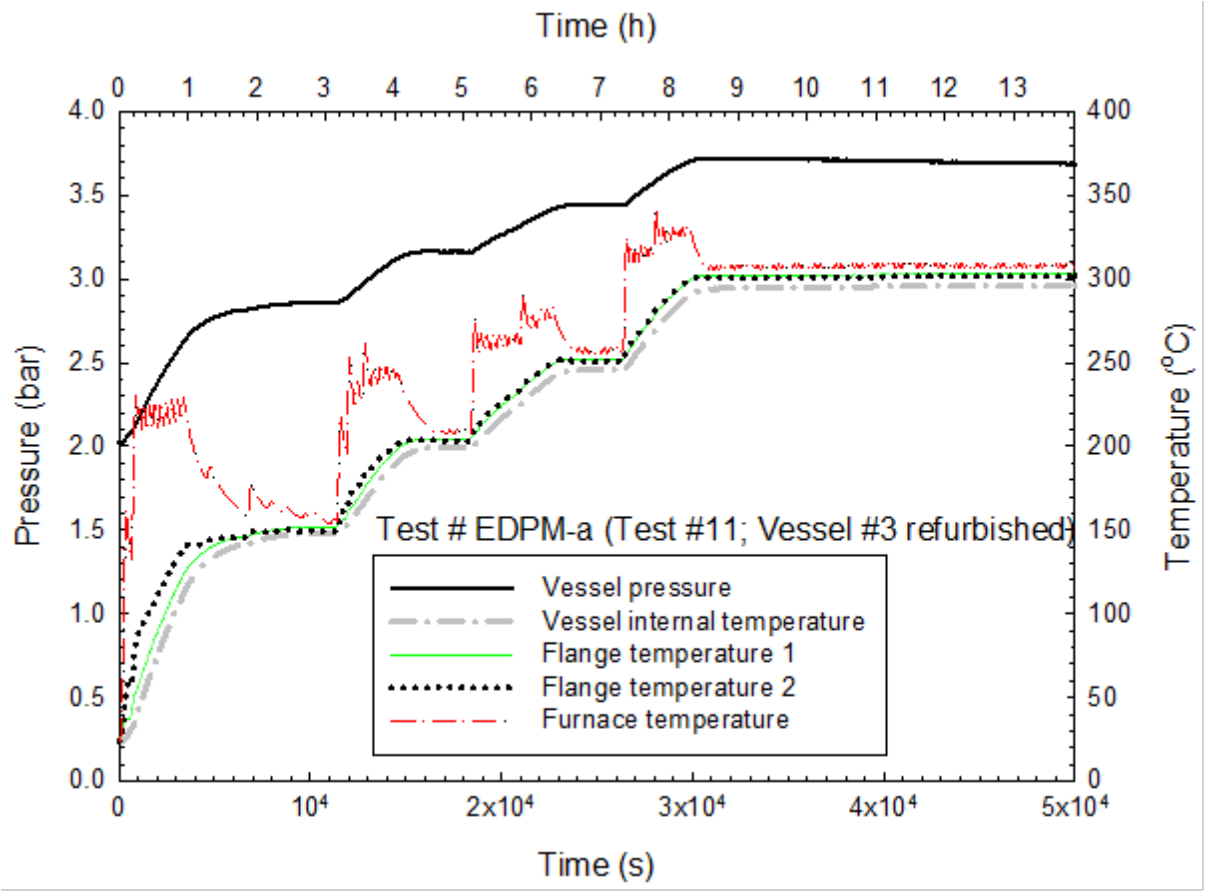

Figure 3-31. Temporal variations of vessel pressure and temperature in Test # EDPM-a (Test #11).

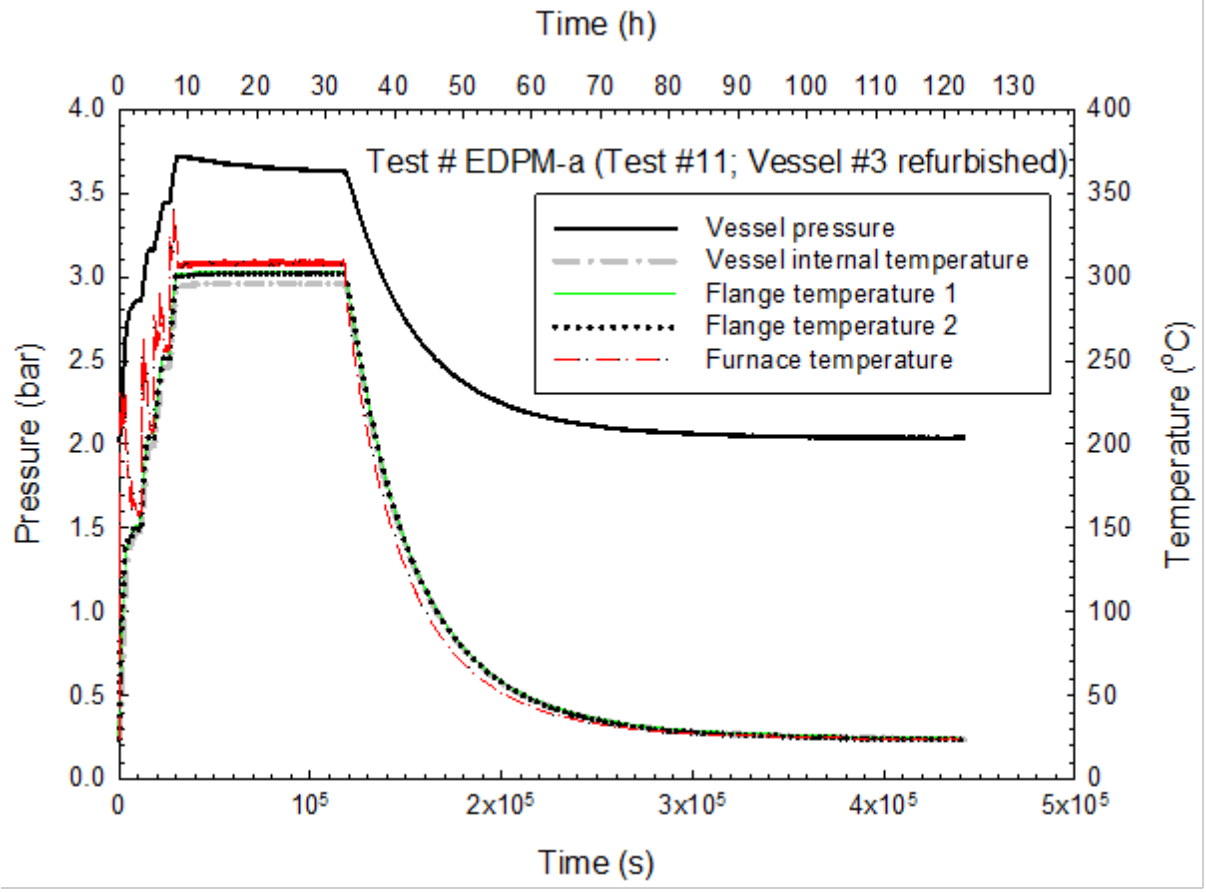

Figure 3-32. Temporal variations of vessel pressure and temperature in Test # EPDM-a (Test #11) with time scale extended, including the complete cool-down phase.

3.1.2.2 Test # EPDM-b (Test #15; Vessel #3 Refurbished)

In Test # EDPM-b (Test #15), an EPDM seal together with the refurbished Vessel #3 (used in Test # EDPM-a) was employed. The refurbishment simply involved cleaning of the O-ring groove and the cavity of the used vessel with ethanol. The vessel was evacuated and charged with helium three times to prepare for the test. The difference between this test and Test # EPDM-a was the temperature used for the thermal exposure test. Instead of 300 °C (572 °F) as used in Test # EPDM-a, a higher temperature, 450 °C (842 °F) was used.

Figure 3-33 shows the first 39 h of the pressure-time and temperature-time histories obtained from this test. The pressure and temperature histories for the complete heating and cooling cycle are given in Figure 3-34. The pressure trace in Figure 3-33 clearly indicates a leak occurred soon after the vessel had attained the nominal target temperature of 450 °C (842 °F). Figure 3-35 shows the calculated reference helium leakage rates over the 25 h isothermal heating period at 450 °C (842 °F) with a time-averaged reference leakage rate of 9.2×10^{-4} ref·cm^3/s.

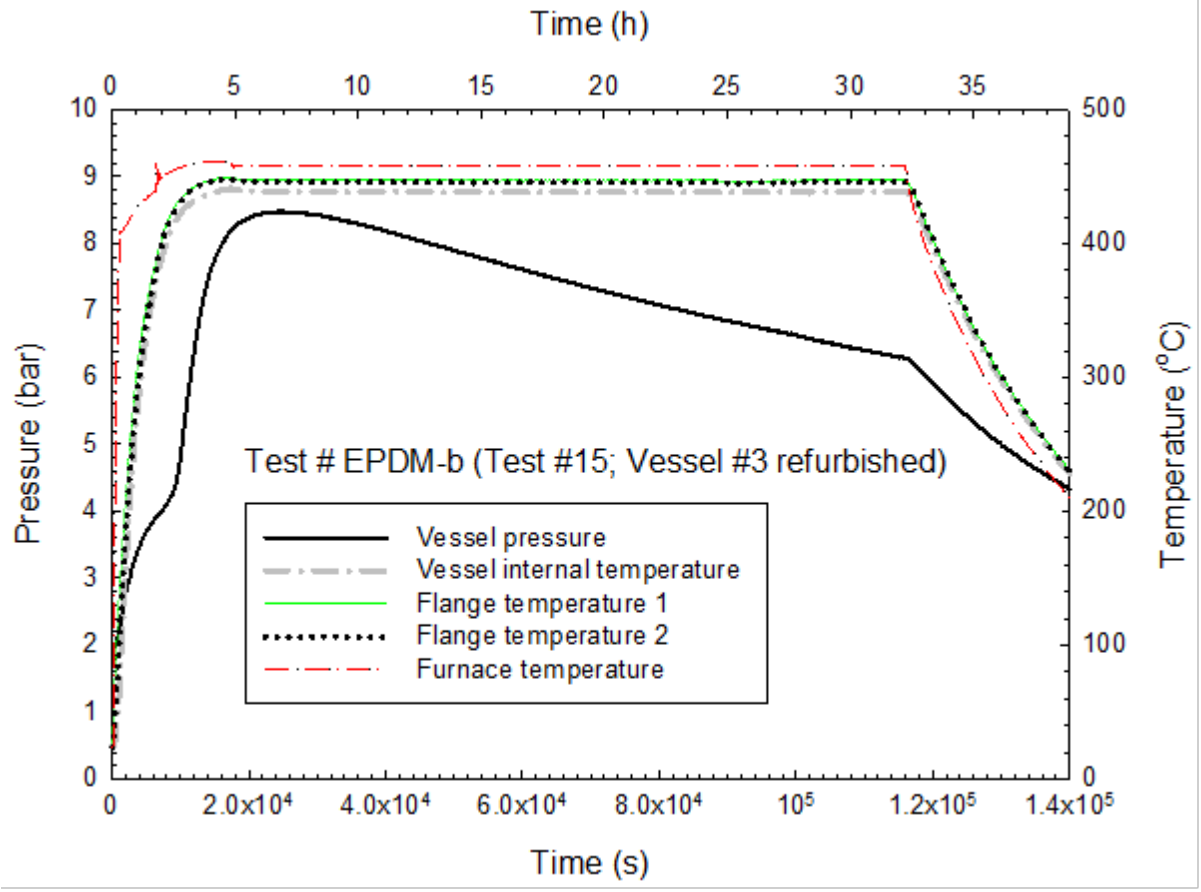

Figure 3-33. Temporal variations of vessel pressure and temperature in Test # EPDM-b (Test #15).

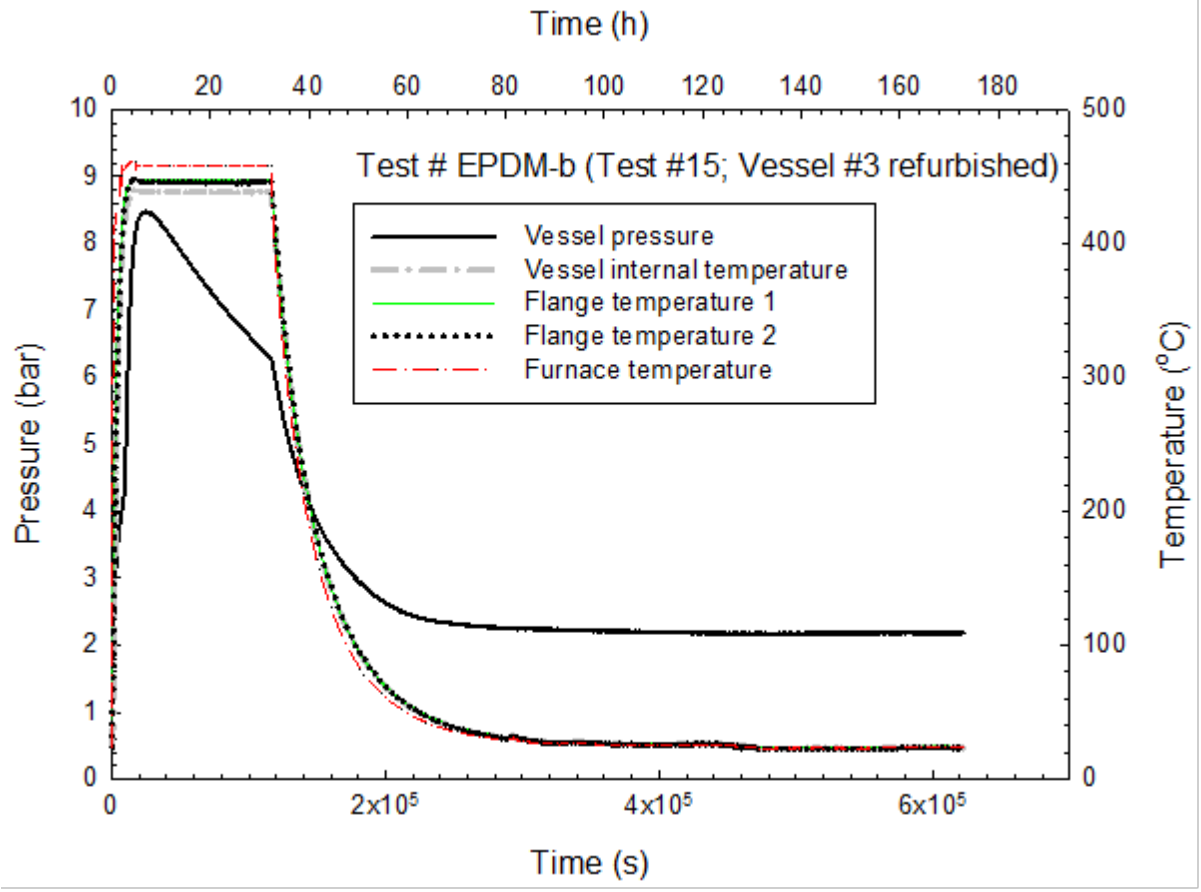

Figure 3-34. Temporal variations of vessel pressure and temperature in Test # EPDM-b (Test #15) with time scale extended, including the complete cool-down phase.

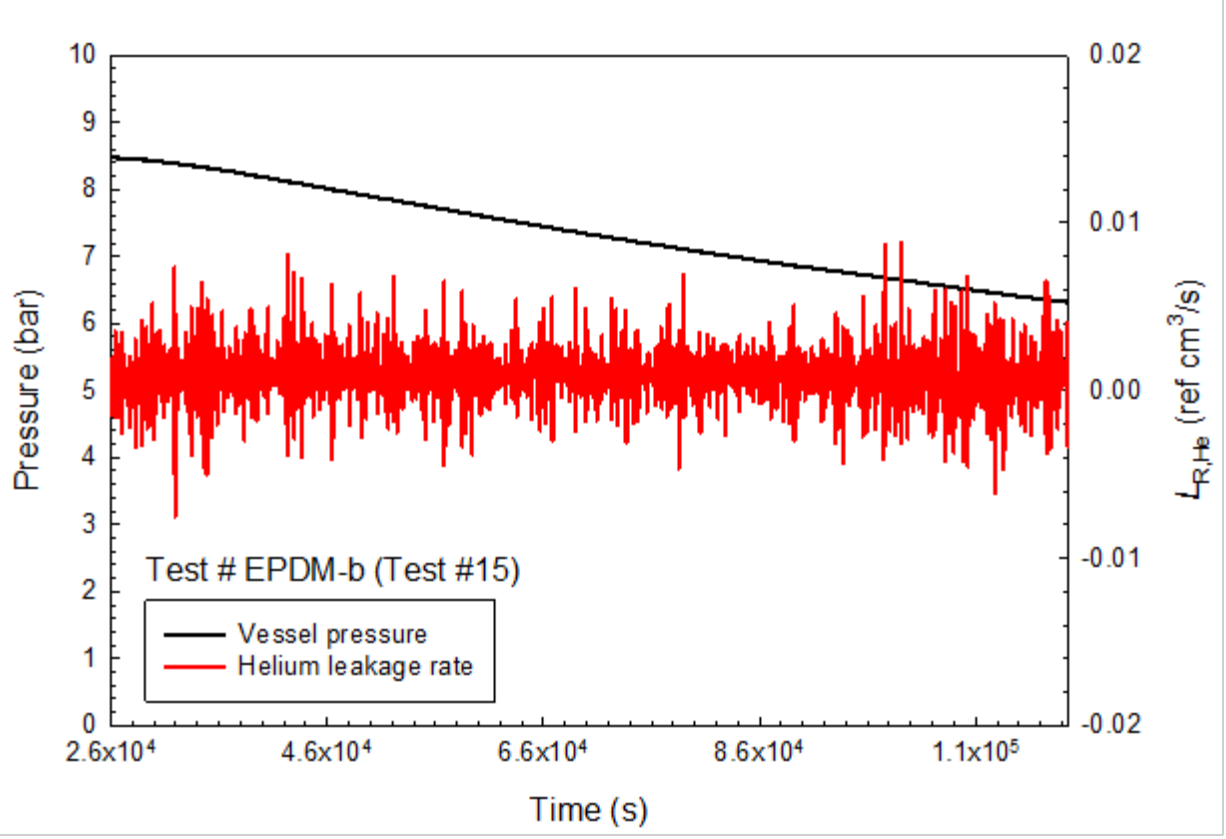

Figure 3-35. Isothermal reference helium leakage rate during the 25 h heating in Test # EPDM-b (Test #15).

From Figure 3-33 and Figure 3-34, a peculiarity is noted. The measured attainable pressure (≈ 8.5 bar) at 450 °C (842 °F) before the leak occurred is noticeably higher than the pressure calculated using the ideal gas law (≈ 4.9 bar), even assuming no thermal expansion of the vessel volume. The addition of vapor mass from the potential thermal decomposition and off-gas of the O-ring and the lubricant used at 450 °C (842 °F) is conjectured to be the cause for this unusually high pressure. Another abnormality is that after the vessel was cooled down to room temperature, the pressure never recovered to its original value (≈ 2 bar) but remained relatively constant at ≈ 2.16 bar over a duration of more than 100 h, implying the O-ring still possessed some residual sealing capability. A post-test inspection of the tested vessel revealed that the interior vessel wall and the thermocouple inserted into the vessel interior were coated with a thin layer of black substance. Although the O-ring was still properly seated in the groove (see Figure 3-36), it had turned into a packed layer of powdery charred material and could not be removed from the groove without destroying its structural integrity (see Figure 3-37). Additional tests would be needed to further examine this finding.

Figure 3-36. Photograph of the EPDM O-ring after thermal exposure.

Figure 3-37. Photograph showing the disintegration of the tested EPDM O-ring when an attempt was made to remove the O-ring from the groove.

3.1.3 PTFE O-Rings

3.1.3.1 Test # PTFE-a (Test #12; Vessel #3 Refurbished)

A PTFE O-ring (DBR Industries 228 PTFE, Lot #04/07 12730-1) with an outer diameter of 6.35 cm (2.5 in.) and a cross section of 0.32 cm (0.125 in.) and refurbished Vessel #3 were used for

this test. The refurbishment of the vessel simply consisted of cleaning of the O-ring groove previously used for the EPDM seal test (Test # EPDM-a). Figure 3-38 and Figure 3-39 show the results during the heating phase and the complete heating-cooling history respectively. During the 22 h heating at 300 °C (572 °F), there was a slight drop in vessel pressure at the end of the isothermal heating phase; however, the pressure decrease was within the measurement uncertainty of the pressure transducer. Figure 3-40, which shows the calculated reference helium leakage rates during the 22 h heating period, indicates a time-averaged reference leakage rate of 4.5×10^{-5} ref·cm^3/s. The fluctuation in the leakage rate data was due to the taking of numerical time derivatives of the unsmoothed pressure-time data. As indicated in the pressure trace, leakage was observed in this test during the cooling phase. The original pressure (≈ 2 bar) did not recover, and the vessel pressure dropped below the original pressure at room temperature. Post-test inspection of the exposed vessel revealed that the compressed O-ring was still intact and could be easily removed from the O-ring groove.

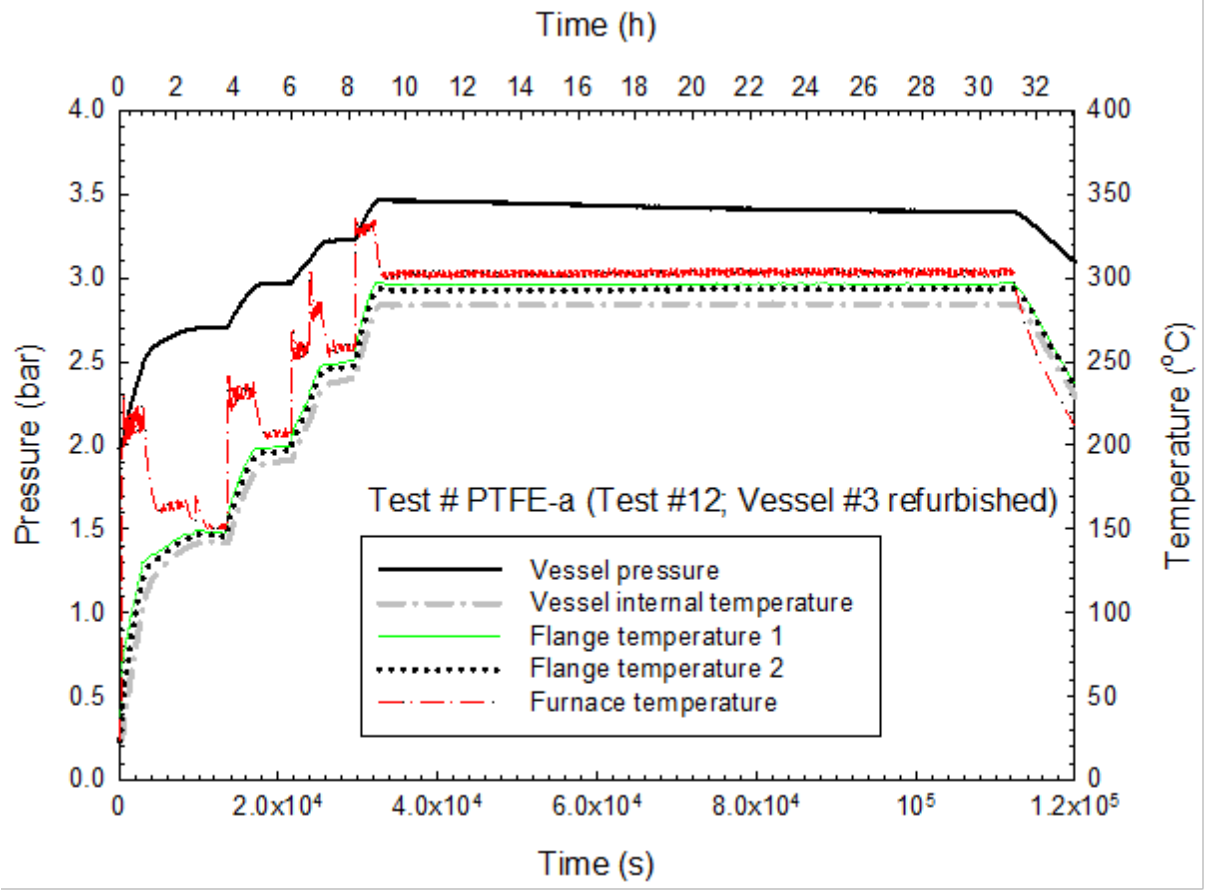

Figure 3-38. Temporal variations of vessel pressure and temperature in Test # PTFE-a (Test #12).

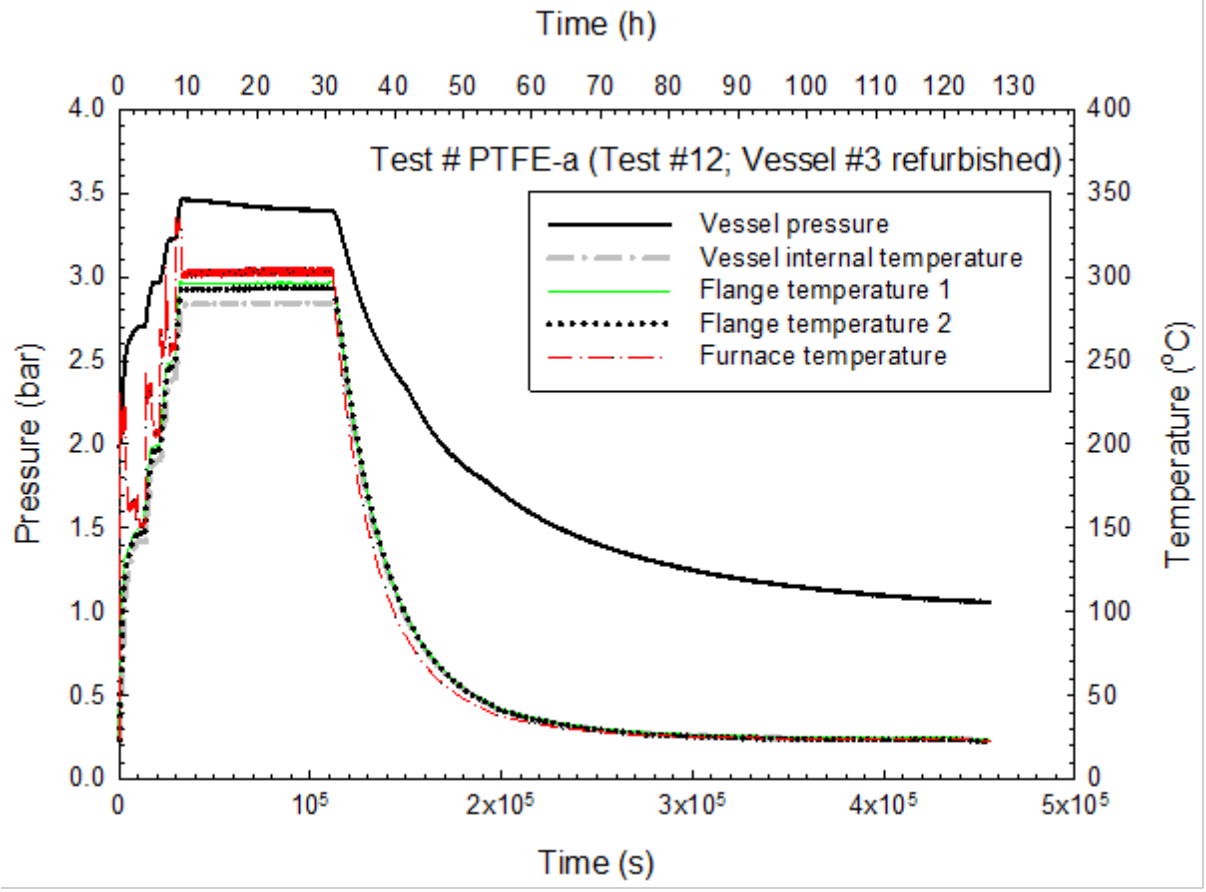

Figure 3-39. Temporal variations of vessel pressure and temperature in Test # PTFE-a (Test #12) with time scale extended, including the complete cool-down phase.

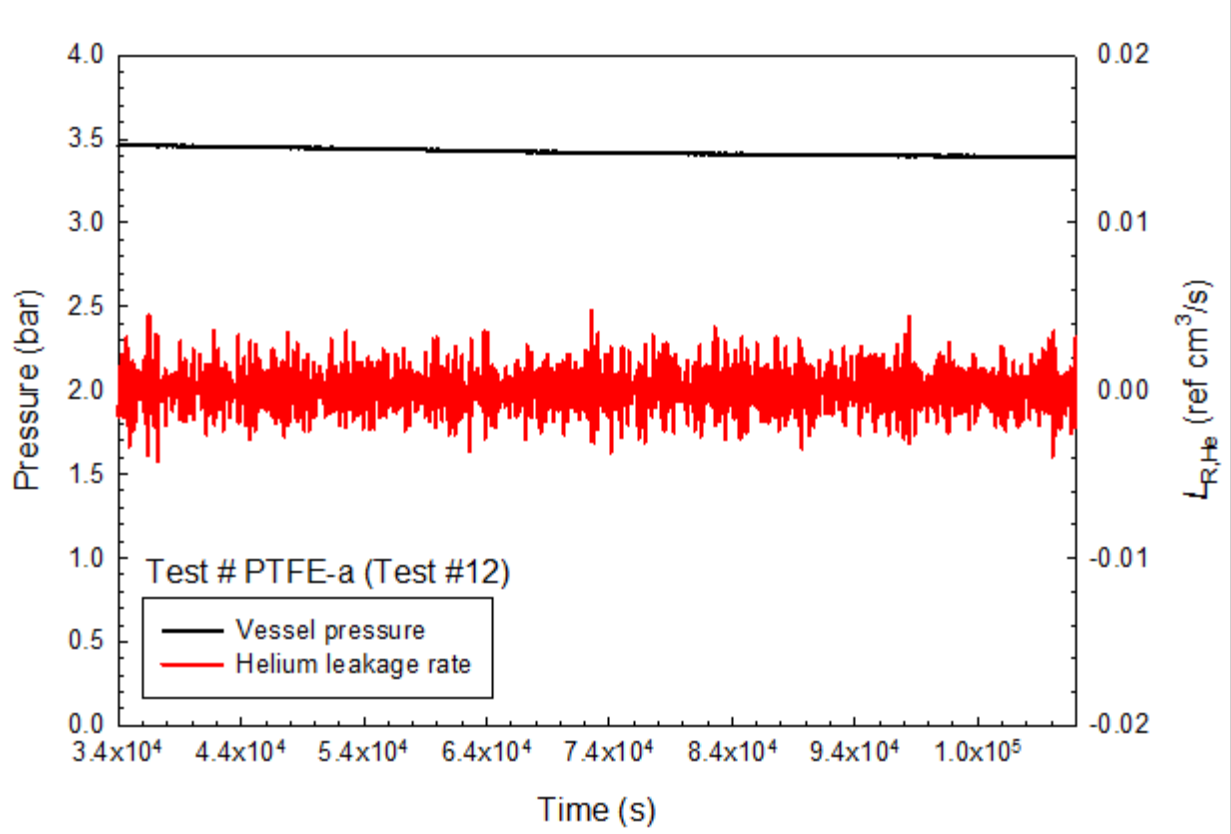

Figure 3-40. Isothermal reference helium leakage rate during the 22 h heating in Test # PTFE-a (Test #12).

3.2 Phase II

3.2.1 EPDM O-Rings

Figure 3-41, Figure 3-42, Figure 3-43, Figure 3-44, Figure 3-45, and Figure 3-46 show the vessel pressure and temperature measurements obtained in Tests # EPDM-1, EPDM-2, EPDM-3, EPDM-4, EPDM-5, and EPDM-6 respectively. Tests # EPDM-1, EPDM-2, EPDM-3, and EPDM-4 were conducted at 316 °C for 9 h, whereas Tests # EPDM-5 and EPDM-6 were performed at 900 °C for 9 h.

In Test # EPDM-1 (Figure 3-41), the vessel pressure decreased by about 0.1 bar over the 8-h test period; however, the corresponding decrease of the vessel internal temperature by 10 °C over the same period was commensurate to a drop in pressure close to 0.1 bar and could easily contribute to this pressure decrease. The temperature fluctuation in this test, first in the leak-rate measurement test series, was the result of constantly adjusting the furnace set-point in an attempt to shorten the vessel heat-up time to reach the test temperature. Therefore, the slight decrease in pressure in this particular test should not be construed as a leak but rather as a result from temperature variation. In Test # EPDM-2 (Figure 3-42), Test # EPDM-3 (Figure 3-43), and Test # EPDM-4 (Figure 3-44), the vessel pressure remained constant during the 8-h test period, and the initial charged pressure was recovered after cool-down, indicating no leak had occurred. Leaks were observed in Tests # EPDM-5 and EPDM-6 before the test temperature was reached in both tests (see Figure 3-45, and Figure 3-46). Since leak occurred during the heat-up period, the isothermal leakage rates could not be estimated.

Post-test inspections of the disassembled test vessels revealed that the EPDM O-rings were thermally degraded due to prolong thermal exposure in all six tests (see Figure 3-47). In Tests # EPDM-1, EPDM-2, EPDM-3, and EPDM-4, when the tested vessel was removed from the furnace, what appeared to be thermally degraded O-ring material was found seeping out from a location of the two-flange interface. The location was where the vessel made contact with and rested on the base of the furnace and was always aligned with the direction of the gravity vector. The location was also marked by a stain on the flange from the O-ring material, which is clearly shown in Figure 3-47. Note that the locations where the seeping of the O-ring material occurred appeared to be different in all four photographs in Figure 3-47 because the disassembled flange was not oriented and placed in the original test position in the furnace when the photographs were taken. The flange with an opening and without an O-ring groove shown only in Test # EPDM-3 in Figure 3-47 was not the vessel cap flange (as shown in the other three photographs) but rather the flange of the vessel body. The O-ring was removed from its groove in the vessel cap flange and adhered to the boss of this flange during the disassembling of the vessel. In Tests # EPDM-5 and EPDM-6, a thin layer of material was found adhered to the vessel interior wall (see Figure 3-48). Similar observations were made in double EPDM-EPDM O-ring tests in Phase III (see Section 3.3.3) although the extent of the layer thickness/area differed in both cases.

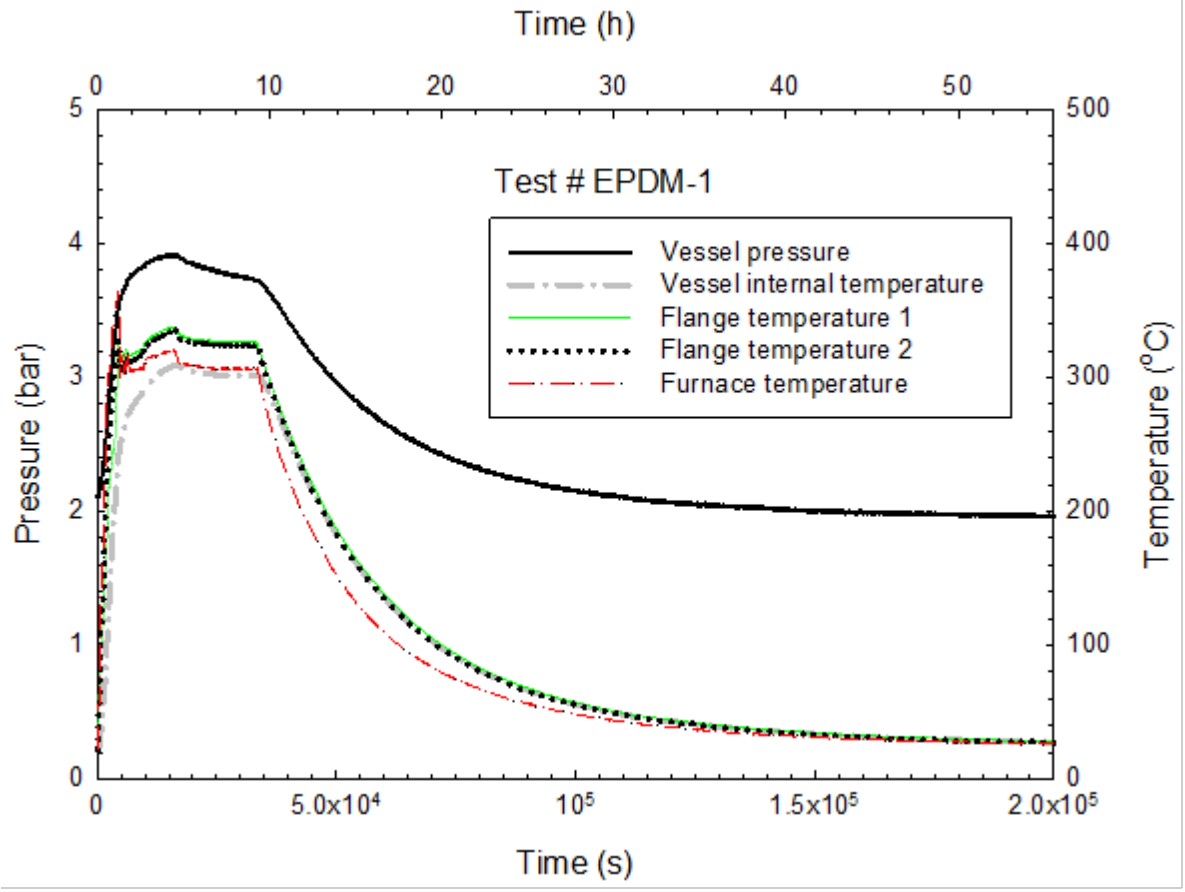

Figure 3-41. Temporal variations of vessel pressure and temperatures in Test # EPDM-1.

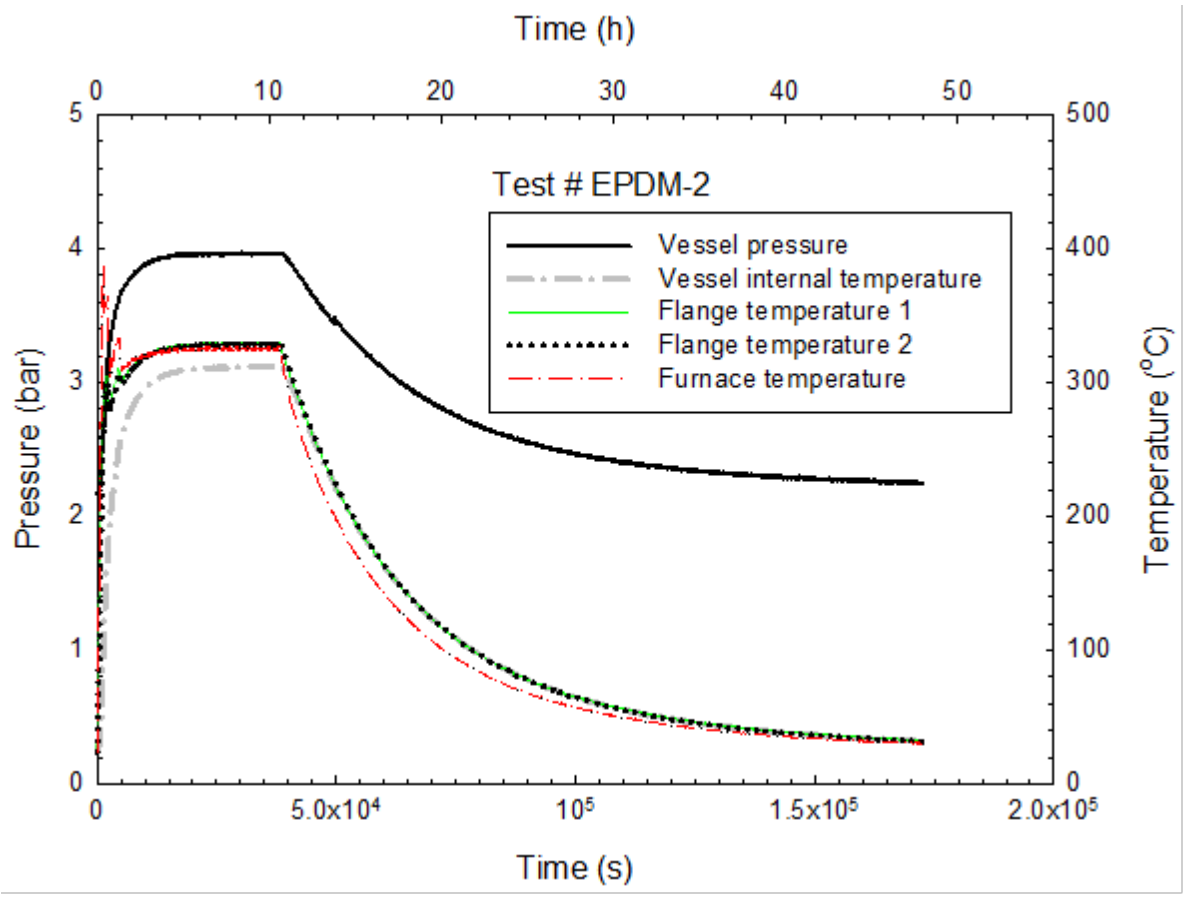

Figure 3-42. Temporal variations of vessel pressure and temperatures in Test # EPDM-2.

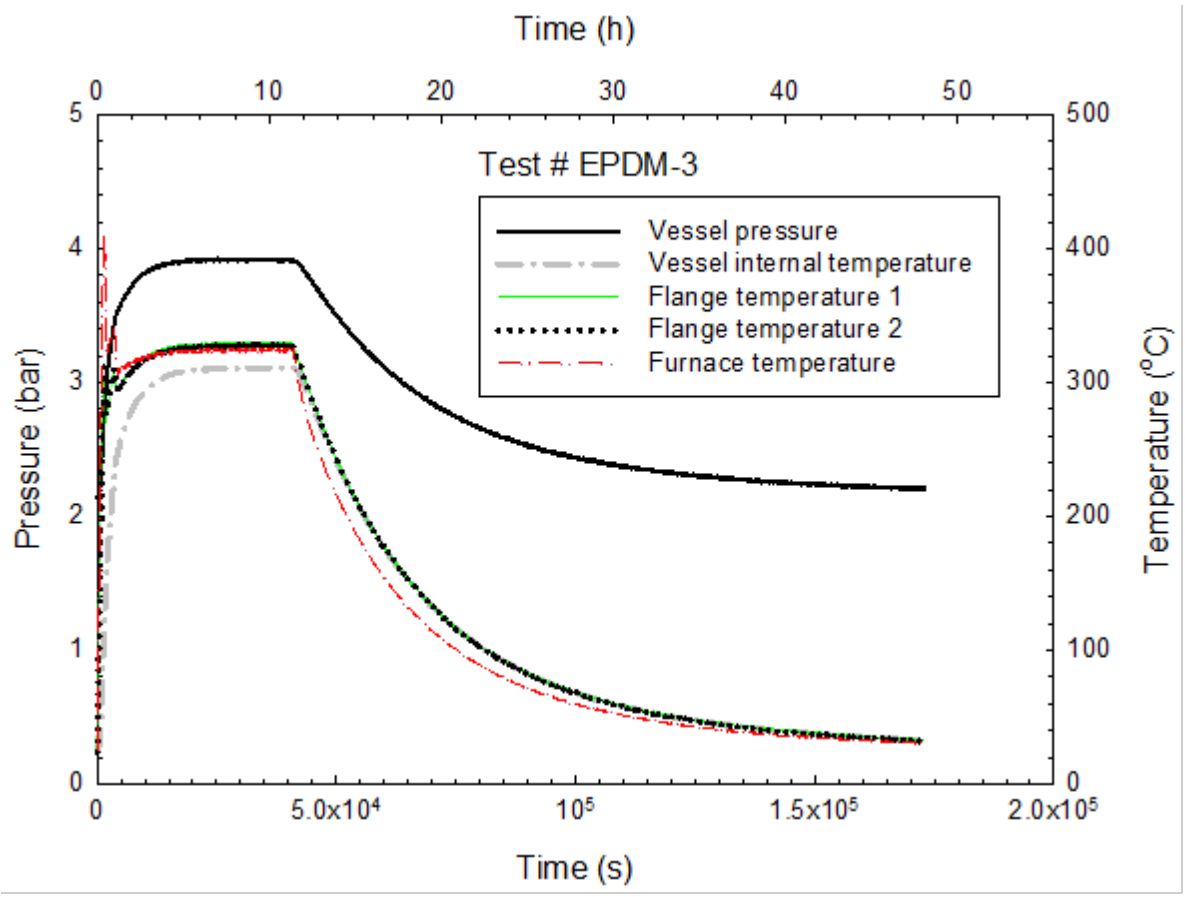

Figure 3-43. Temporal variations of vessel pressure and temperatures in Test # EPDM-3.

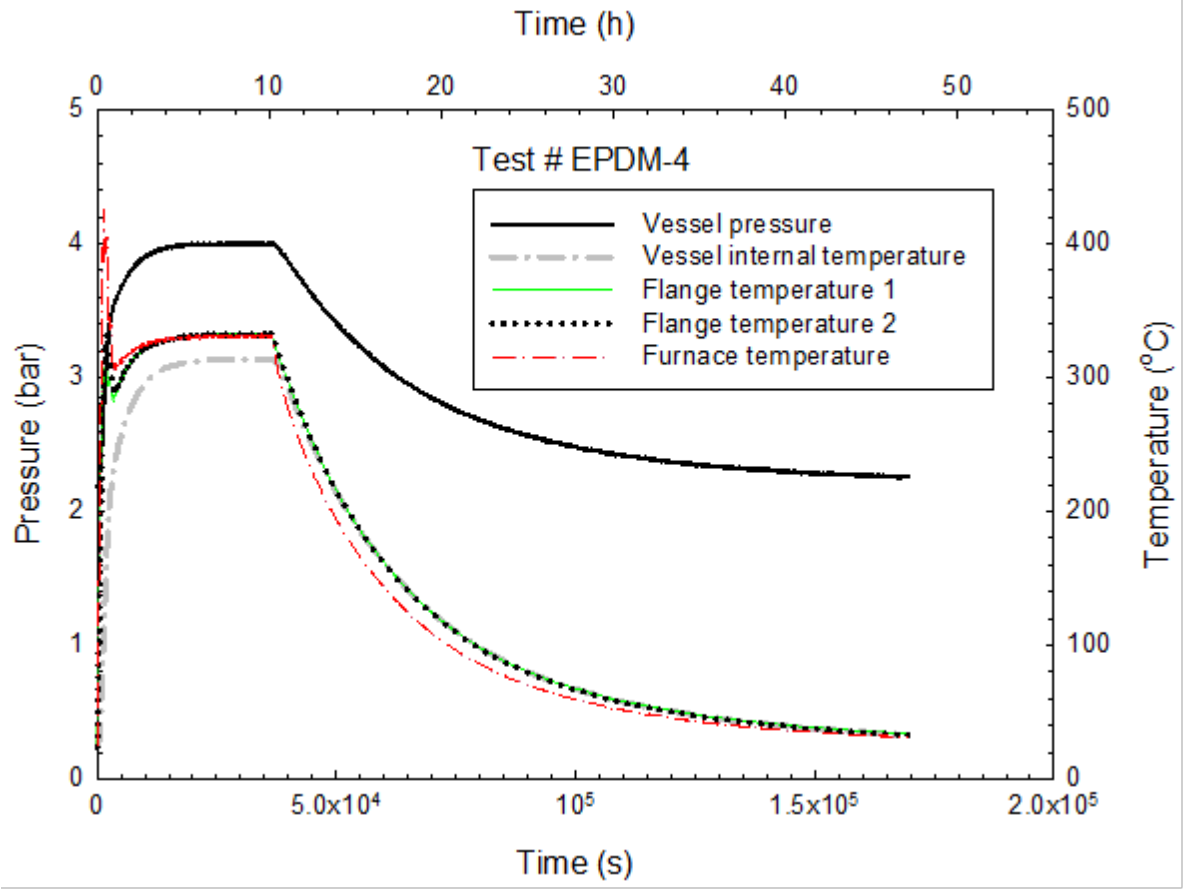

Figure 3-44. Temporal variations of vessel pressure and temperatures in Test # EPDM-4.

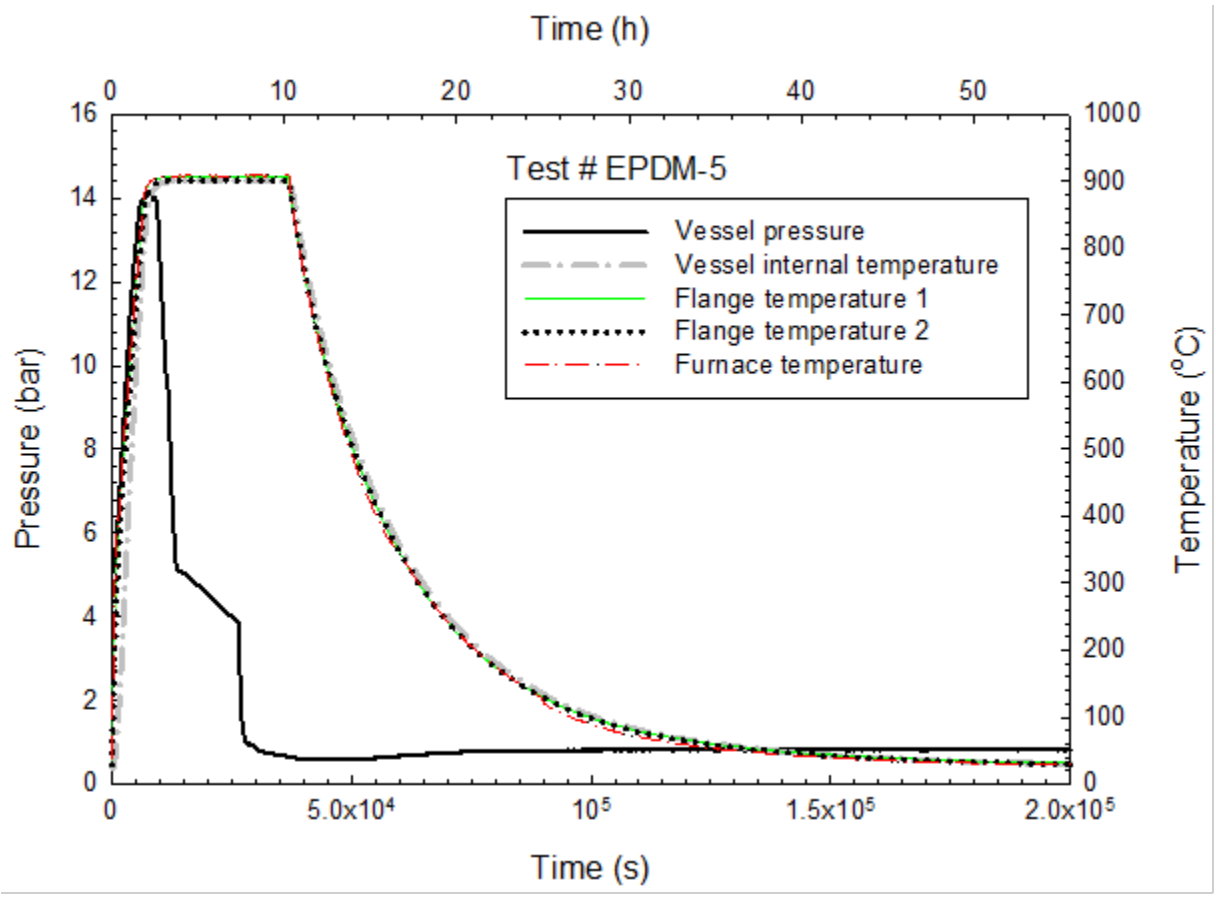

Figure 3-45. Temporal variations of vessel pressure and temperatures in Test # EPDM-5.

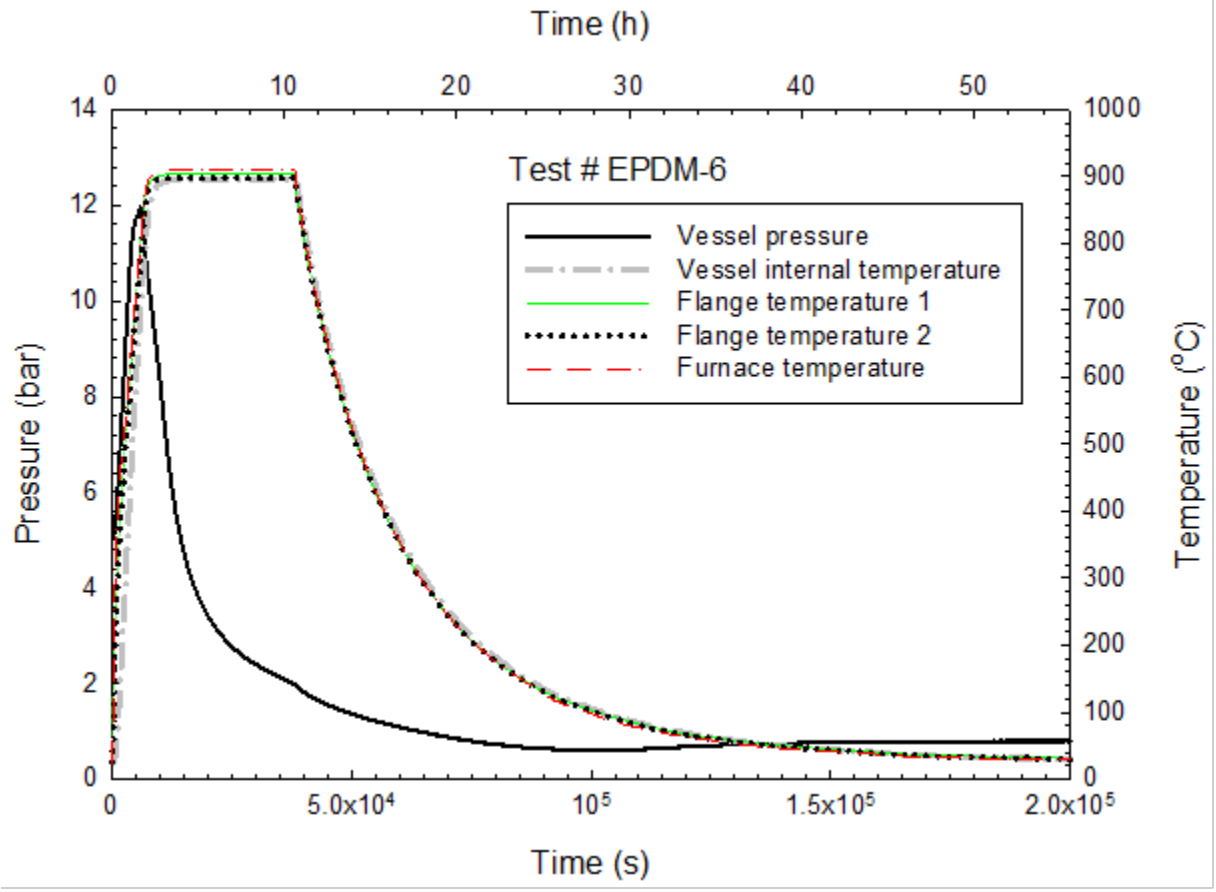

Figure 3-46. Temporal variations of vessel pressure and temperatures in Test # EPDM-6.

Figure 3-47. Photographs showing the thermally degraded EPDM O-ring after 8-h thermal exposure at 316 °C (600 °F) from the four EPDM O-ring tests (Tests # EPDM-1, EPDM-2, EPDM-3, and EPDM-4). Tests # EPDM-5 and # EPDM-6 were conducted at 900 °C for 9 h.

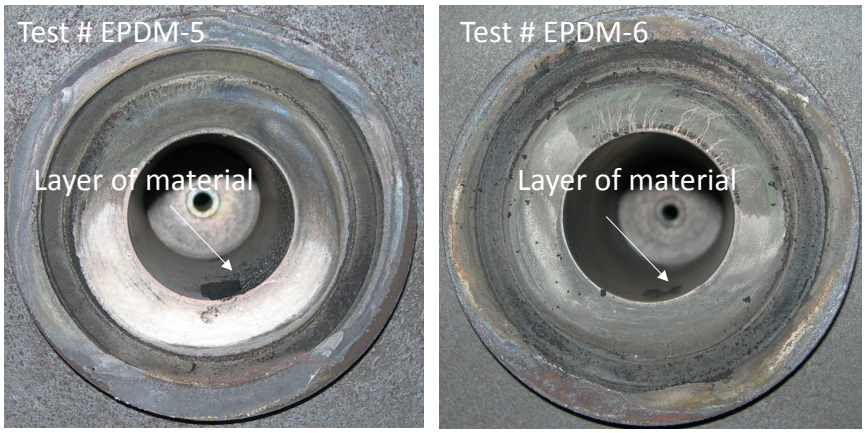

Figure 3-48. Photographs showing the vessel interiors after 9 h thermal exposure at 900 °C from Tests # EPDM-5 and EPDM-6.

3.2.2 Silicone O-Rings

Figure 3-49, Figure 3-51, Figure 3-52, and Figure 3-53 show the temporal variations of the vessel internal pressure and temperature, two flange temperatures and furnace temperature for the four silicone O-ring tests, Test # Silicone-1, Test # Silicone-2, Test # Silicone-3, and Test #

Silicone-4, respectively.

In Test # Silicone-1 (Figure 3-49), the vessel internal pressure started to drop after about 2 h into the test. At the end of the test period (8 h), the pressure had decreased by approximately 0.5 bar. The drop in vessel pressure during the test period and the subsequent further reduction of the vessel pressure to ambient pressure (~ 1 bar) and the inability to regain the initial charged pressure during the cool-down phase were indicative of a leak. Figure 3-50 shows the calculated reference helium leakage rate, and a time-averaged reference leakage rate of 2.4×10^{-3} ref cm^3/s was obtained over the time interval from 25,000 s to 37,000 s.

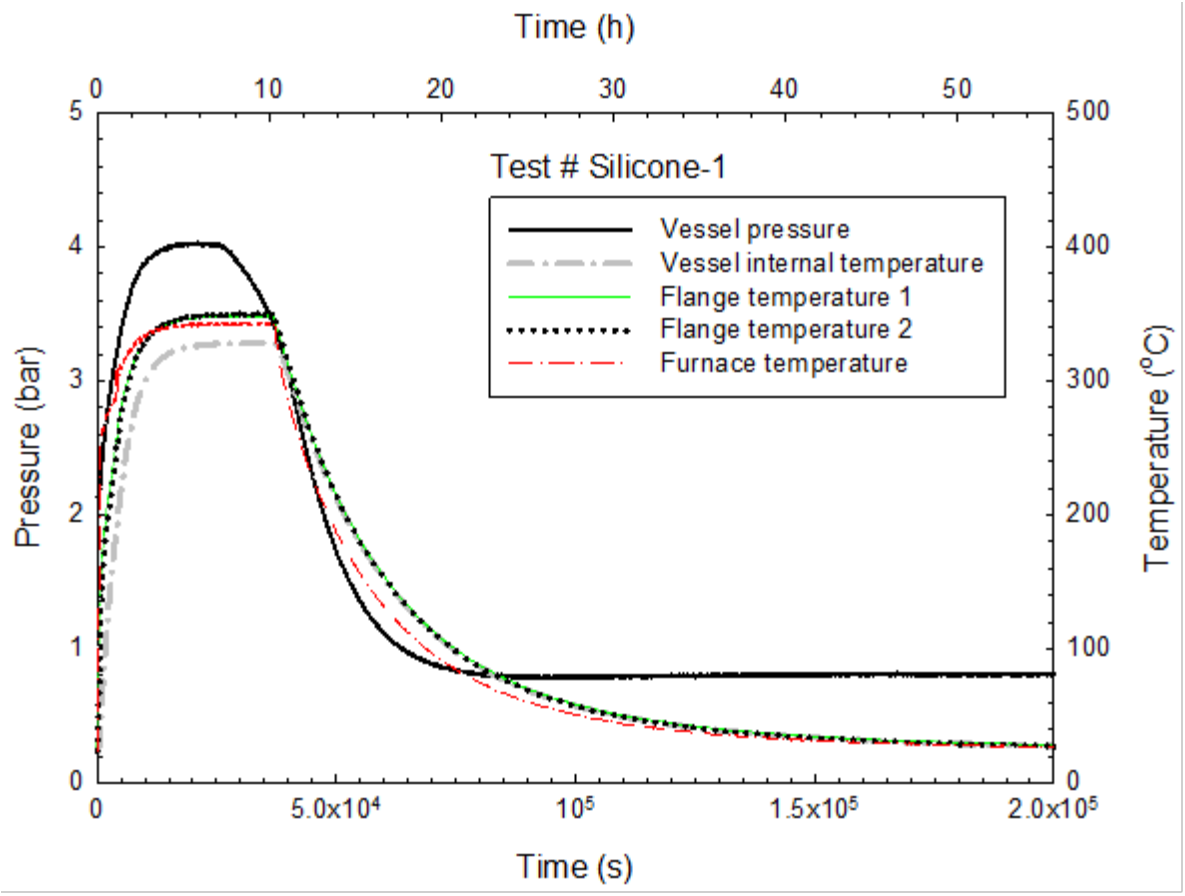

Figure 3-49. Temporal variations of vessel pressure and temperatures in Test # Silicone-1.

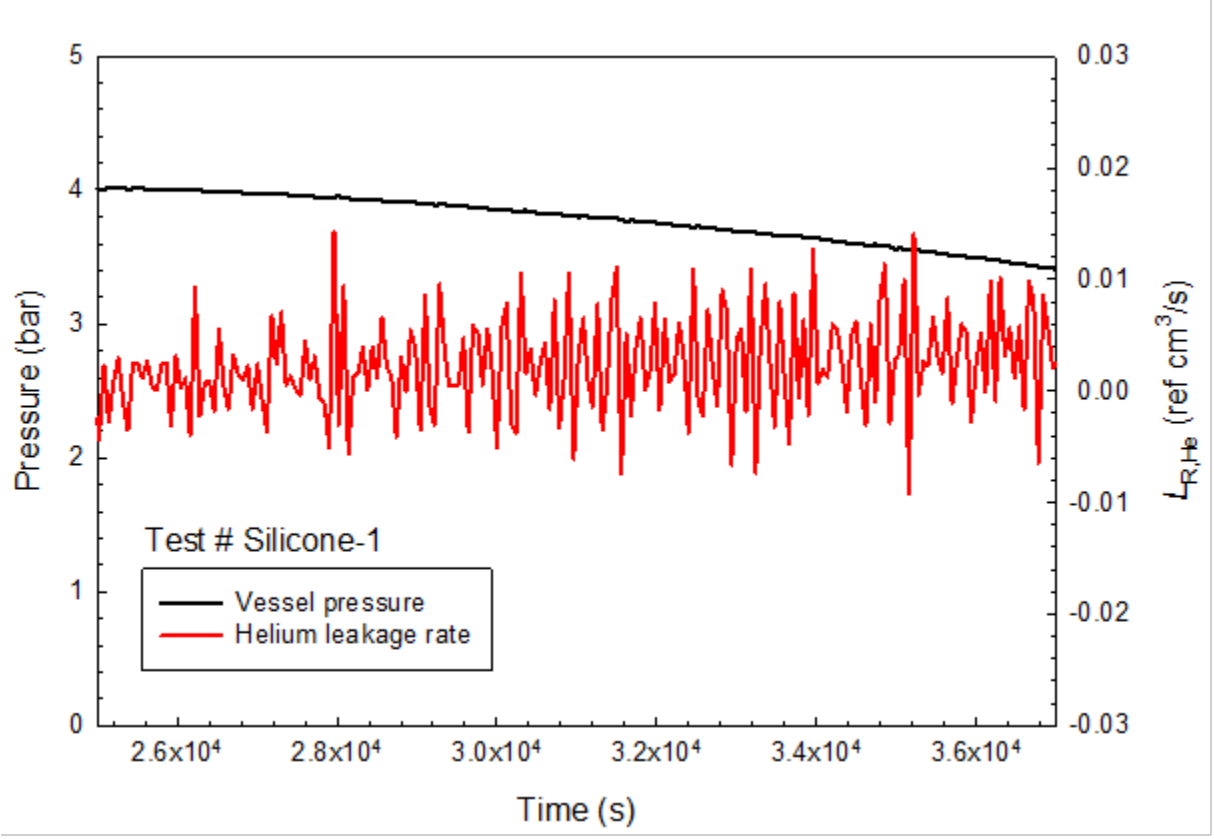

Figure 3-50. Calculated isothermal reference helium leakage rate in Test # Silicone-1.

In Test # Silicone-2[15] (Figure 3-51) and Test # Silicone-3 (Figure 3-52), the vessel pressure decreased by less than 0.1 bar, which was within the measurement uncertainty of the pressure transducer, over the 8-h test period. However, the initial charged pressure was recovered after the cool-down phase. The occurrence of a leak was proved to be inconclusive in these two tests.

In Test # Silicone-4 (Figure 3-53), the vessel pressure remained unchanged during the 8-h test period, and the initial charged pressure was also regained after the cool-down phase. Based on these observations, the absence of a leak was concluded.

Post-test inspections of the disassembled test vessel revealed that the silicone O-rings were thermally degraded due to prolong thermal exposure in all four tests (see Figure 3-54). When the tested vessel was removed from the furnace, a globule of O-ring material was observed to ooze out from a location of the two-flange interface. Similar to the EPDM O-ring tests, the location was where the vessel made contact with and rested on the base of the furnace and was always aligned with the direction of the gravity vector. As explained in Section 3.2.1, the locations where the seeping of the O-ring material occurred were different in all four photographs in Figure 3-54 as the result of how the disassembled flange was placed when the

[15] The DAQ was inadvertently turned off during the first hour of the heat-up period, and the data was not logged. The time zero in the figure was the time when the DAQ was switched back on. The data collected over the 8-h test period were never affected.

photographs were taken. The flange with an opening and without an O-ring groove shown only in Test # Silicone-1 in Figure 3-54 was the result of the O-ring adhering to the boss of the opposite flange of the vessel body during disassembly of the vessel. In addition, the degree of thermal damage to the O-rings, as shown in the figure, might not completely represent the actual *in situ* damage condition because the already thermally degraded O-ring could potentially be further damaged when the vessel cap and body were pulled apart during disassembly of the vessel for post-test inspection.

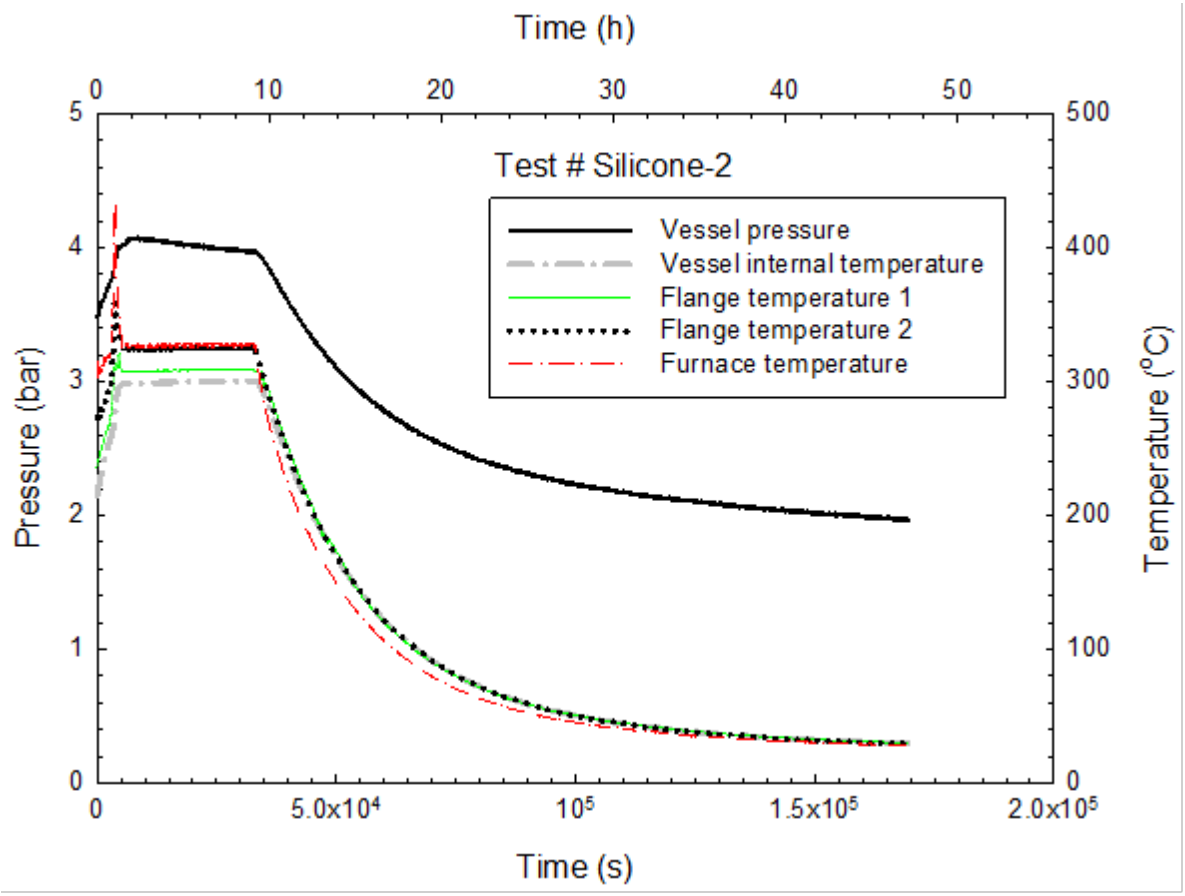

Figure 3-51. Temporal variations of vessel pressure and temperatures in Test # Silicone-2.

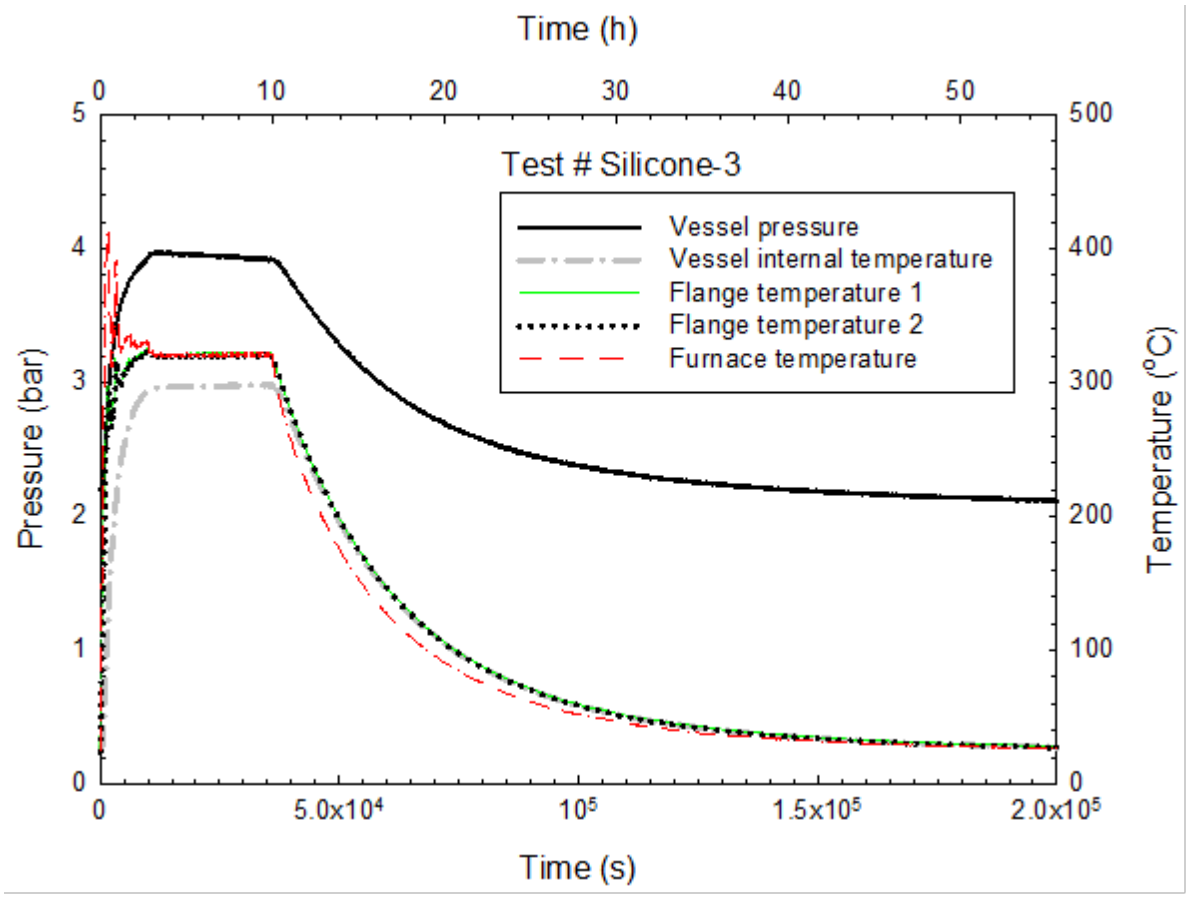

Figure 3-52. Temporal variations of vessel pressure and temperatures in Test # Silicone-3.

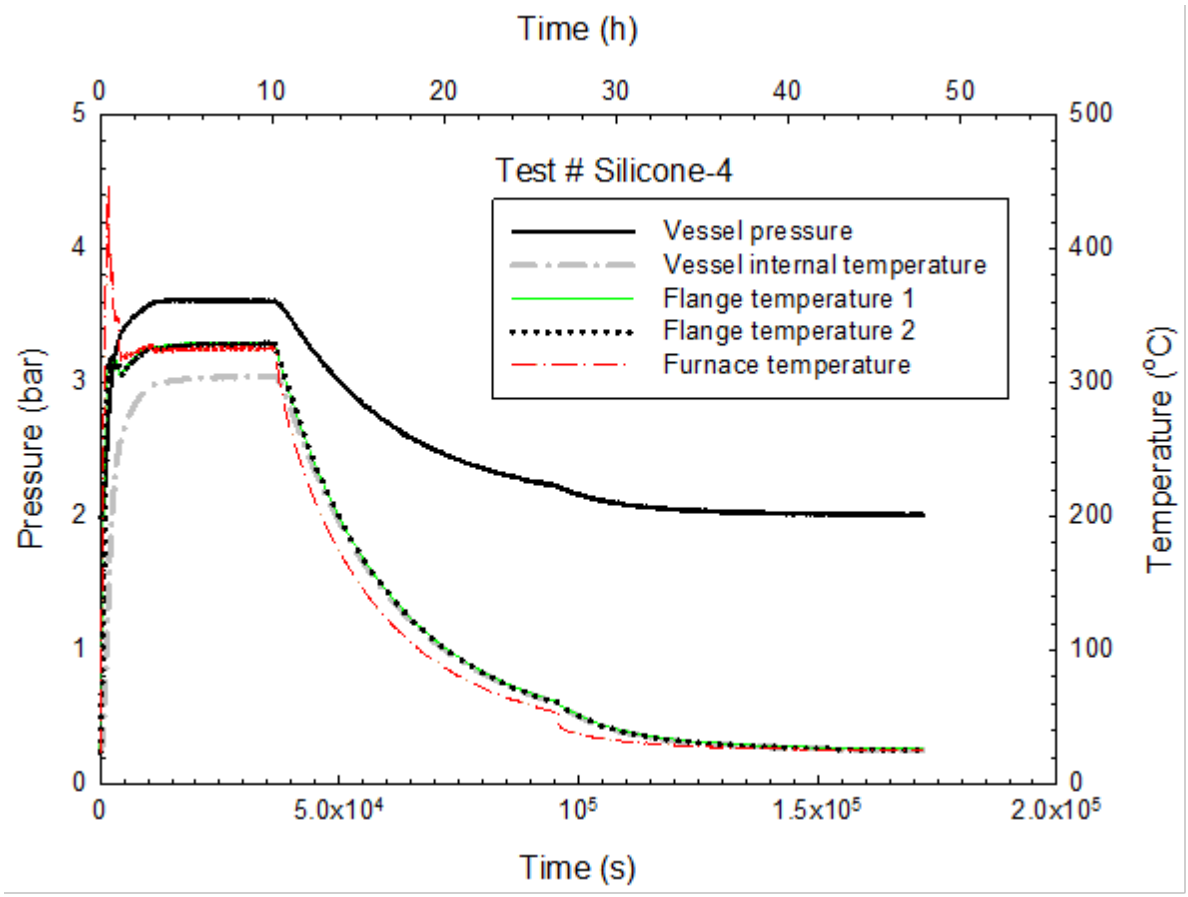

Figure 3-53. Temporal variations of vessel pressure and temperatures in Test # Silicone-4.

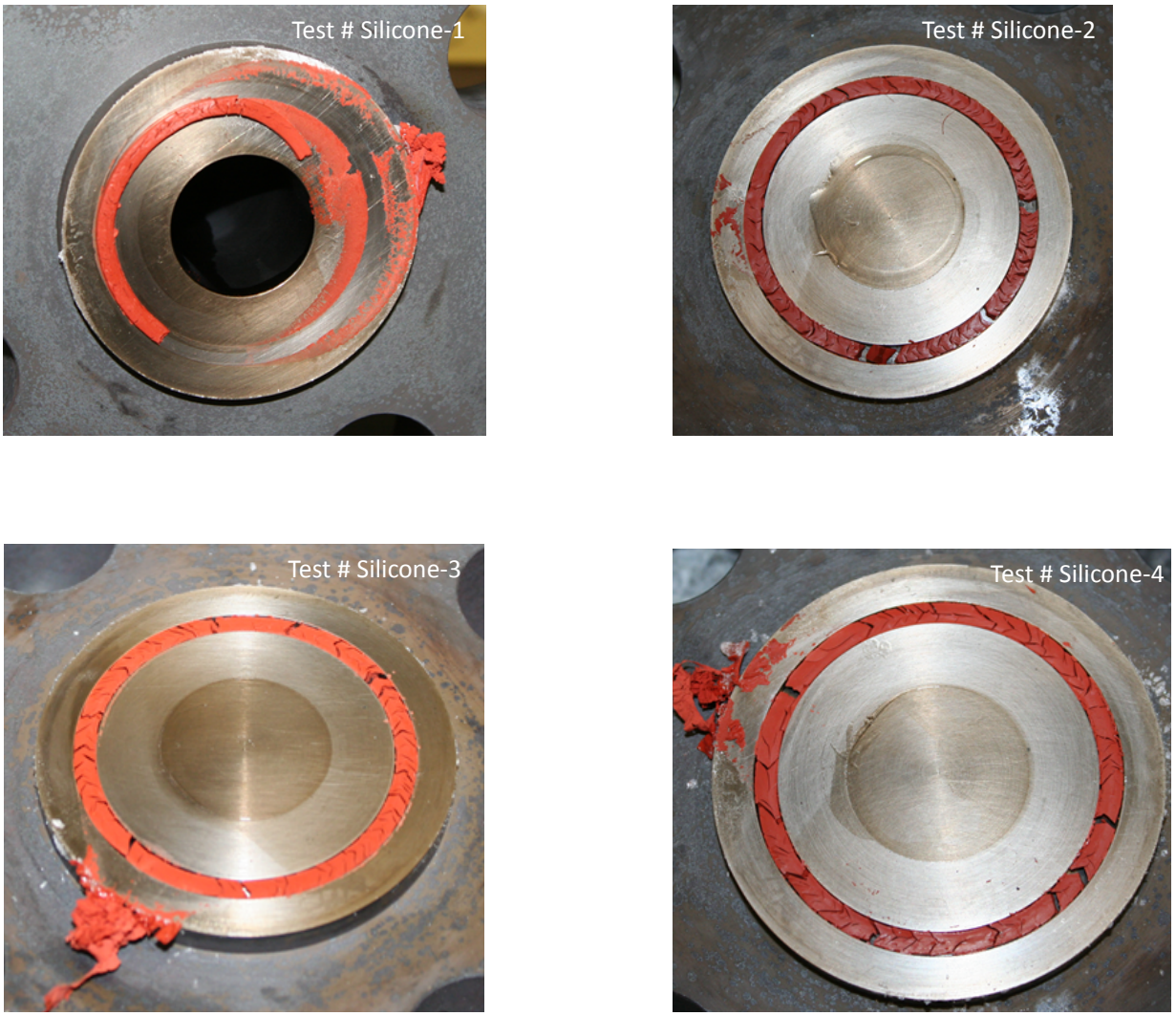

Figure 3-54. Photographs showing the thermally degraded silicone O-ring after 8-h thermal exposure at 316 °C (600 °F) for the four silicone O-ring tests.

3.2.3 Butyl O-Rings

Figure 3-55, Figure 3-56, and Figure 3-57 show the temporal variations of the vessel internal pressure and temperature, two flange temperatures and furnace temperature for the three Butyl O-ring tests, Test # Butyl-1, Test # Butyl-2, and Test # Butyl-3, respectively. The variation in pressure within the measurement uncertainty and no loss in pre-test vessel pressure after cool-down indicate the absence of a leak in these three tests.

Figure 3-58 shows the photographs taken during post-test inspections of the thermally damaged butyl O-rings in the three tests. The explanations of the features in the photographs are similar to those described in the EPDM and silicone O-ring tests in Sections 3.2.1 and 3.2.2.

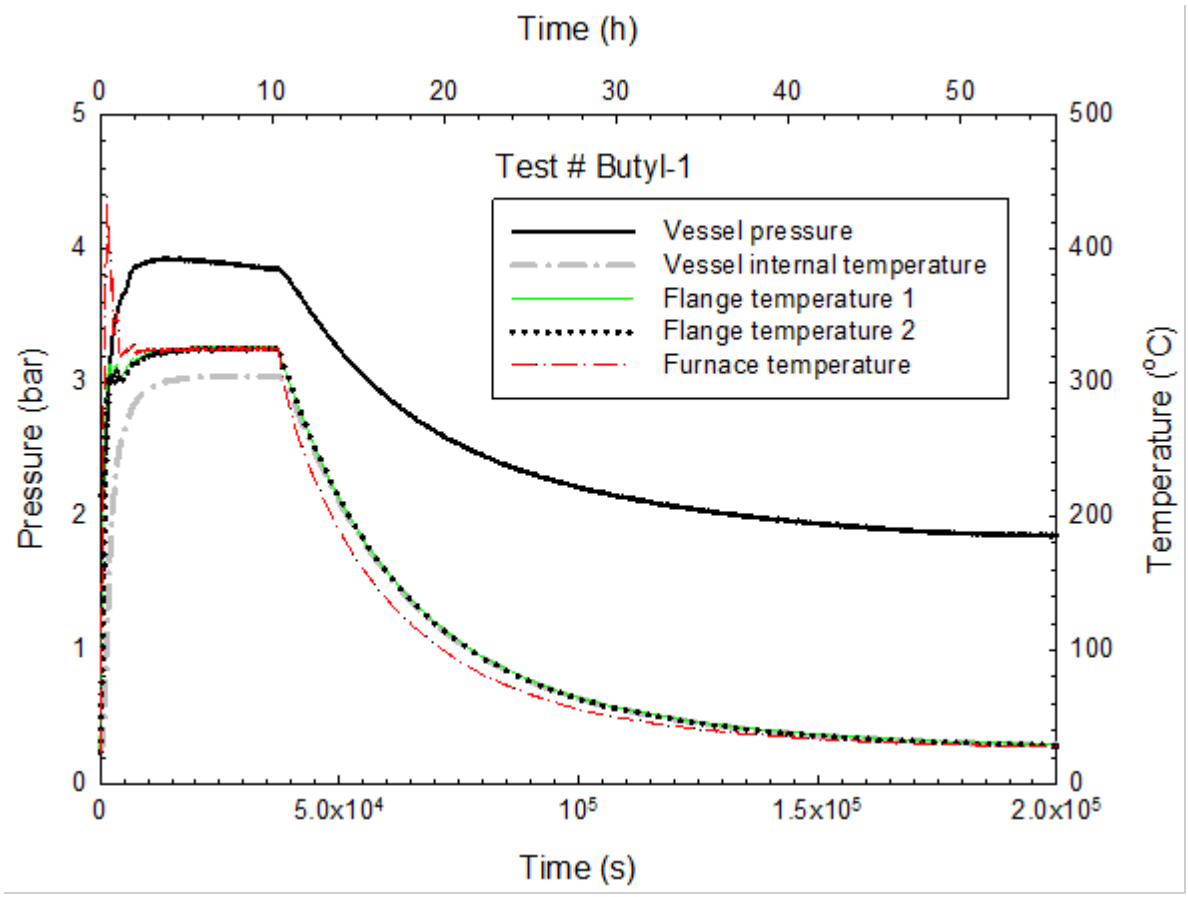

Figure 3-55. Temporal variations of vessel pressure and temperatures in Test # Butyl-1.

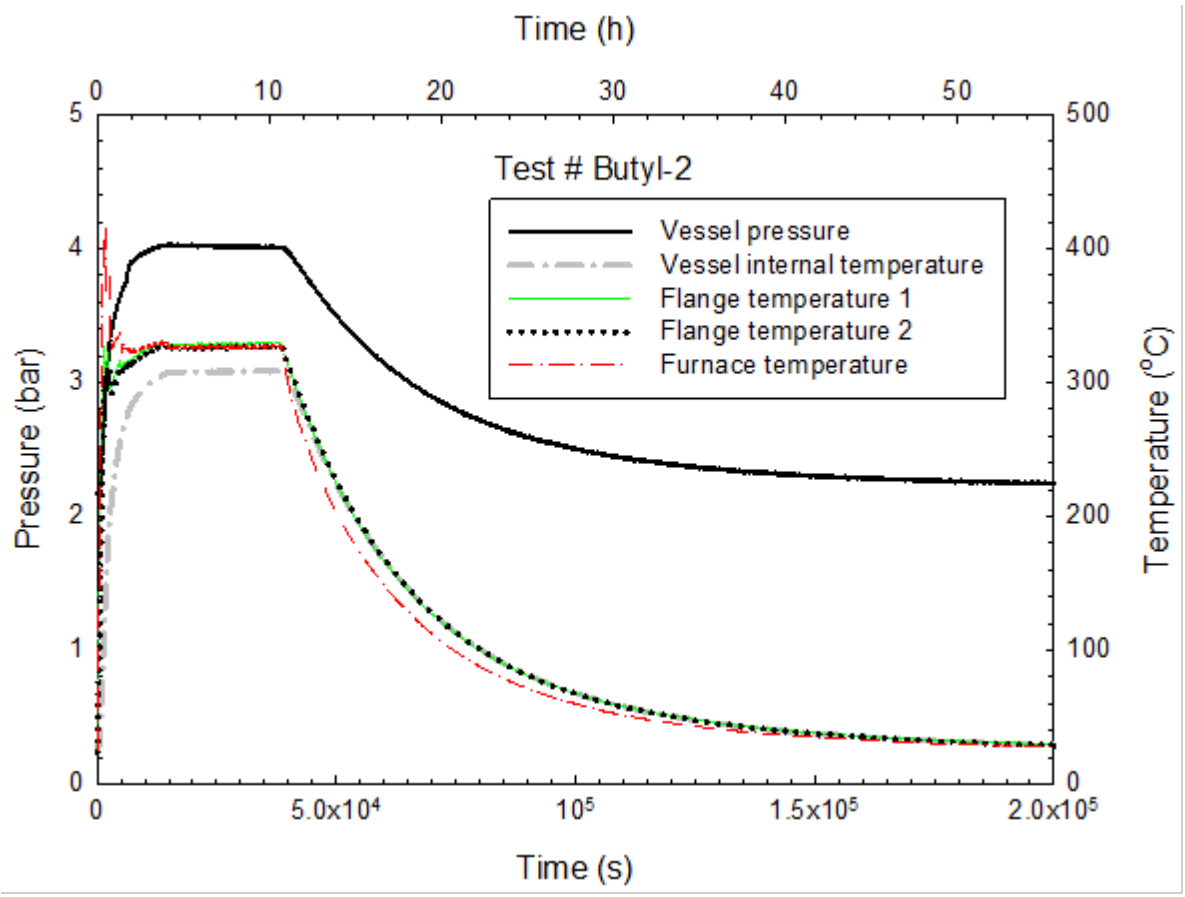

Figure 3-56. Temporal variations of vessel pressure and temperatures in Test # Butyl-2.

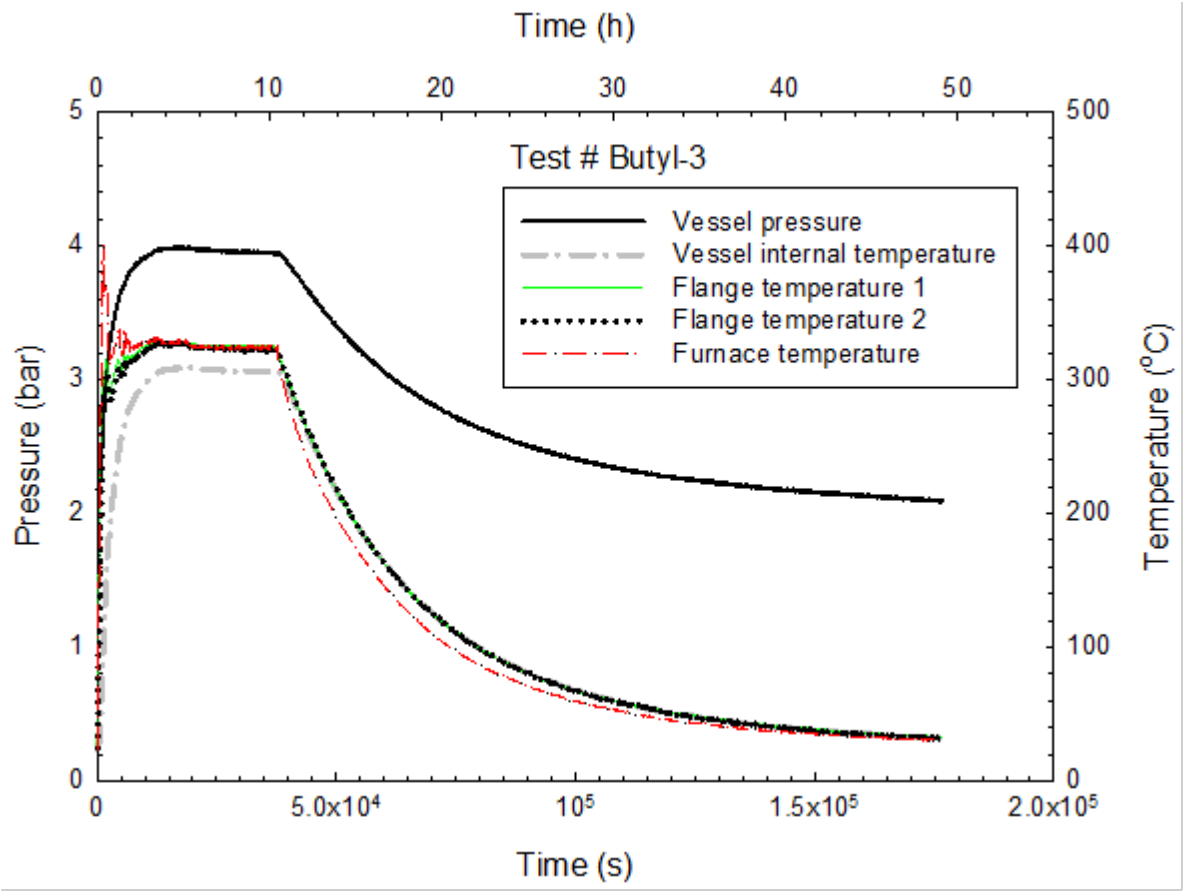

Figure 3-57. Temporal variations of vessel pressure and temperatures in Test # Butyl-3.

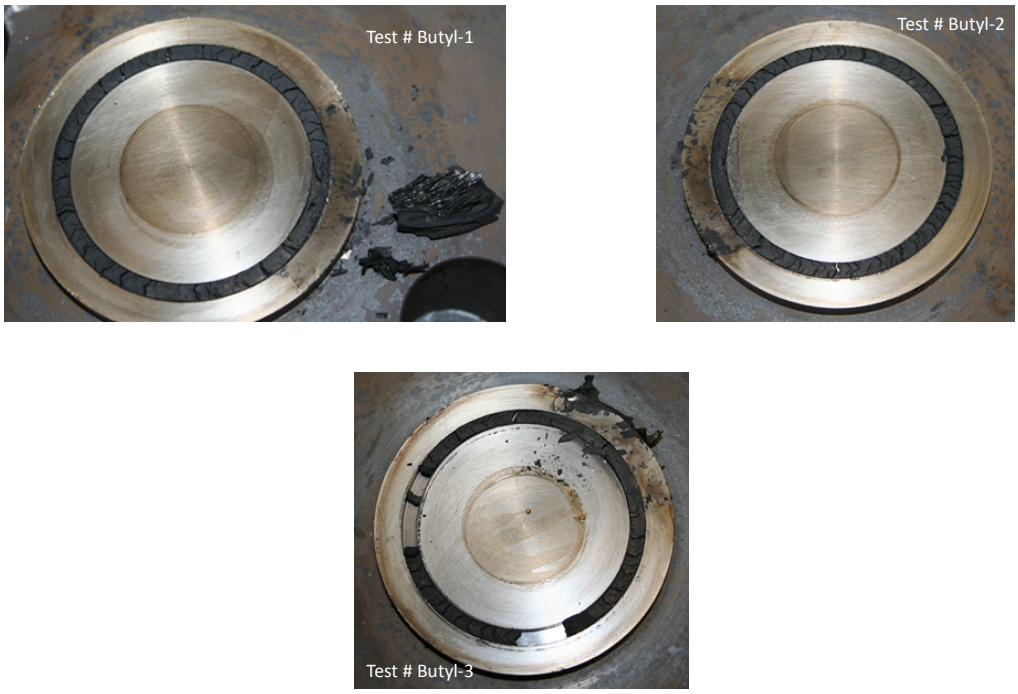

Figure 3-58. Photographs showing the thermally degraded butyl O-ring after 8-h thermal exposure at 316 °C (600 °F) for the three butyl O-ring tests.

3.2.4 Viton O-Rings

Figure 3-59, Figure 3-60, Figure 3-61, and Figure 3-62 show the temporal variations of the vessel internal pressure and temperature, two flange temperatures and furnace temperature for the four Viton O-ring tests, Test # Viton-1, Test # Viton-2, Test # Viton-3, and Test # Viton-4, respectively.

In all four tests, the pressure was not constant but varied during the 8-h test period. In Test # Viton-1 (Figure 3-59), Test # Viton-3 (Figure 3-61), and Test # Viton-4 (Figure 3-62), the vessel pressure increased in the early part of the 8-h test period but remained relative constant at the later part. In Test # Viton-2 (Figure 3-60), the pressure increased continuously over the entire 8-h test period. The rate of pressure increase was irregular and not reproducible in all four tests. The increase in pressure at the isothermal test condition and the subsequent attainment of vessel pressure greater than the pre-test initial charge pressure after cool-down suggested the addition of material to the vessel interior. The origin of the material remains unknown. This peculiarity in vessel pressure behavior was also observed in Test #15 in Phase I using an EPDM O-ring exposed at 450 °C (842 °F) for more than 25 h.

Figure 3-63 shows the photographs taken during post-test inspections of the thermally damaged Viton O-rings in the four tests. The explanations of the features in the photographs are similar to those described in the EPDM, silicone, and butyl O-ring tests (see Sections 3.2.1, 3.2.2, and 3.2.3).

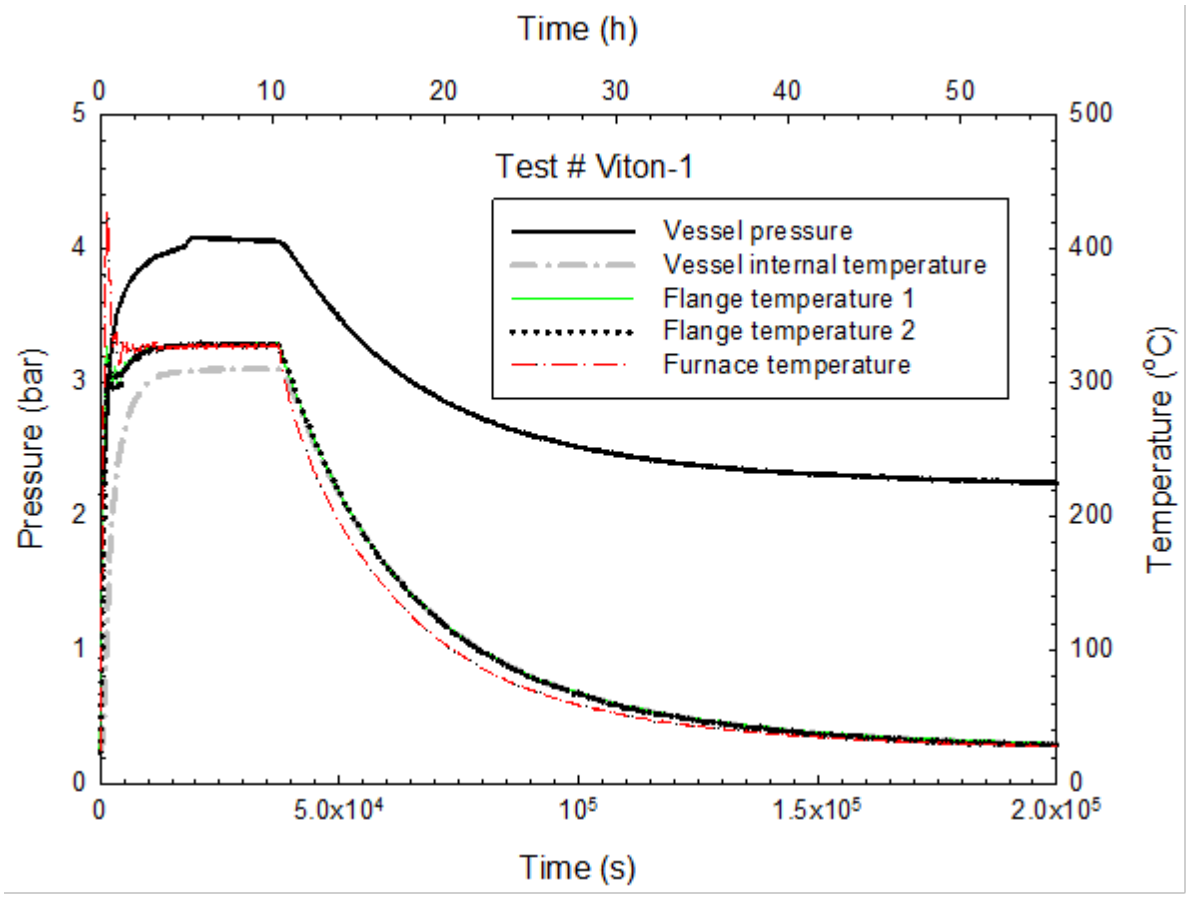

Figure 3-59. Temporal variations of vessel pressure and temperatures in Test # Viton-1.

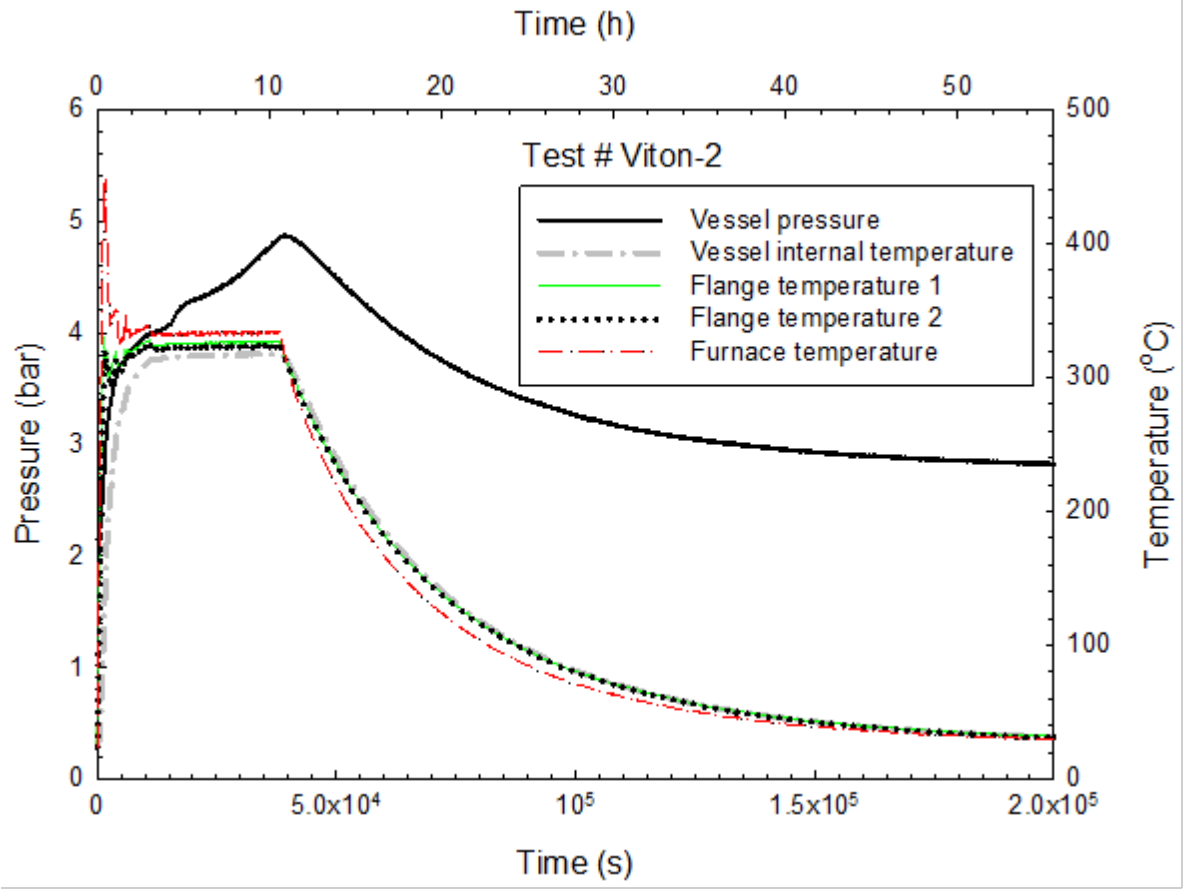

Figure 3-60. Temporal variations of vessel pressure and temperatures in Test # Viton-2.

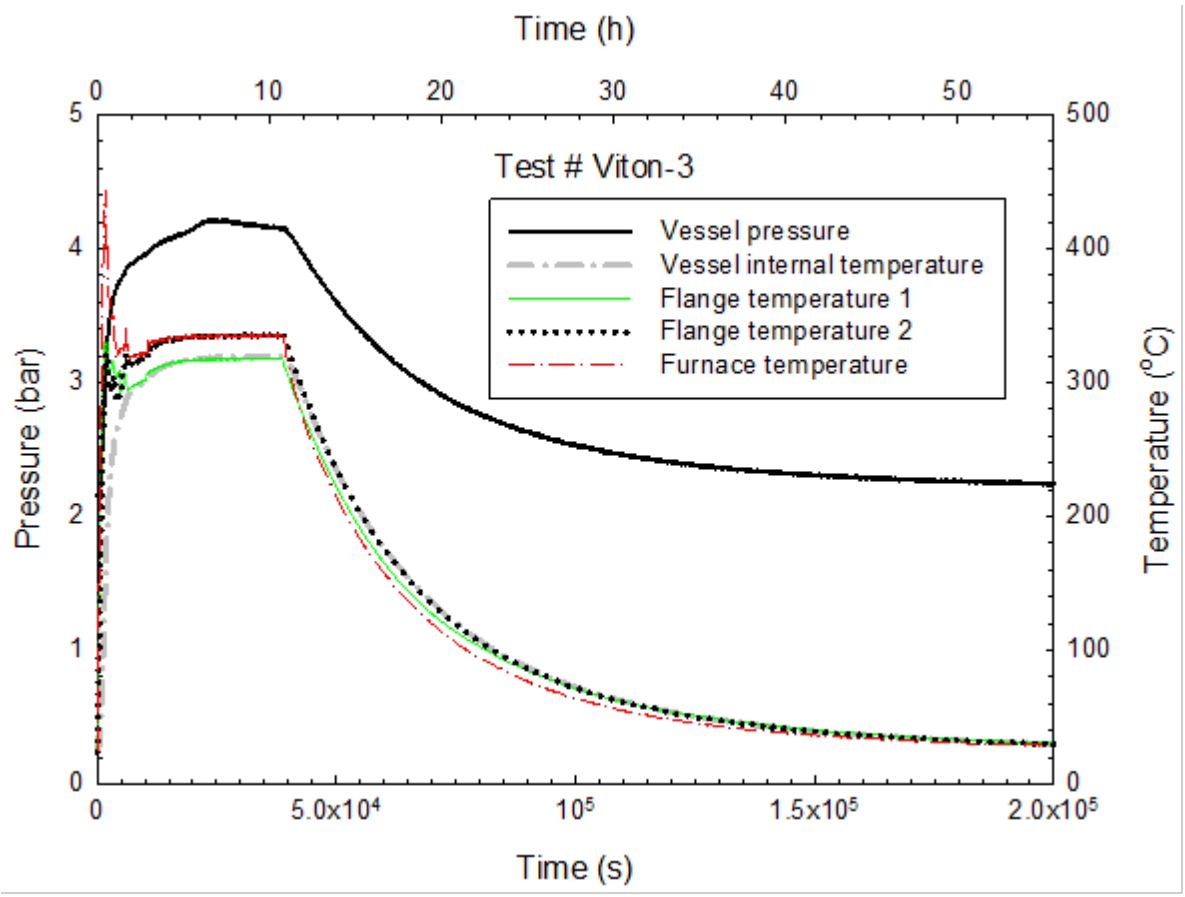

Figure 3-61. Temporal variations of vessel pressure and temperatures in Test # Viton-3.

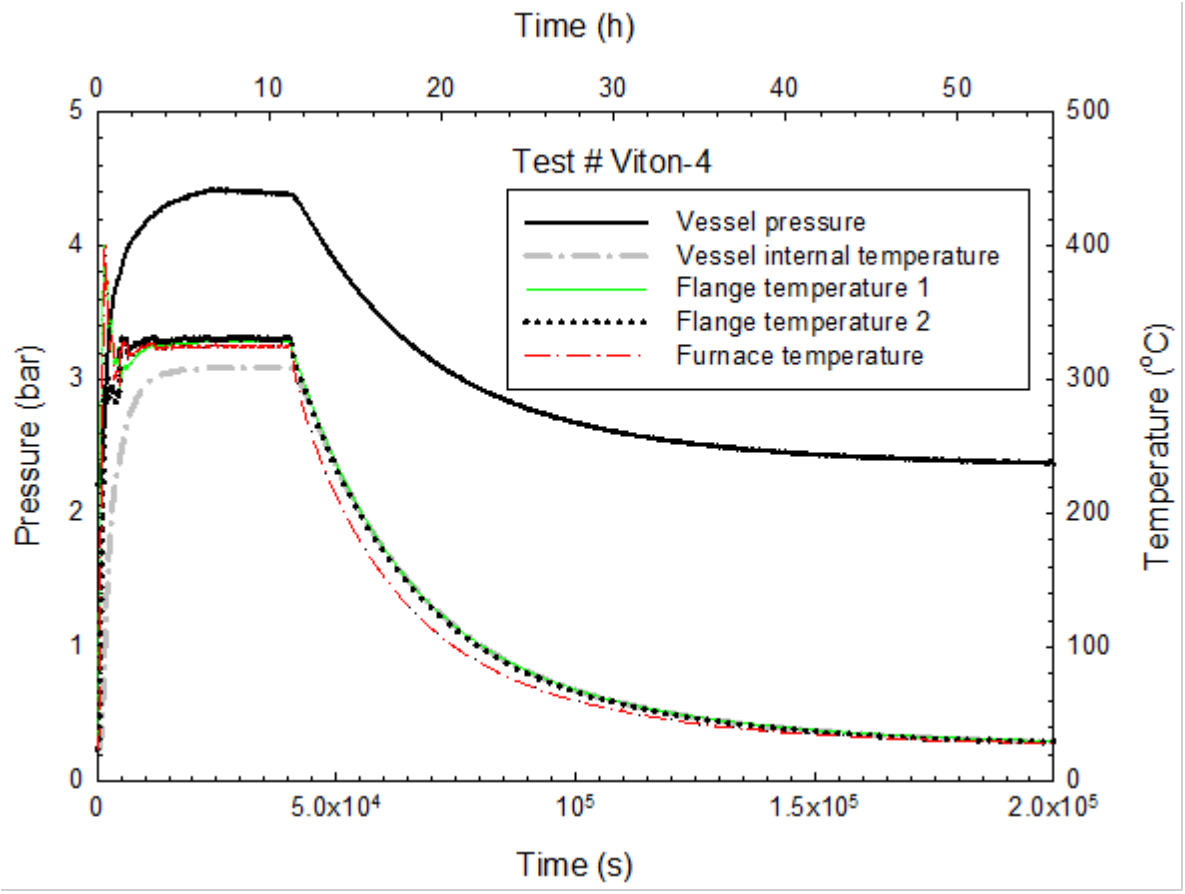

Figure 3-62. Temporal variations of vessel pressure and temperatures in Test # Viton-4.

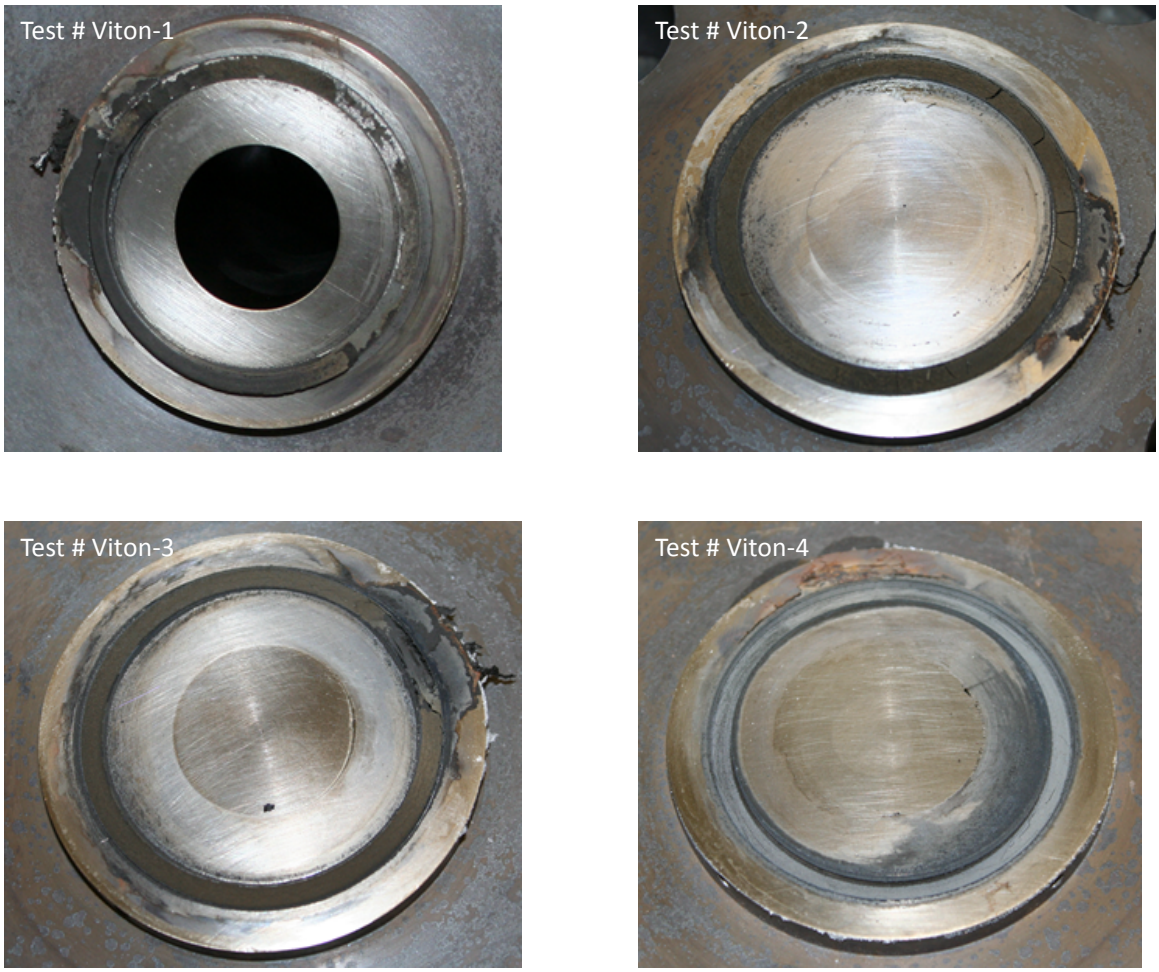

Figure 3-63. Photographs showing the thermally degraded Viton O-ring after 8-h thermal exposure at 316 °C (600 °F) for the four Viton O-ring tests.

3.2.5 PTFE O-Rings

Figure 3-64, Figure 3-65, and Figure 3-66 show the temporal variations of the vessel internal pressure and temperature, two flange temperatures and furnace temperature for the three PTFE O-ring tests, Test # PTFE-1, Test # PTFE-2, and Test # PTFE-3, respectively. The lack of detectable pressure drop during the 8-h test period and the recovery of initial charged pressure after the cool-down phase are indicative of the absence of a leak.

Figure 3-67 shows three photographs of the thermally exposed PTFE O-rings taken during post-test inspections. The tested O-rings remained intact but flattened due to the clamping forces of the bolts and thermal exposure, and no PTFE material had oozed out at the flange interface. However, a minute amount of PTFE powder was observed when the two vessel flanges were separated and the O-ring groove was exposed.

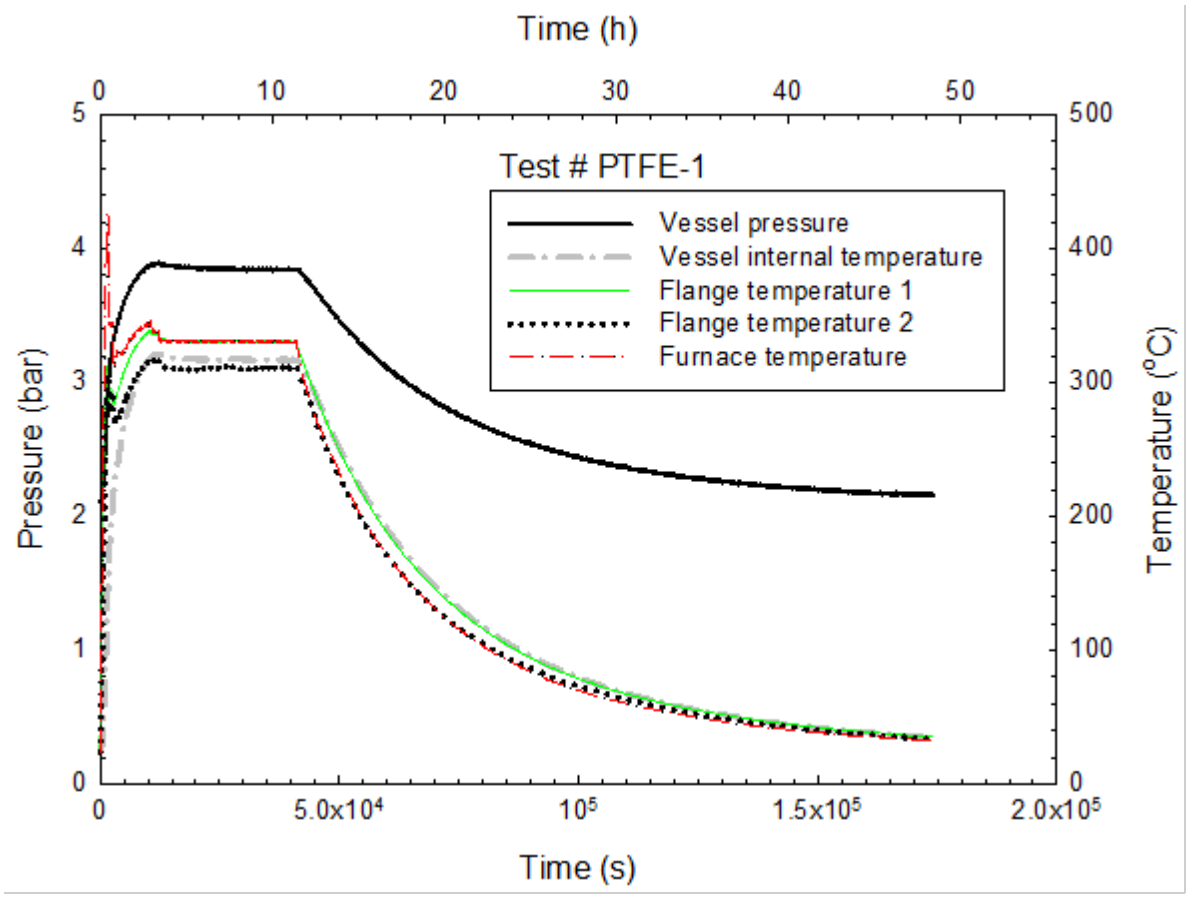

Figure 3-64. Temporal variations of vessel pressure and temperatures in Test # PTFE-1.

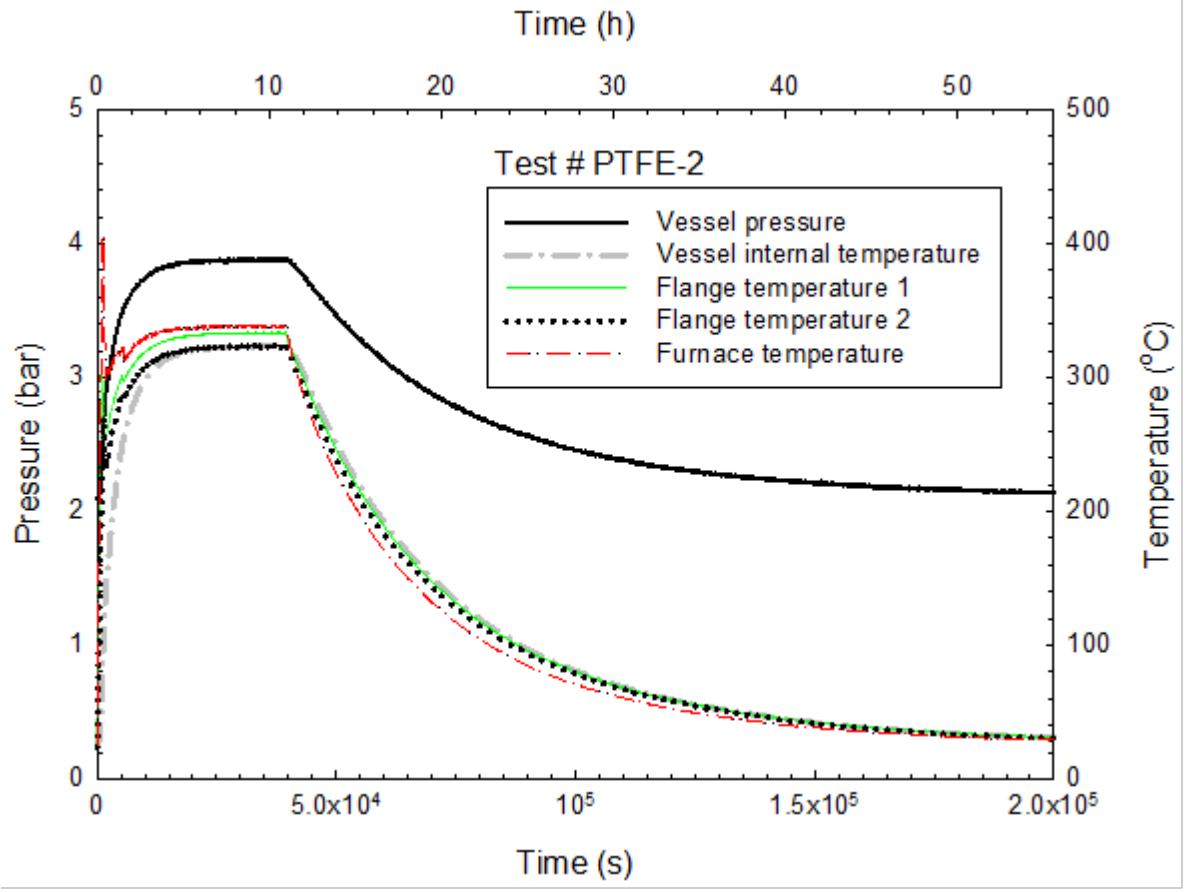

Figure 3-65. Temporal variations of vessel pressure and temperatures in Test # PTFE-2.

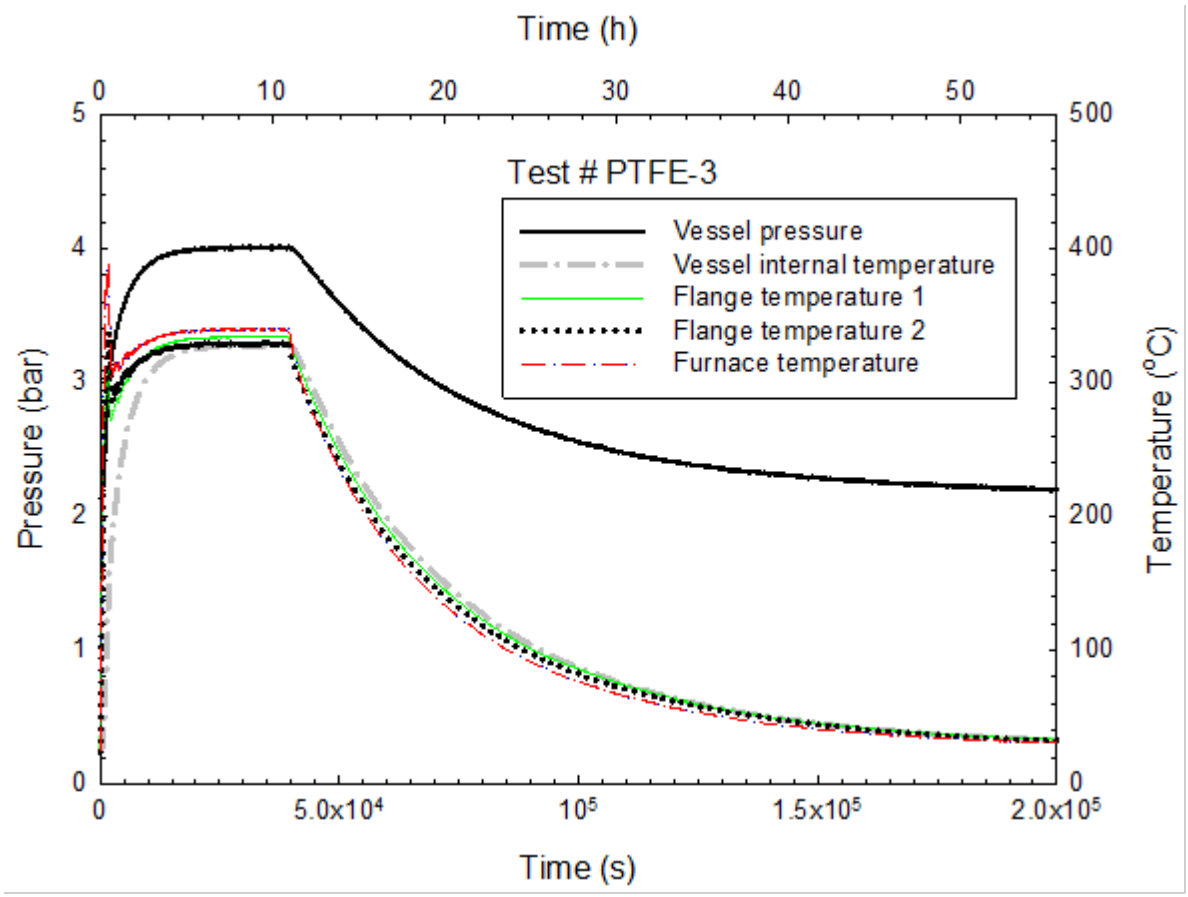

Figure 3-66. Temporal variations of vessel pressure and temperatures in Test # PTFE-3.

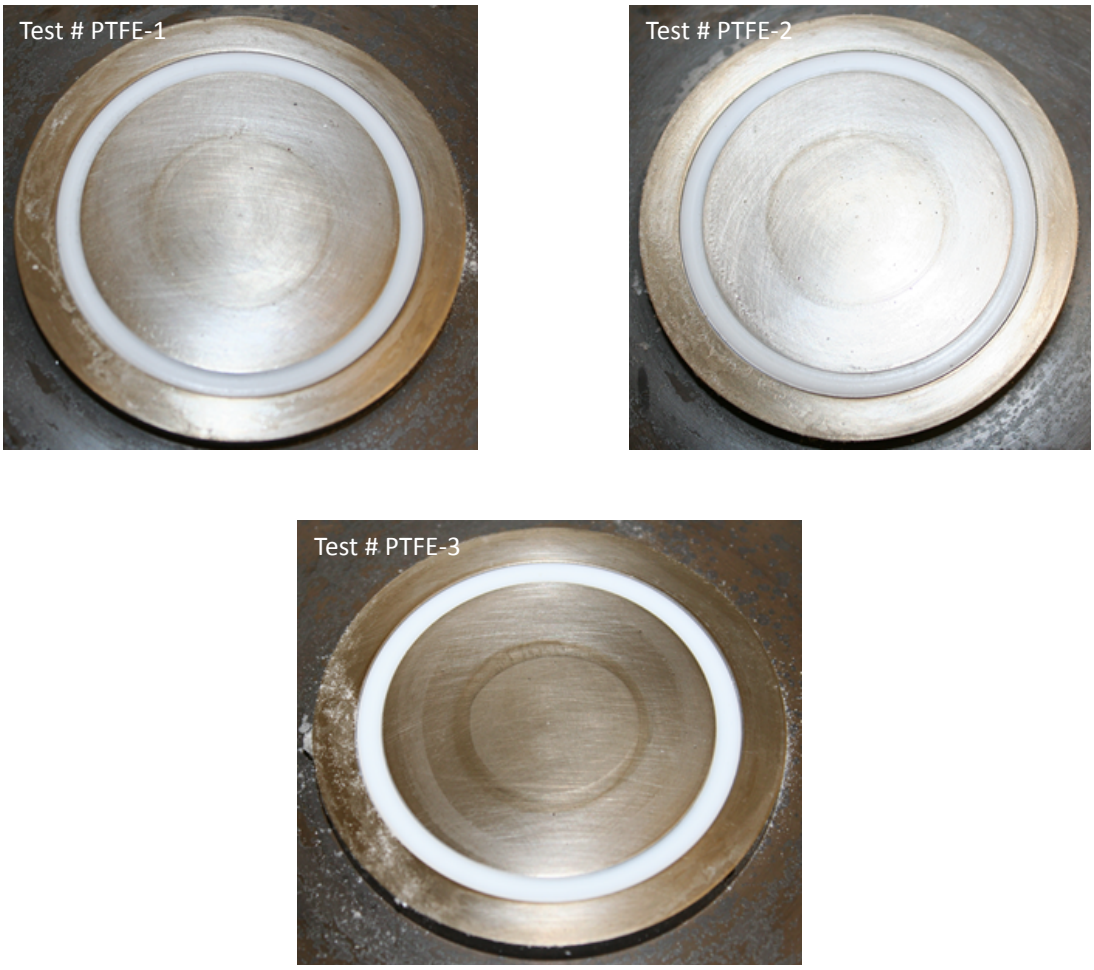

Figure 3-67. Photographs showing the thermally degraded PTFE O-ring after 8-h thermal exposure at 316 °C (600 °F) for the three PTFE O-ring tests.

3.3 Phase III

3.3.1 EPDM-Metallic O-Rings

Figure 3-68, Figure 3-69, and Figure 3-70 show the temporal variations of the vessel internal pressure and temperature, two flange temperatures and furnace temperature for the Test # EPDM-Metallic-1[16], Test # EPDM-Metallic-2, and Test # EPDM-Metallic-3, respectively. New vessels (body and cap) were used in the first two tests[17]. For Test # EPDM-Metallic-3, a new vessel cap and a used vessel body with re-surfaced boss were used, and the test was conducted at 900 °C (1652 °F), instead of 800 °C (1472 °F).

In all three tests, the maintenance of unchanged vessel pressure over the 9-h thermal exposure period and the recovery of the initial vessel pressure at room temperature after the cool-down phase indicate the absence of a leak[18]. It should be noted that in Phase I, a leak was evident after a few hours into the thermal exposure period in three of the five tests using a single metallic O-ring configuration, and a leak was also observed in a single exploratory test using a single EPDM O-ring immediately after the vessel had attained the test temperature of 450 °C (842 °F).

[16] The DAQ was inadvertently turned off during the heat-up period, and the data was not logged. The time zero in the figure was the time when the DAQ was initiated at the beginning of the 9-h thermal exposure period. The data collected over the 9-h test period were never affected or compromised.
[17] The numbering sequence for the vessel designation continues from Phase I.
[18] The data logging was terminated during the cooling phase of Test # EPDM-Metallic-3 due to site power-outage; however, the recovery of the initial vessel pressure was manually noted from the computer display when the vessel was cooled to room temperature after the power outage was over.

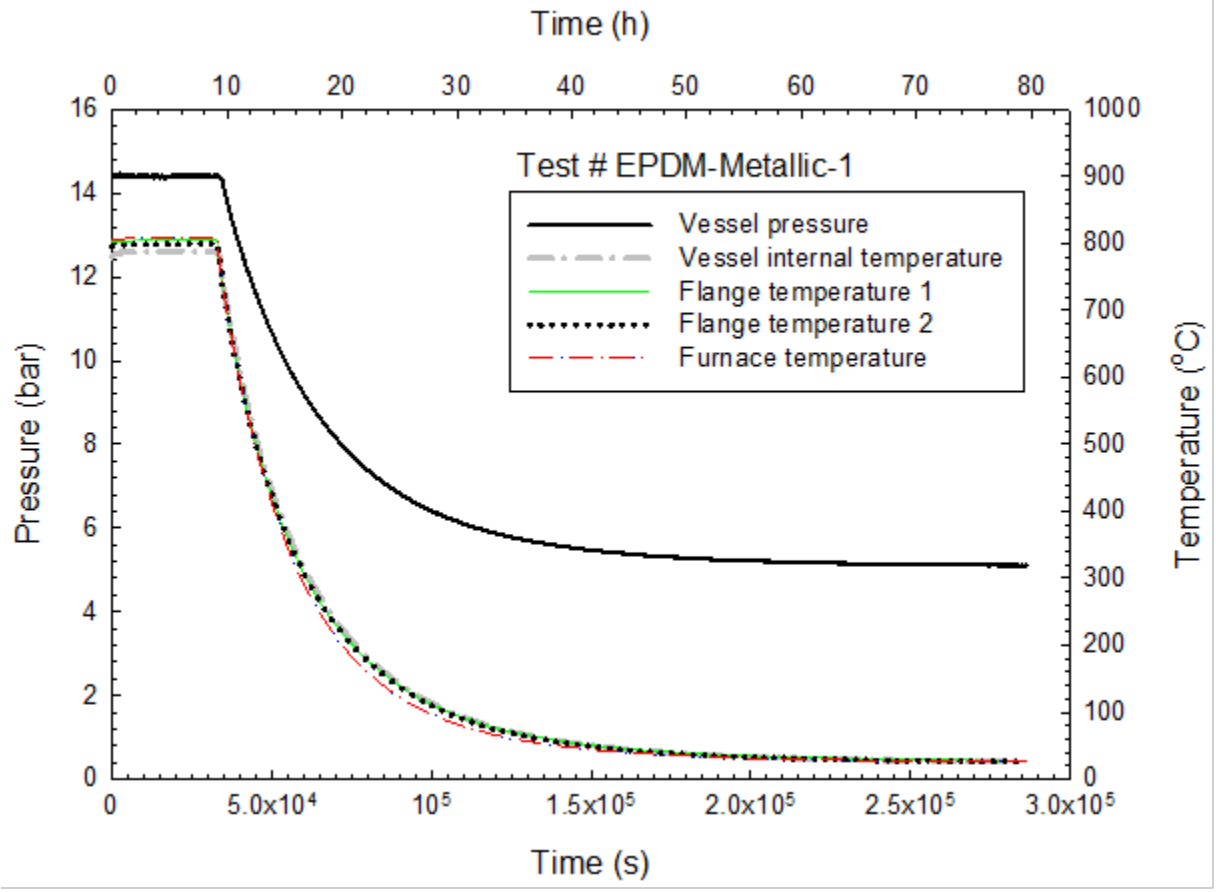

Figure 3-68. Temporal variations of vessel pressure and temperatures in Test # EPDM-Metallic-1 (Vessel #10).

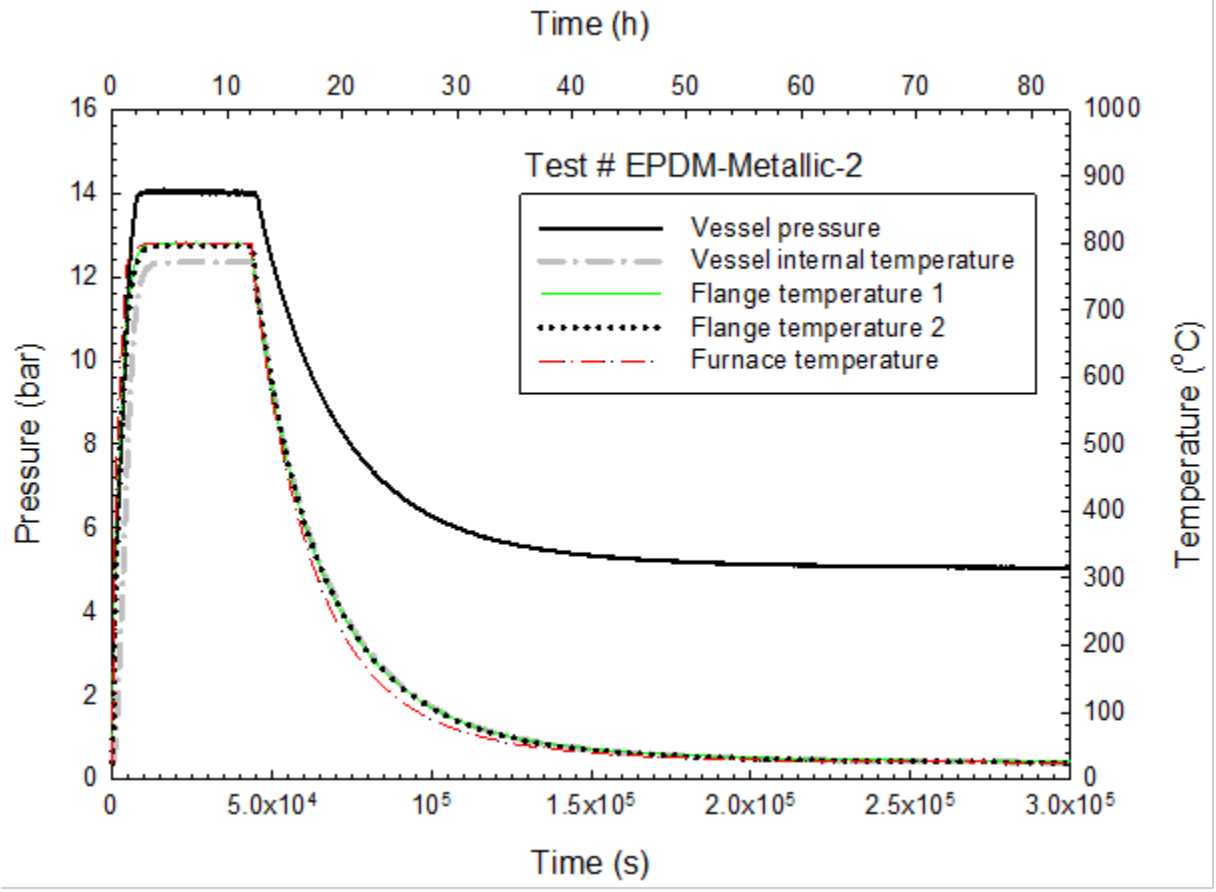

Figure 3-69. Temporal variations of vessel pressure and temperatures in Test # EPDM-Metallic-2 (Vessel #11).

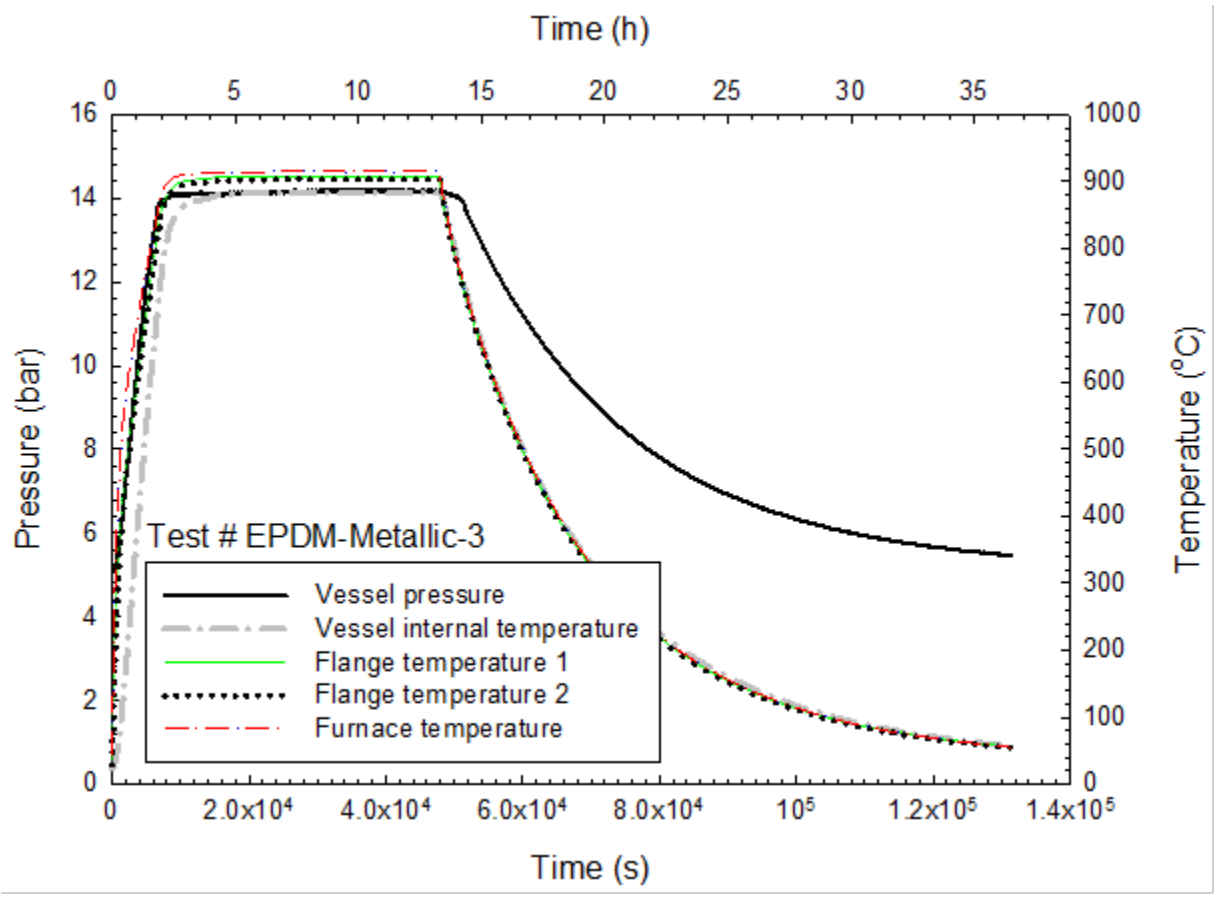

Figure 3-70. Temporal variations of vessel pressure and temperatures in Test # EPDM-Metallic-3 using the cap of Vessel #12 and the body (with boss re-surfaced) of Vessel #10.

Figure 3-71 shows the photographs taken after the vessels were disassembled for post-test inspection for the three tests. Unlike the observations made in the single EPDM O-ring tests (see Section 3.2.1), a globule of O-ring material was not observed to seep out at the interface between the two flanges of the vessel when the test vessel was first removed from the furnace after the test. However, upon disconnecting the two flanges, char residues left by the EPDM O-ring materials were apparent on both bosses at the vicinity of the EPDM O-ring groove, indicating that oozing of the EPDM O-ring material had occurred during the thermal exposure and the materials that had seeped out from the interface were completely charred. The tested EPDM O-ring turned into a thick layer of highly compacted powdery char in the O-ring groove and could not be removed from the groove without destroying the structural integrity of the char layer. It should be noted that the condition of the EPDM O-ring depicted in Figure 3-71 does not truly represent the actual in situ condition of the tested O-ring because the damage to the O-ring might have been further exacerbated when the two flanges were forcibly removed and separated for post-test inspection. Similar to the observations made in Phase I, the metallic O-ring was partially bonded to the boss of the vessel body flange when it was disconnected from the flange of the vessel cap. The O-ring groove was coated with silver from the melted metallic O-ring.

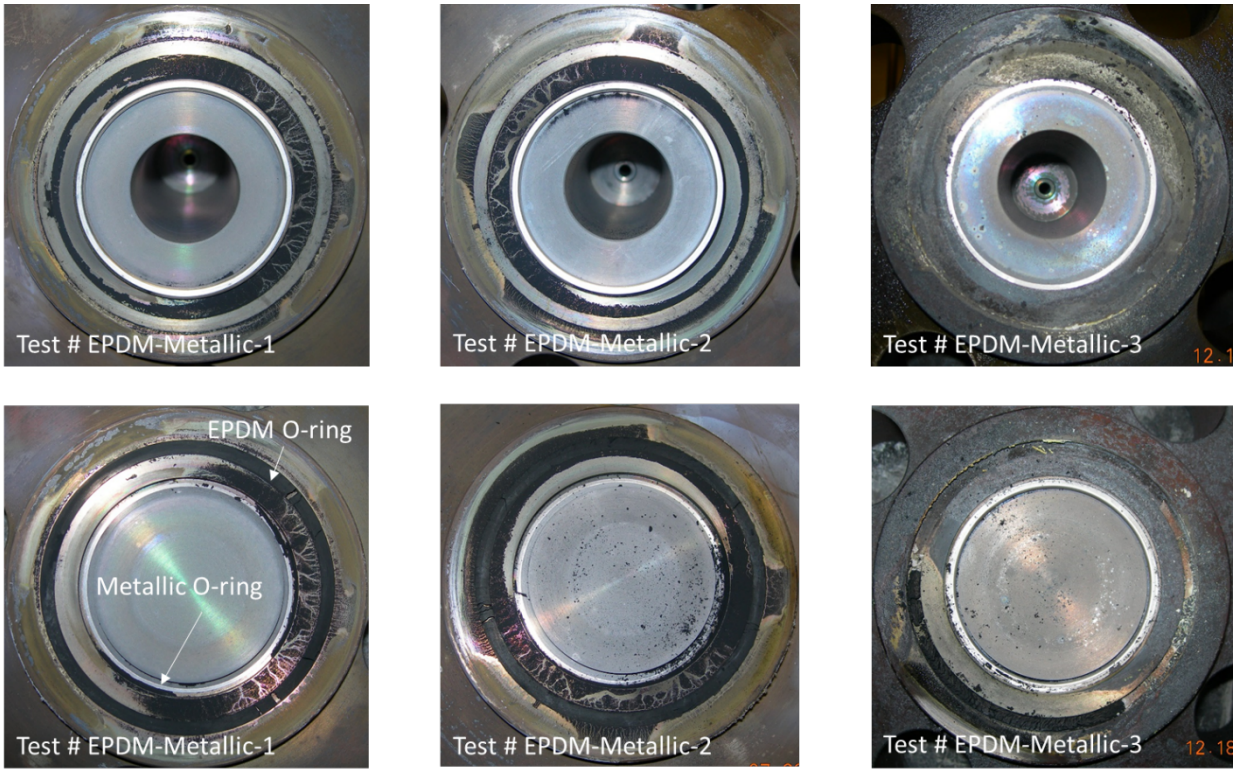

Figure 3-71. Photographs showing the thermally degraded EPDM-Metallic O-rings after 9-h thermal exposure at 800 °C (1472 °F) for the two EPDM-Metallic O-ring tests.

3.3.2 Blank-Metallic O-Ring

In this test, the cap of Vessel #13 (with double O-ring configuration) and the body (with boss re-surfaced) of Vessel #11 was used; however, the outer O-ring groove was left blank and a metallic O-ring was placed in the inner groove. Figure 3-72 shows the temporal variations of the vessel internal pressure and temperature, two flange temperatures and furnace temperature for Test # Blank-Metallic-1. As indicated in the figure, the vessel pressure remained unchanged during the 9 h constant-temperature heating period, and no leakage was observed during this test. Figure 3-73 shows the photographs taken after the vessel were dismantled for post-test inspection. The thermally-exposed O-ring was observed to suffer damages similar to those sustained in the double metallic O-rings tested at 900 °C (1652 °F).

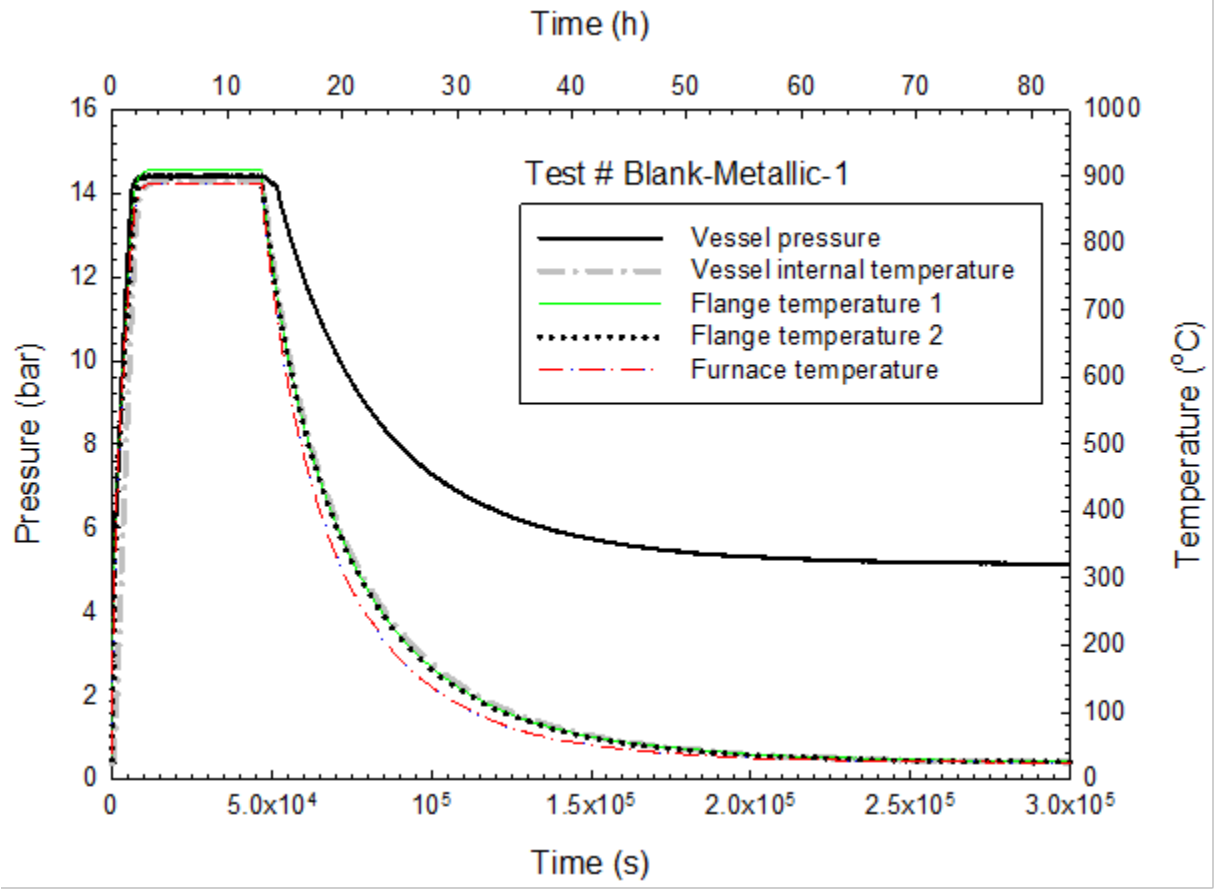

Figure 3-72. Temporal variations of vessel pressure and temperatures in Test # Blank-Metallic-1 using the cap of Vessel #13 and the body (with boss re-surfaced) of Vessel #11.

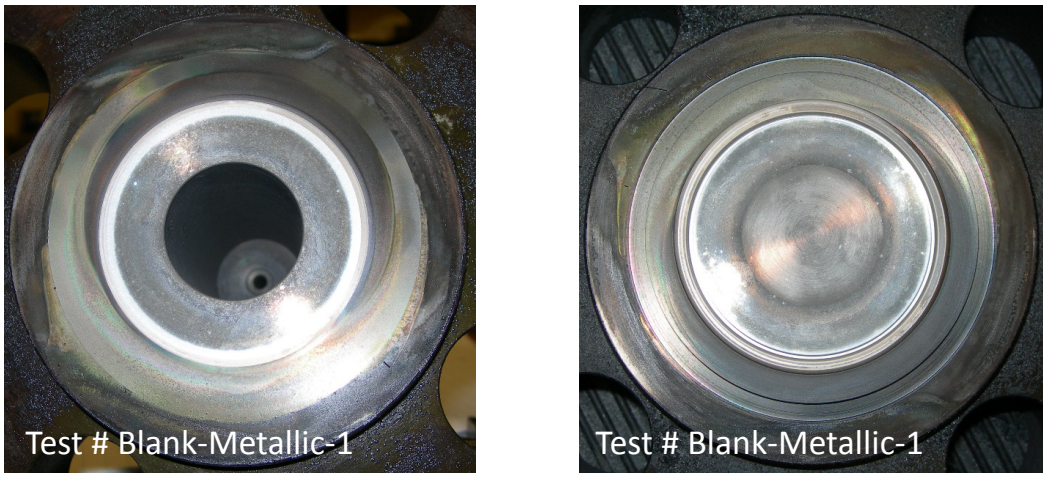

Figure 3-73. Photographs showing the thermally degraded Metallic O-ring after 9-h thermal exposure at 900 °C (1652 °F) for the Blank-Metallic O-ring test.

3.3.3 EPDM-EPDM O-Rings

Two tests (Test # EDPM-EDPM-1 and Test # EPDM-EPDM-2) were conducted at 900 °C (1652 °F) using the EPDM-EPDM double O-ring configuration. Figure 3-74 and Figure 3-75 show the temporal variations of vessel pressure and temperatures for these two tests. Leaks occurred before the test vessel reached the target temperature of 900 °C (1652 °F)[19]. Note that in the two figures, the four temperatures were off-scale for less than 1 h but returned to normal due to the problems associated with the thermocouples and the DAQ system. The DAQ recorded unrealistically high temperatures from the four thermocouples. The photographs in Figure 3-76 illustrate the extent of damage to the O-rings after the thermal exposure tests. The black powdery materials (most likely from metal dusting) on of the flange came from the vessel wall and was the result of striking the vessel with a mallet in order to loosen the bolts and other mechanical actions taken to dismantle the vessel for post-test inspection. In addition, the vessel interior wall was found to be coated with a very thin layer of what appeared to be metallic material. The isothermal leakage rates could not be estimated because the pressure drop occurred during the heat-up period. Tests # EPDM-5 and # EPDM-6 also revealed a smaller layer of material under the same thermal exposure condition (see Section 3.2.1).

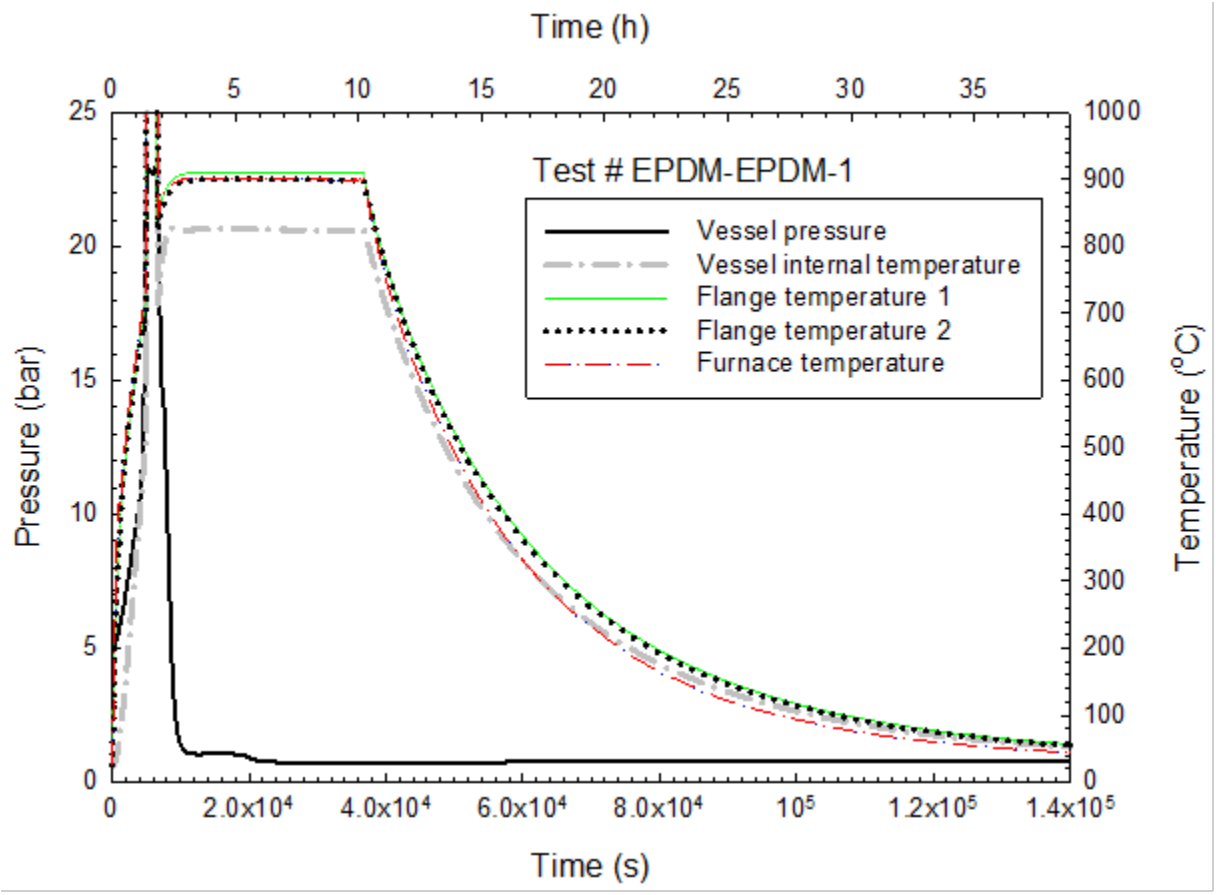

Figure 3-74. Temporal variations of vessel pressure and temperatures in Test # EPDM-EPDM-1 using Vessel #16.

[19] The method for leak rate estimation described in Appendix D could not be used to estimate the leak rate because the heat-up period was not isothermal.

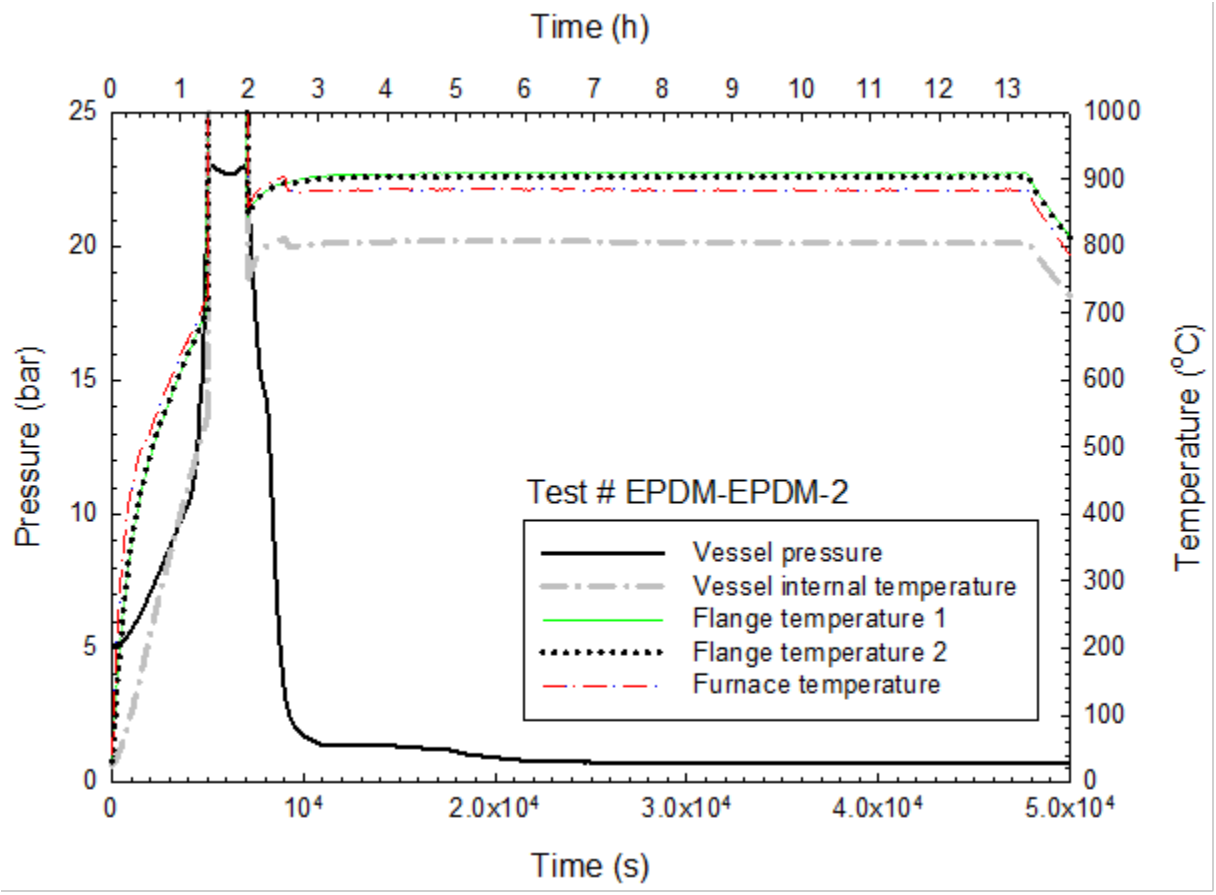

Figure 3-75. Temporal variations of vessel pressure and temperatures in Test # EPDM-EPDM-2 using Vessel #17.

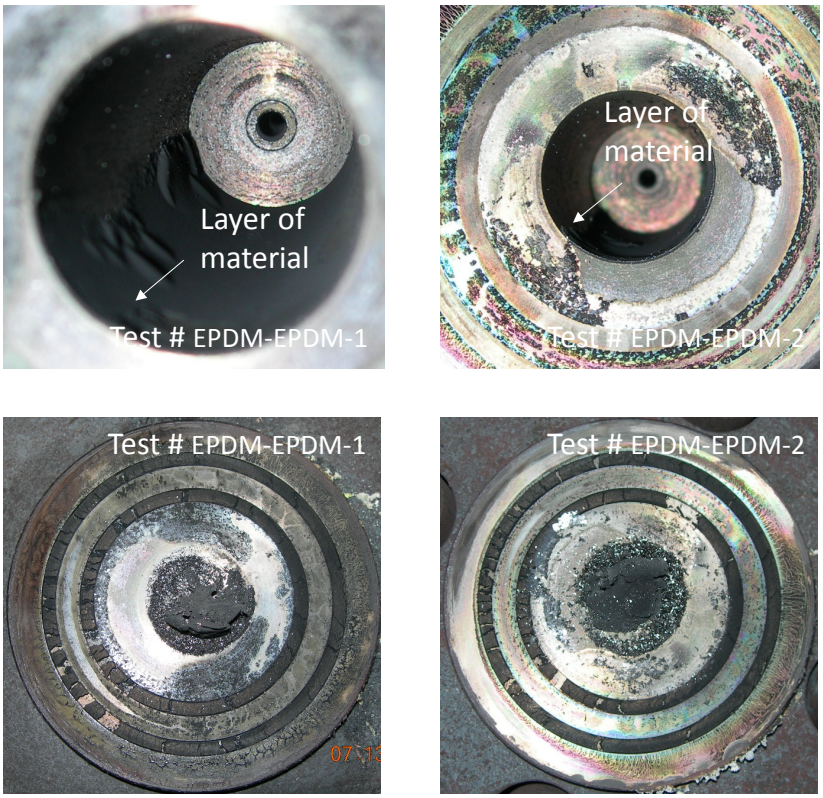

Figure 3-76. Photographs showing the thermally degraded EPDM O-rings after 9-h thermal exposure at 900 °C (1652 °F) for the EPDM-EPDM O-ring test.

3.3.4 Butyl-Butyl O-Rings

One exploratory test was performed using a double butyl O-ring configuration. Vessel #16 was cleaned and re-used for this test. Figure 3-77 shows the test results. Similar to the EPDM-EPDM tests, a leak occurred before the target temperature of 900 °C (1652 °F) was attained, and a layer of material of metallic nature was also formed on the interior wall of the vessel (see Figure 3-78)[19]. Incidentally, all four thermocouples also failed to function for about one hour.

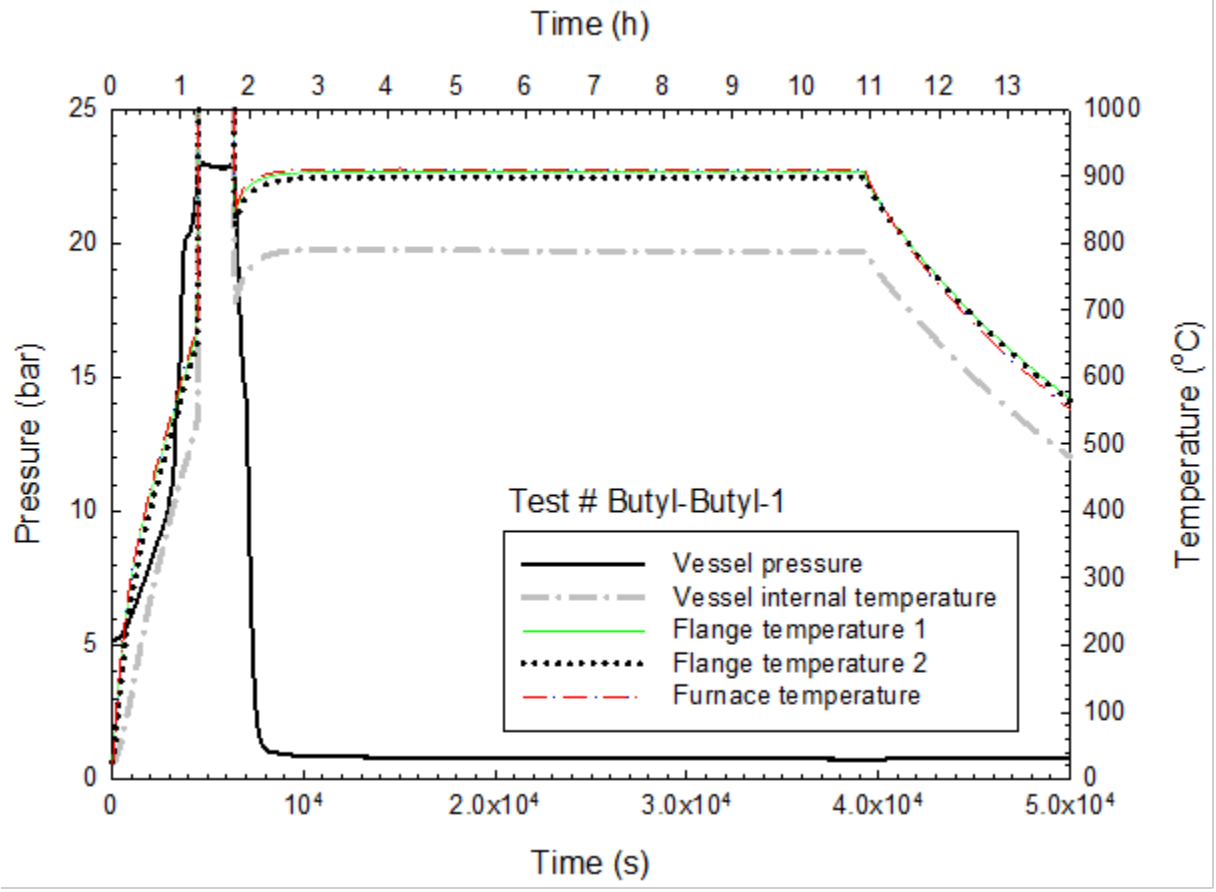

Figure 3-77. Temporal variations of vessel pressure and temperatures in Test # Butyl-Butyl-1 using Vessel #16.

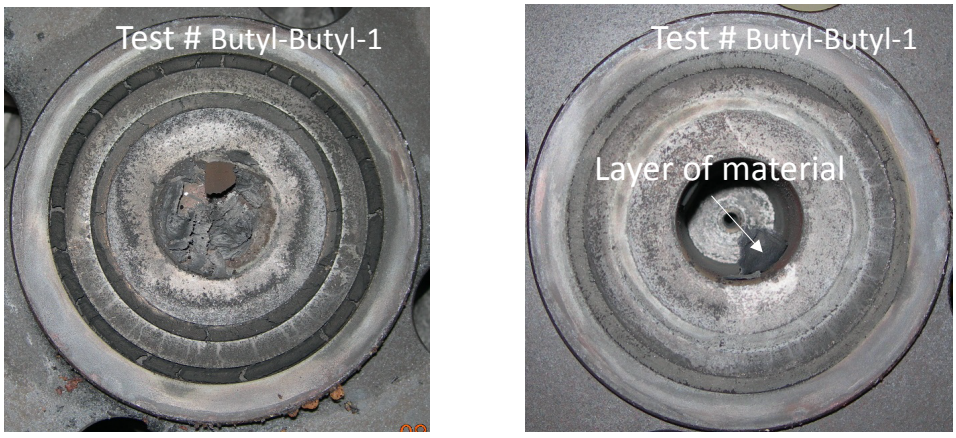

Figure 3-78. Photograph showing the thermally degraded butyl O-rings after 9-h thermal exposure at 900 °C (1652 °F) for the butyl-butyl O-ring test.

3.3.5 Metallic-Metallic O-Rings

Four tests (Test # Metallic-Metallic-1, Test # Metallic-Metallic-2, Test # Metallic-Metallic-3, and Test # Metallic-Metallic-4) were conducted. For Test # Metallic-Metallic-1, the cap of Vessel #14 and the body of Vessel #12 was used. For Test # Metallic-Metallic-2, the cap of Vessel #15 and the body of Vessel #13 was used. Test # Metallic-Metallic-3 and Test # Metallic-Metallic-4 used Vessel # 18 and Vessel # 19 respectively. As described in Section 2.1.3, Test # Metallic-Metallic-1 and Test # Metallic-Metallic-2 used 416 N m (307 lb ft) torque, whereas Test # Metallic-Metallic-3, and Test # Metallic-Metallic-4 used 976 N m (720 lb ft) torque.

Figure 3-79 shows the temporal variations of the vessel internal pressure and temperature, two flange temperatures and furnace temperature[20] for Test # Metallic-Metallic-1. The vessel pressure started to decrease after more than 4 h at 900 °C (1652 °F) and continued to decrease over the remaining test period. The gradual decrease in vessel pressure during the thermal exposure and the failure to recover the original vessel pressure (≈ 5 bar) at room temperature after the cool-down phase are the two indicators of a leak. However, after the vessel cooled to room temperature, the vessel pressure did not ever equilibrate with atmospheric pressure, but remained at elevated pressure (≈ 2 bar), implying that the O-rings still retained some residual sealing capability after the thermal exposure. Figure 3-80 shows the calculated reference helium leakage rates during the 9 h isothermal heating period at 900 °C (1652 °F).

Figure 3-81 shows the temporal variations of the vessel internal pressure and temperature, two flange temperatures and furnace temperature for Test # Metallic-Metallic-2. This test is subtly different from Test # Metallic-Metallic-1 in that the vessel pressure abruptly (within minutes) dropped from ≈ 14 bar to ≈ 11 bar after more than 4 h at 900 °C (1652 °F), and then continued to decrease gradually over the remaining test period. Other observations remain similar to Test # Metallic-Metallic-1. Figure 3-82 shows the calculated reference helium leakage rates over the 9 h isothermal heating period at 900 °C (1652 °F). The sudden drop in vessel pressure is clearly marked as a spike in the leakage rate plot.

Figure 3-83 shows the temporal variations of the vessel internal pressure and temperature, two flange temperatures and furnace temperature for Test # Metallic-Metallic-3. The vessel held pressure for about 8 h at 900 °C before a leak occurred. It is interesting to note that when the vessel cooled to room temperature after 9-h thermal exposure, the vessel pressure still maintained a pressure of about 1.6 bar before the vessel was dismantled for post-test inspection more than a week later. Figure 3-84 shows the calculated reference helium leakage rates over the isothermal heating period at 900 °C (1652 °F) where the leak occurred. The sudden drop in vessel pressure is again clearly marked as a spike in the leakage rate plot. In this test, the vessel pressure was stabilized and maintained eventually at about 1.7 bar as the vessel was cooled to room temperature.

[20] The furnace temperature readings in this figure are somewhat (about 40 °C) lower than those reported in other figures due to the slight misplacement of the furnace thermocouple, but the furnace own temperature read-out indicted that the furnace was at the set-point temperature.

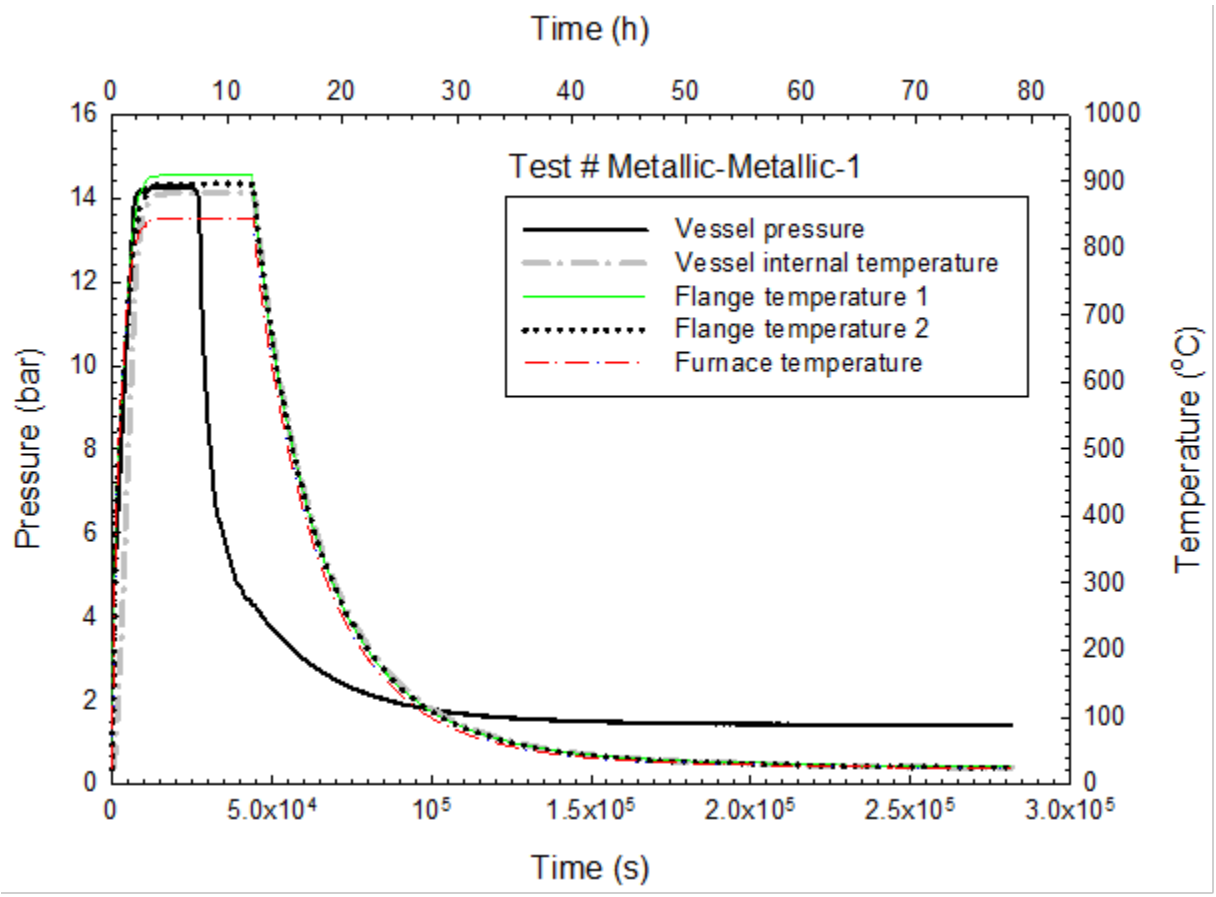

Figure 3-79. Temporal variations of vessel pressure and temperatures in Test # Metallic-Metallic-1 using the cap of Vessel #14 and the body of Vessel #12.

Figure 3-85 shows the temporal variations of the vessel internal pressure and temperature, two flange temperatures and furnace temperature for Test # Metallic-Metallic-4. The vessel was maintaining pressure for about 2 h before the leak occurred, as indicted by the sudden drop of vessel pressure. Contrary to the observations made in Test # Metallic-Metallic-3, the leak occurred much sooner in this test although both tests were prepared and conducted at the same conditions. In addition, the vessel pressure never stabilized and continued to drop to atmospheric value as the vessel cooled to room temperature. Figure 3-86 shows the calculated reference helium leakage rates over the isothermal heating period at 900 °C (1652 °F) where the leak occurred.

Figure 3-87 shows the photographs taken after the vessels were disassembled for post-test inspection for the four tests. The thermally-exposed O-rings were observed to suffer damages similar to those sustained in the metallic O-rings tested at 800 °C (1472 °F).

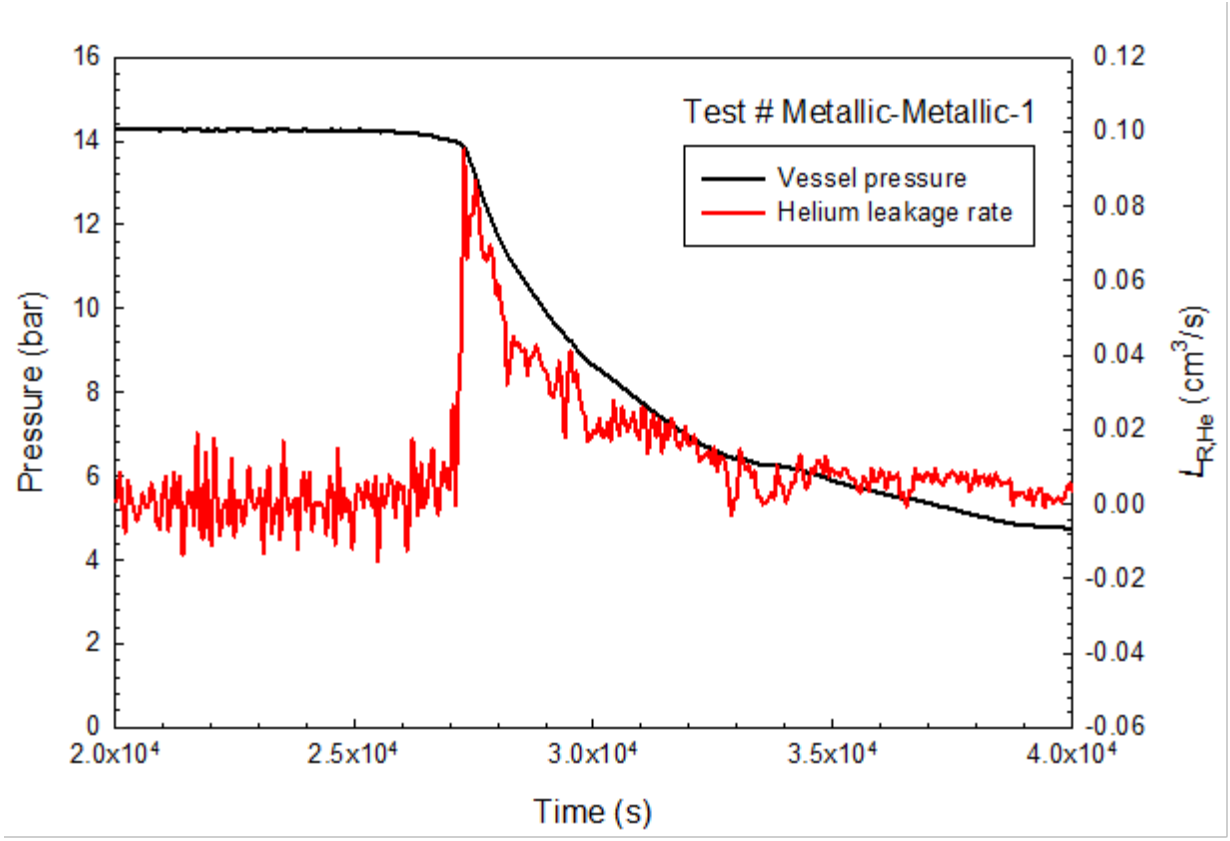

Figure 3-80. Isothermal reference helium leakage rate during the 9 h heating in Test # Metallic-Metallic-1 using the cap of Vessel #14 and the body of Vessel #12.

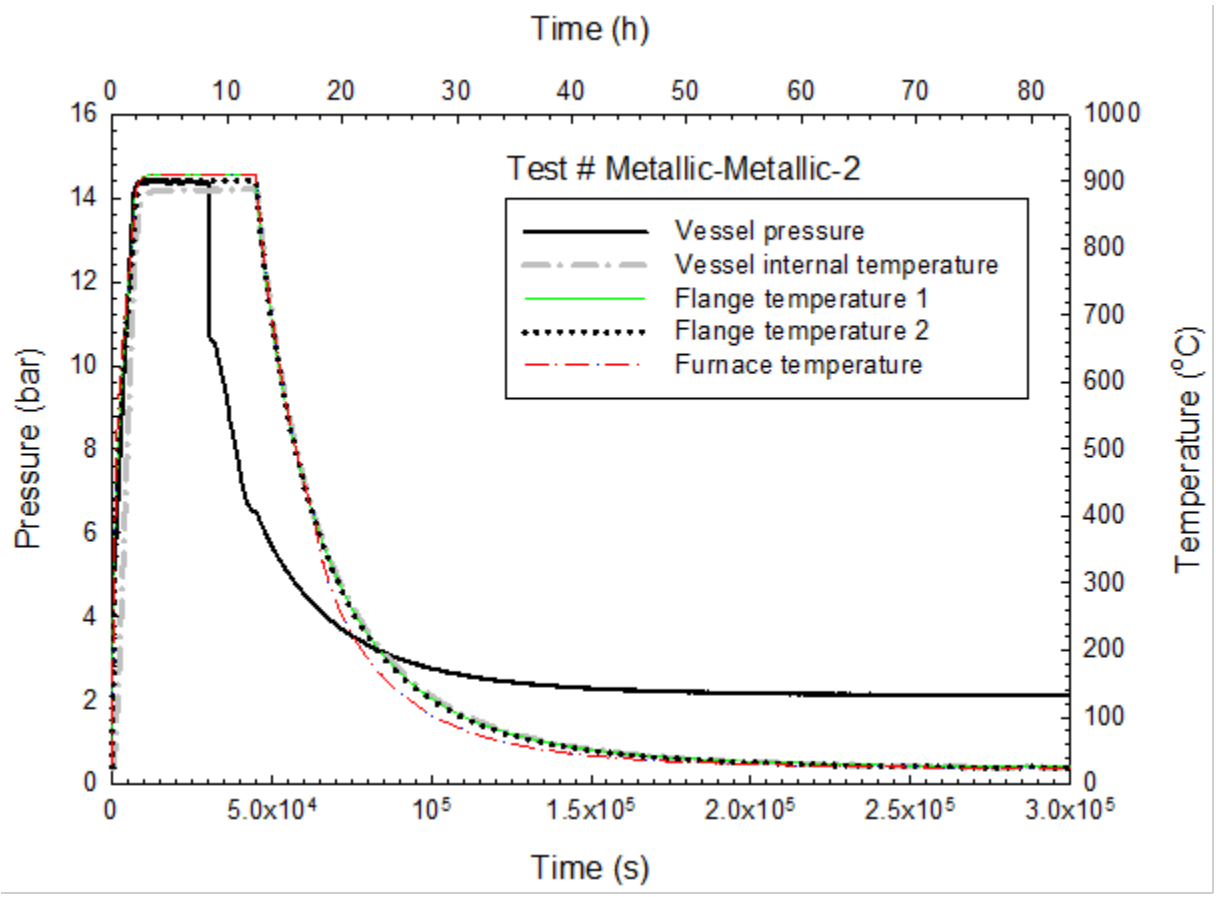

Figure 3-81. Temporal variations of vessel pressure and temperatures in Test # Metallic-Metallic-2 using the cap of Vessel #15 and the body of Vessel #13.

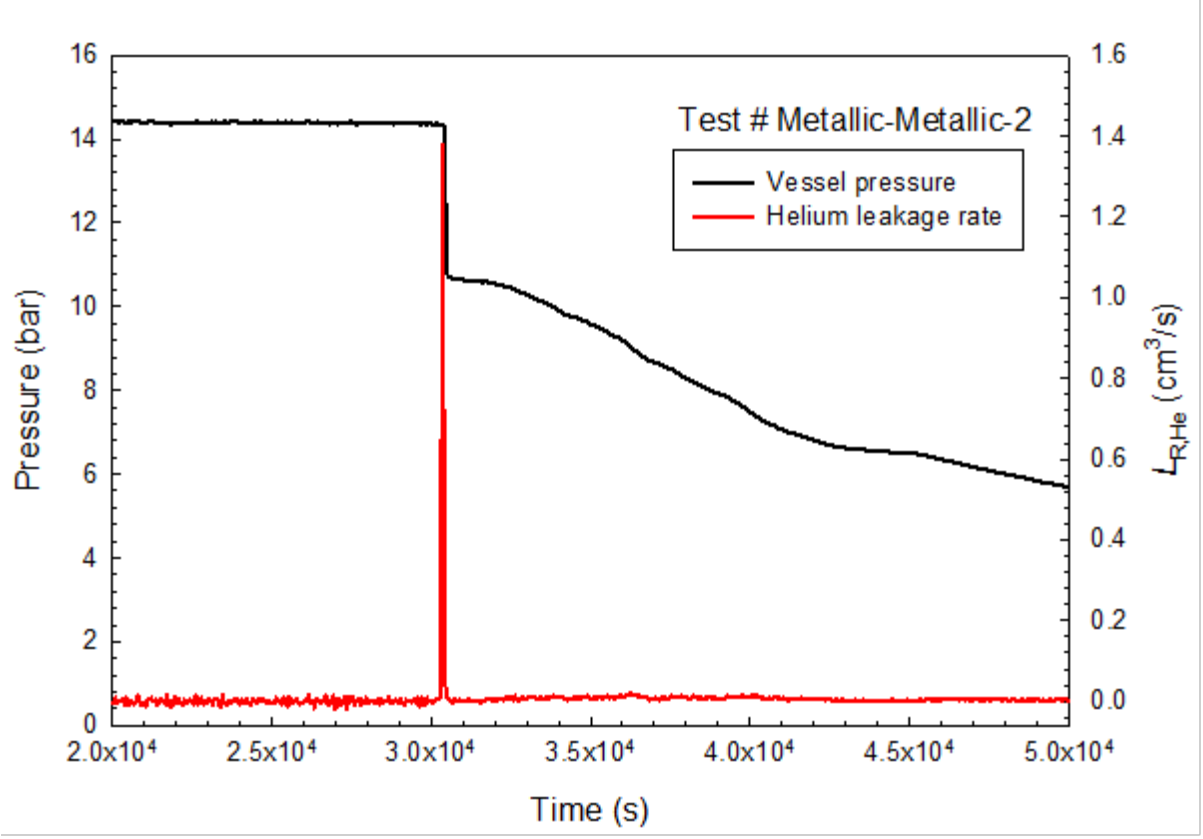

Figure 3-82. Isothermal reference helium leakage rate during the 9 h heating in Test # Metallic-Metallic-2 using the cap of Vessel #15 and the body of Vessel #13.

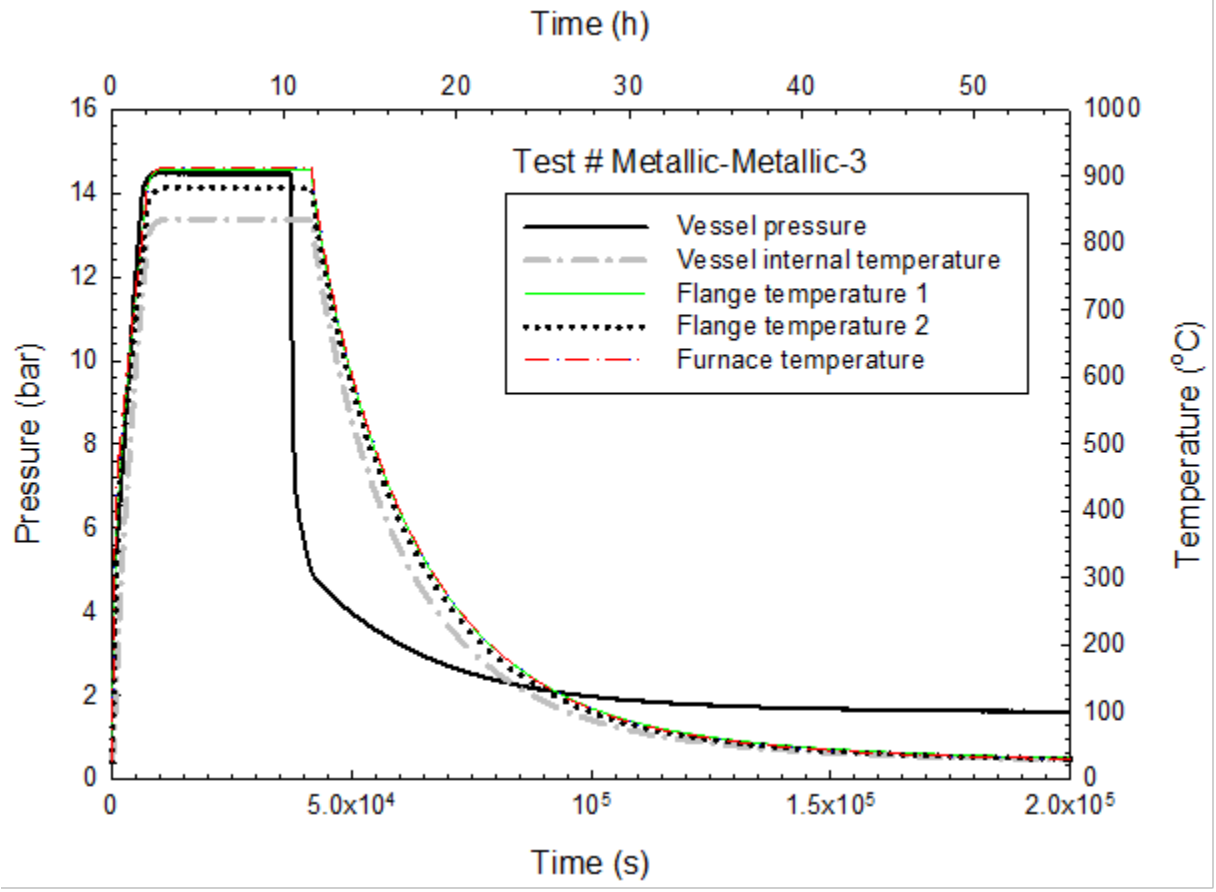

Figure 3-83. Temporal variations of vessel pressure and temperatures in Test # Metallic-Metallic-3 using Vessel #18.

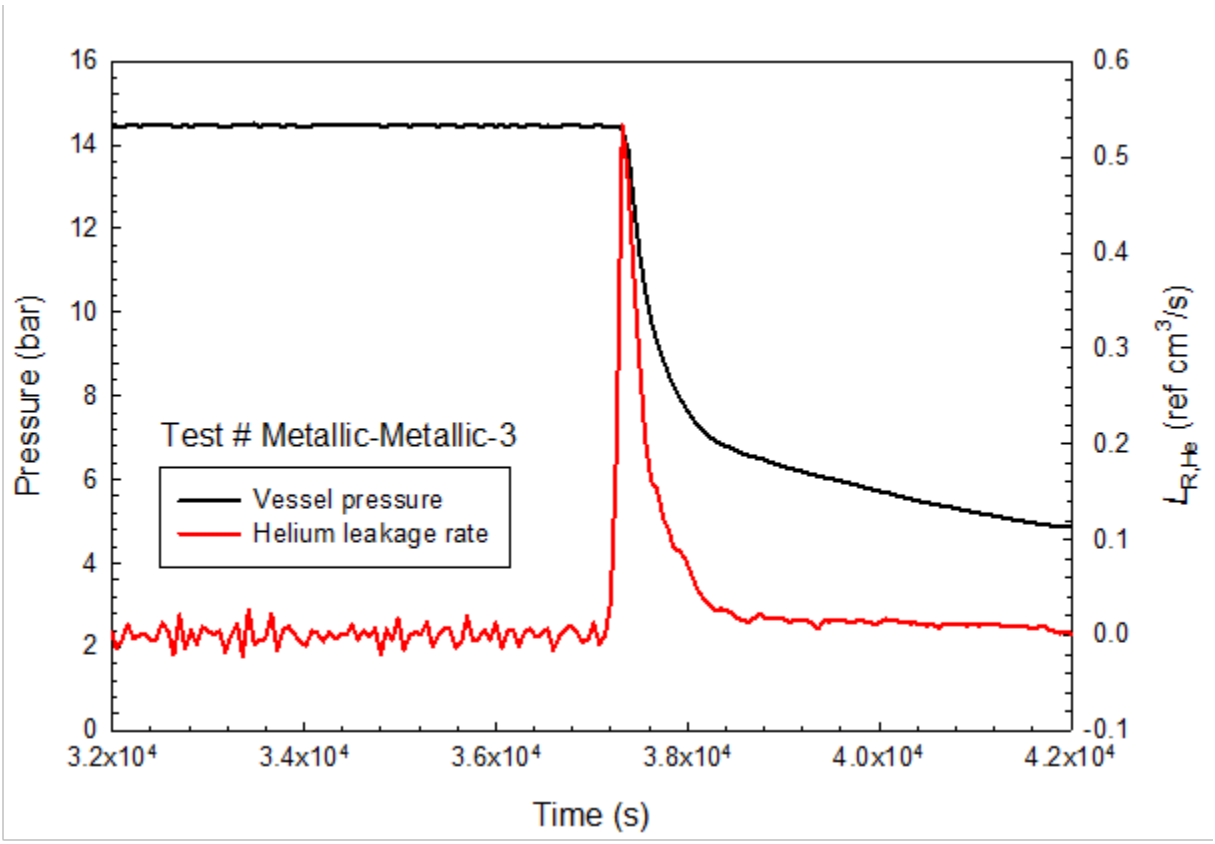

Figure 3-84. Isothermal reference helium leakage rate during the 9 h heating in Test # Metallic-Metallic-3 using the cap of Vessel #18.

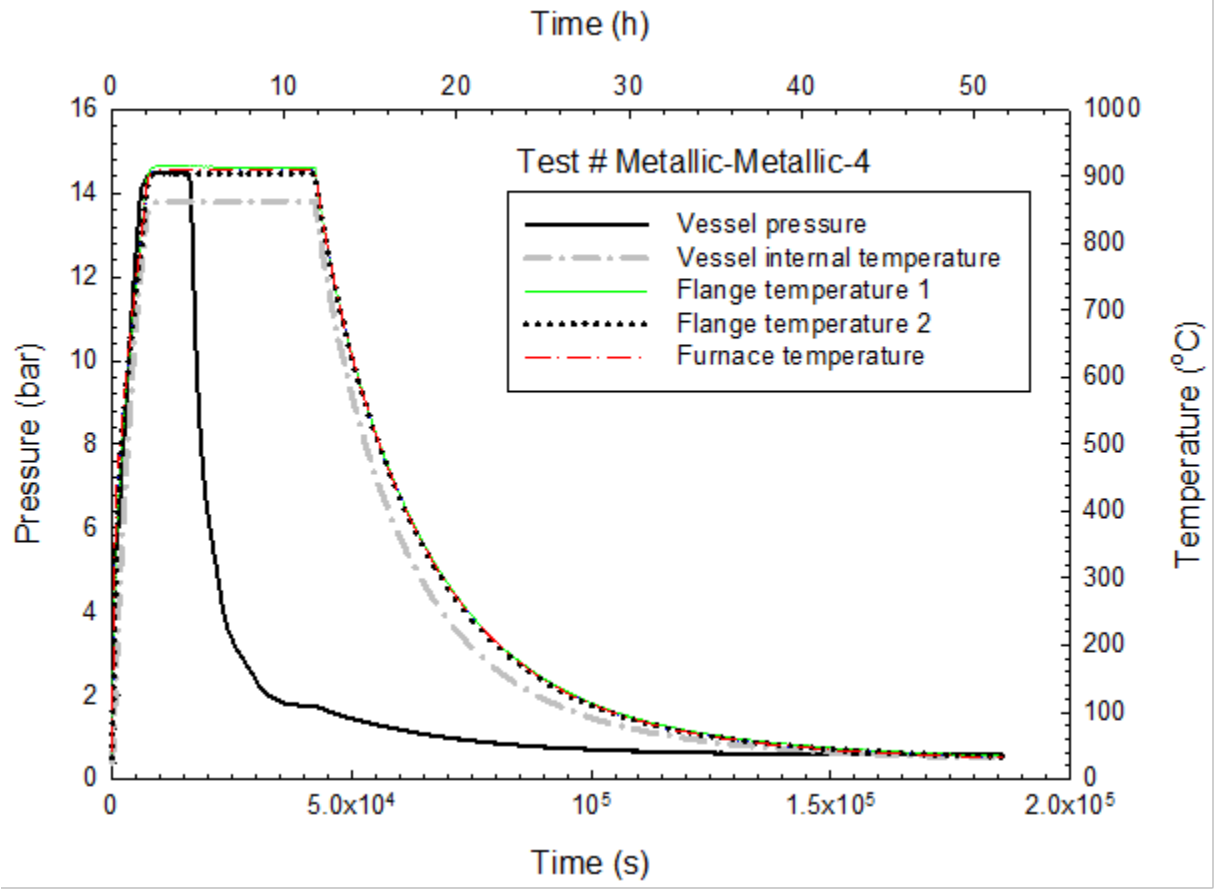

Figure 3-85. Temporal variations of vessel pressure and temperatures in Test # Metallic-Metallic-4 using Vessel #19.

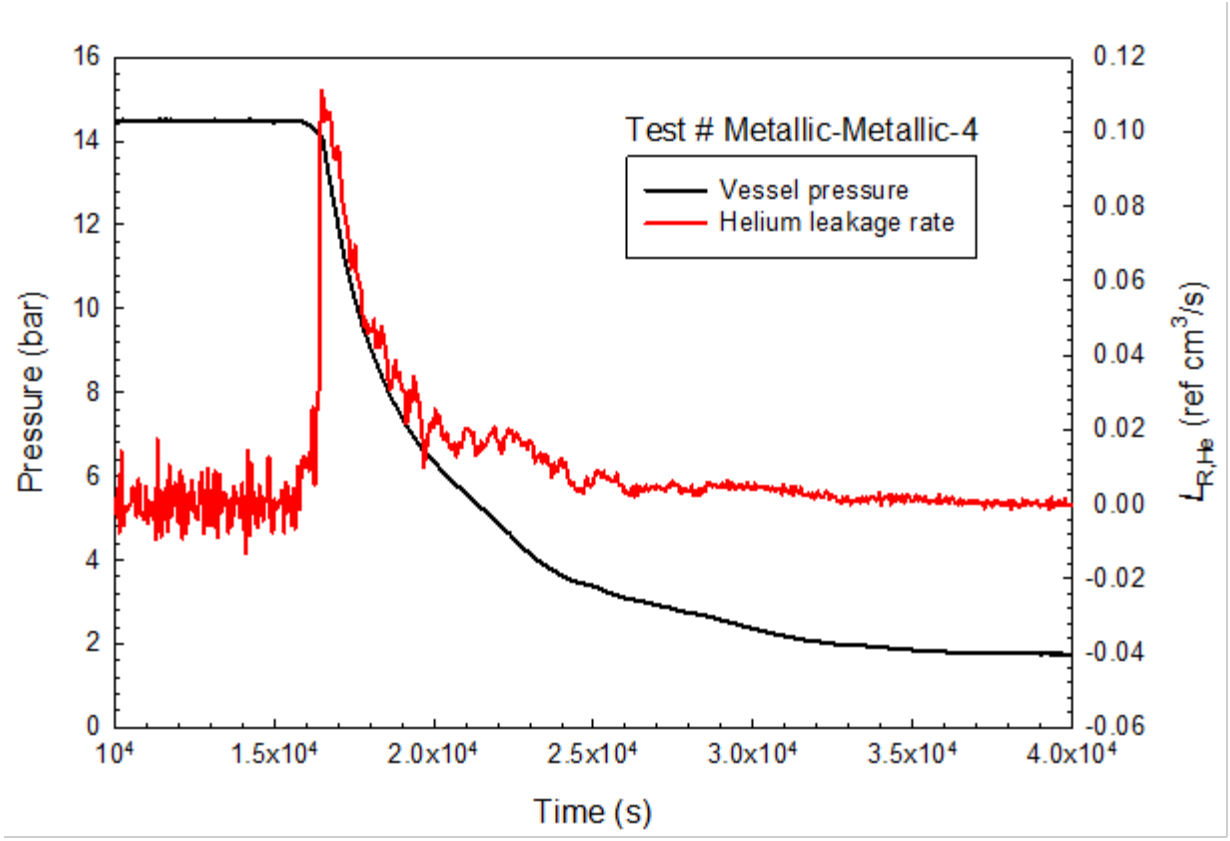

Figure 3-86. Isothermal reference helium leakage rate during the 9 h heating in Test # Metallic-Metallic-4 using Vessel #19.

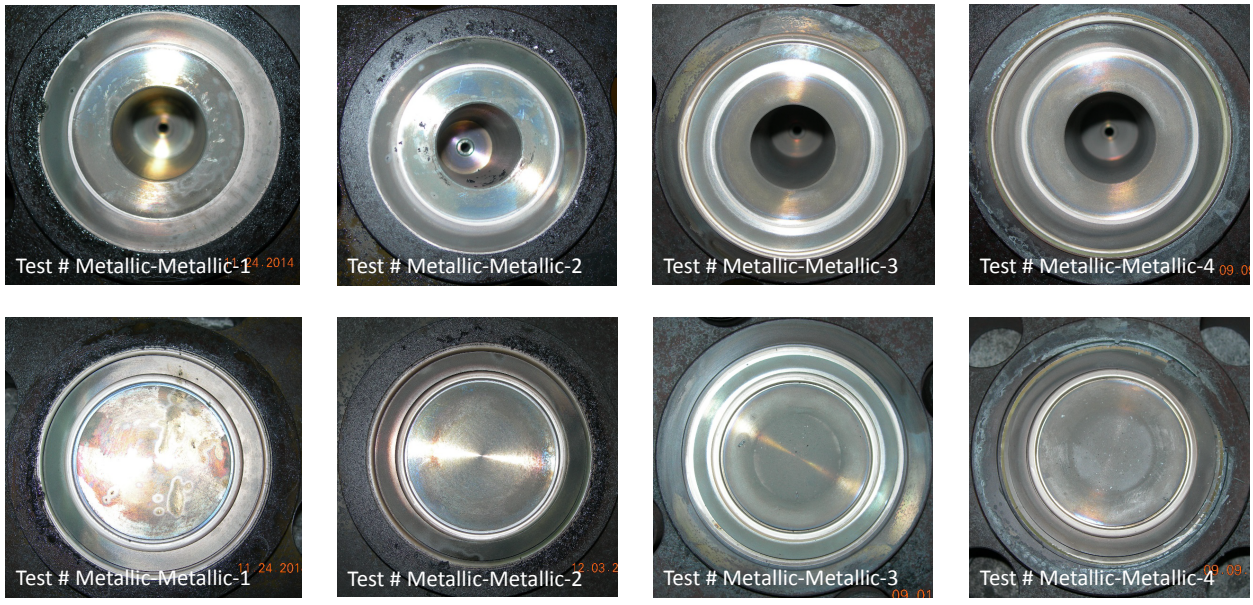

Figure 3-87. Photographs showing the thermally degraded Metallic-Metallic O-rings after 9-h thermal exposure at 900 °C (1652 °F) for the two Metallic-Metallic O-ring tests.

4 SUMMARY

This study provides experimental seal performance data for metallic and polymeric seals typically used in radioactive material transportation packages for beyond-design-basis temperature excursions. Tests were conducted using a small-scale test package. The study was divided into three phases. Phases I and II used a single O-ring configuration, whereas Phase III used a double O-ring configuration.

In Phase I, fifteen tests including two shakedowns were performed including some at beyond-design-basis thermal exposure conditions. Of the tests conducted, 12 tests used metallic seals, two used EPDM seals, and one used a PTFE seal.

Of the five repeat metallic-seal tests (Tests # Metallic-2, # Metallic-3, # Metallic-4, # Metallic-8, and # Metallic-12), leakage (decreasing vessel pressure) was observed in three of the tests (Tests # Metallic-3, # Metallic-4, and # Metallic-8) during the 9 h 800 °C (1472 °F) exposure. The times when the leakage occurred (the vessel pressure started to decrease) varied in the three tests performed. In Test # Metallic-3, measurable leakage occurred approximately 6.9 h after the test temperature 800 °C (1472 °F) had been reached. In Test # Metallic-4, measurable leakage occurred about 2.8 h into the 800 °C (1472 °F) exposure. In Test # Metallic-8, leakage was observed roughly 3 h into the test. The two shakedown tests (Tests # Metallic-1 and # Metallic-9) were conducted using a 30 min and 4 h exposure to 800 °C (1472 °F), respectively, and the seal appeared to hold vessel pressure. No leakage (unchanged vessel pressure within the pressure measurement uncertainty) was also observed in the two metallic seal tests that used 100 °C (212 °F) incremental heating from 427 °C (800 °F) to 627 °C (1161 °F) and from 427 °C (800 °F) to 727 °C (1341 °F), respectively, with at least 9 h exposure at each temperature increment. Three repeat metallic seal tests were also conducted at the seal maximum operating temperature of 427 °C (800 °F) for 9 h. The seal maintained vessel pressure within the measurement uncertainty of the pressure transducer in all three tests.

No leakage was observed in one EPDM seal tested at 300 °C (572 °F) for more than 20 h (Test # EPDM-a); however, leakage was observed immediately after the vessel had attained the nominal target temperature of 450 °C (842 °F) in another EPDM seal test (Test # EPDM-b). Leakage was also observed in the test (Test # PTFE-a) that used a PTFE seal after it had been subjected to 300 °C (572 °F) exposure for 22 h during the cooling phase.

In Phase II, additional experimental seal performance data for the two polymeric (EPDM and PTFE) O-ring seals were obtained. For exploratory purposes, three additional O-ring seals made of other polymeric materials (butyl, Viton, and silicone) were also studied. Thermal exposure tests were conducted at 316 °C (600 °F) for 8 h.

A total of eighteen tests were performed: four tests used EPDM O-rings, four used Viton, four used silicone, three used butyl, and three used PTFE. For the EPDM, butyl, PTFE, and silicone O-rings, the results, except one silicone O-ring test (Test # Silicone-1), showed that no leak was observed within measurement uncertainty. For all the Viton O-ring tests, the vessel pressure peculiarly increased during the thermal exposure, and the reason for this increase remains unresolved.

In Phase III, leak tests were performed using a double O-ring configuration. The outer-inner O-ring combinations were metallic-metallic, EPDM-metallic, blank-metallic, EPDM-EPDM, and butyl-butyl. Thermal exposure tests were conducted at 800 °C (1472 °F) or 900 °C (1652 °F) for 9 h. A total of eleven tests were carried out using a double O-ring configuration: four tests used

metallic-metallic, three used EPDM-metallic, one used blank (no O-ring)-metallic, two used EPDM-EPDM, and one used butyl-butyl. No leaks were observed with the EPDM-metallic double O-ring configuration. For the four metallic-metallic O-ring tests, leak was observed in the two tests when the same torque for single metallic O-ring was used. Even when the appropriate torque value was applied for the double O-ring configuration, the other two metallic-metallic tests leaked, but only after being at a 900°C environment between 2 h and 8 h; there was no leakage prior to that period. No leak was observed in the blank-metallic test. Leaks were detected in all the EPDM-EPDM and butyl-butyl tests even before the test temperature was reached. Table 4-1 provides a detailed summary of all the tests where constant vessel pressure was not observed during thermal exposure, and Table 4-2 provides a concise summary of all the tests.

Table 4-1. Summary of tests where constant vessel pressure was not observed during thermal exposure

Test Phase	Test # and seal material	Comments	Exposure conditions	Nominal initial vessel condition	Seal configuration
I	Metallic-3	Measurable leakage occurred at approximately 6.9 h after the test temperature of 800 °C (1472 °F) had been reached.	Heat-up + 9 h at 800 °C (1475 °F) + cool-down	24 °C at 5 bar	Single
	Metallic-4	Measurable leakage occurred about 2.8 h into the 800 °C (1472 °F) exposure.			
	Metallic-8	Leakage was observed roughly 3 h after reaching the target temperature.			
	PTFE-a	Leakage was observed in the test after it had been subjected to 300 °C (572 °F) exposure for 22 h during the cooling phase.	8 h of incremental heating from 150 ºC to 300 ºC (572°F) + more than 20 h at 300 ºC (572 °F) + cool-down	24 °C at 2 bar	
	EPDM-b	Leakage was observed immediately after the vessel had attained the nominal target temperature of 450 °C (842 °F).	Heat-up + more than 24 h at 450 ºC (842 °F)		
II	Silicone-1	Leakage was observed after about 2 h at the target temperature.	Heat-up + 8 h at 316°C + cool-down		
	Viton-1	For all the Viton O-ring tests, the vessel pressure peculiarly increased during the thermal exposure, and the reason for the pressure increase remains unresolved.			
	Viton-2				
	Viton-3				
	Viton-4				
III	EPDM-EPDM-1	Leakage occurred before test temperature was reached.	Heat-up + 9 h at 900 °C + cool-down	24 °C at 5 bar	Double
	EPDM-EPDM-2				
	Butyl-Butyl-1				
	Metallic-Metallic-1	Leakage occurred when the torque for a single metallic O-ring was used.			
	Metallic-Metallic-2				
	Metallic-Metallic-3	Leakage occurred even when the appropriate torque was used.			
	Metallic-Metallic-4				

Table 4-2. Summary of all the test results

Phase	Test #	Nominal initial vessel conditions	Exposure conditions	Leakage
I	Metallic-1	24 °C at 5 bar	30 min at 800 °C	
	Metallic-2	24 °C at 5 bar	9 h at 800 °C	
	Metallic-3	24 °C at 5 bar	9 h at 800 °C	Yes
	Metallic-4	24 °C at 5 bar	9 h at 800 °C	Yes
	Metallic-5	24 °C at 5 bar	9 h at 427 °C	
	Metallic-6	24 °C at 5 bar	9 h at 427 °C	
	Metallic-7	24 °C at 5 bar	9 h at 427 °C	
	Metallic-8	24 °C at 5 bar	9 h at 800 °C	Yes
	Metallic-9	24 °C at 5 bar	427 °C and then to 800 °C for about 4 h	
	Metallic-10	24 °C at 5 bar	427 °C to 627 ºC with 100 ºC increment	
	Metallic-11	24 °C at 5 bar	427 °C to 727 ºC with 100 °C increment	
	Metallic-12	24 °C at 5 bar	9 h at 800 °C	
	EPDM-a	24 °C at 2 bar	150 ºC to 300 °C with 50 ºC increment	
	EPDM-b	24 °C at 2 bar	> 24 h at 450 ºC	Yes
	PTFE-a	24 °C at 2 bar	150 ºC to 300 °C with 50 ºC increment	Yes
II	EDPM-1	24 °C at 2 bar	8 h at 316 °C	
	EPDM-2	24 °C at 2 bar	8 h at 316 °C	
	EPDM-3	24 °C at 2 bar	8 h at 316 °C	
	EPDM-4	24 °C at 2 bar	8 h at 316 °C	
	EPDM-5	24 °C at 5 bar	9 h at 900 °C	
	EPDM-6	24 °C at 5 bar	9 h at 900 °C	
	Silicone-1	24 °C at 2 bar	8 h at 316 °C	Yes
	Silicone-2	24 °C at 2 bar	8 h at 316 °C	
	Silicone-3	24 °C at 2 bar	8 h at 316 °C	
	Silicone-4	24 °C at 2 bar	8 h at 316 °C	
	Butyl-1	24 °C at 2 bar	8 h at 316 °C	
	Butyl-2	24 °C at 2 bar	8 h at 316 °C	
	Butyl-3	24 °C at 2 bar	8 h at 316 °C	
	Viton-1	24 °C at 2 bar	8 h at 316 °C	
	Viton-2	24 °C at 2 bar	8 h at 316 °C	
	Viton-3	24 °C at 2 bar	8 h at 316 °C	
	Viton-4	24 °C at 2 bar	8 h at 316 °C	
	PTFE-1	24 °C at 2 bar	8 h at 316 °C	
	PTFE-2	24 °C at 2 bar	8 h at 316 °C	
	PTFE-3	24 °C at 2 bar	8 h at 316 °C	
III	EPDM-Metallic-1	24 °C at 5 bar	9 h at 800 °C	
	EPDM-Metallic-2	24 °C at 5 bar	9 h at 800 °C	
	EPDM-Metallic-3	24 °C at 5 bar	9 h at 900 °C	
	Metallic-Metallic-1	24 °C at 5 bar	9 h at 900 °C	Yes
	Metallic-Metallic-2	24 °C at 5 bar	9 h at 900 °C	Yes
	Metallic-Metallic-3	24 °C at 5 bar	9 h at 900 °C	Yes
	Metallic-Metallic-4	24 °C at 5 bar	9 h at 900 °C	Yes
	Blank-Metallic-1	24 °C at 5 bar	9 h at 900 °C	
	EPDM-EPDM-1	24 °C at 5 bar	9 h at 900 °C	Yes
	EPDM-EPDM-2	24 °C at 5 bar	9 h at 900 °C	Yes
	Butyl-Butyl-1	24 °C at 5 bar	9 h at 900 °C	Yes

5 REFERENCES

Adkins, H.E., Jr., Koeppel, B.J., Cuta, J.M., Guzman, A.D., and Bajwa, C.S, "Spent Fuel Transportation Package Response to the Caldecott Tunnel Fire Scenario," US NRC NUREG/CR-6894, Rev. 1, PNNL-15346, 2007.

Adkins, H.E., Jr., Cuta, J.M., Koeppel, B.J., Guzman, A.D., and Bajwa, C.S., "Spent Fuel Transportation Package Response to the Baltimore Tunnel Fire Scenario," US NRC NUREG/CR-6886, Rev. 2, PNNL-15313, 2007.

American National Standard for Radioactive Materials – Leakage Tests on Packages for Shipment, ANSI N14.5-1997.

ASME B16.5-2009, Pipe Flanges and Flanged Fittings NPS ½ through NPS 24 Metric/Inch Standard.

ASME Boiler and Pressure Vessel Code Section VIII – Rules for Construction of Pressure Vessels Division 1 (BPVC-VIII-1-2007).

Bronowski, D.R., "Performance Testing of Elastomeric Seal Materials under Low- and High-Temperature Conditions: Final Report," Sandia Report SAND94-2207, Sandia National Laboratories, June 2000.

Dunn, D.S., Shewmaker, R.E., and Chowdhury, A.H., "Analysis of Structural Materials Exposed to a Severe Fire Environment," US NRC NUREG/CR-6987, 2009.

ISO Guide to the Expression of Uncertainty in Measurement, first edition, 1993, International Organization for Standardization, Geneva, Switzerland.

ISO 12807 (1996) Safe Transport of Radioactive Materials – Leakage Testing on Packages. ISO, International Organization for Standardization.

Marlier, R., "First tests results for determination of seal life of EPDM O-rings at high temperature (determined by unique method)," Packaging, Transport, Storage and Security of Radioactive Material 21 (1):37-40 (2010).

McGrattan, K.B. and Hamins, A. "Numerical Simulation of the Howard Street Tunnel Fire, Baltimore, Maryland, July 2001," U.S. NRC NUREG/CR-6793, 2003.

Title 10, Code of Federal Regulations (CFR), Part 71, Packaging and Transportation of Radioactive Material, January 1, 2010, U.S. Government Printing Office, Washington, DC.

APPENDIX A DESIGN DRAWINGS OF TEST VESSEL

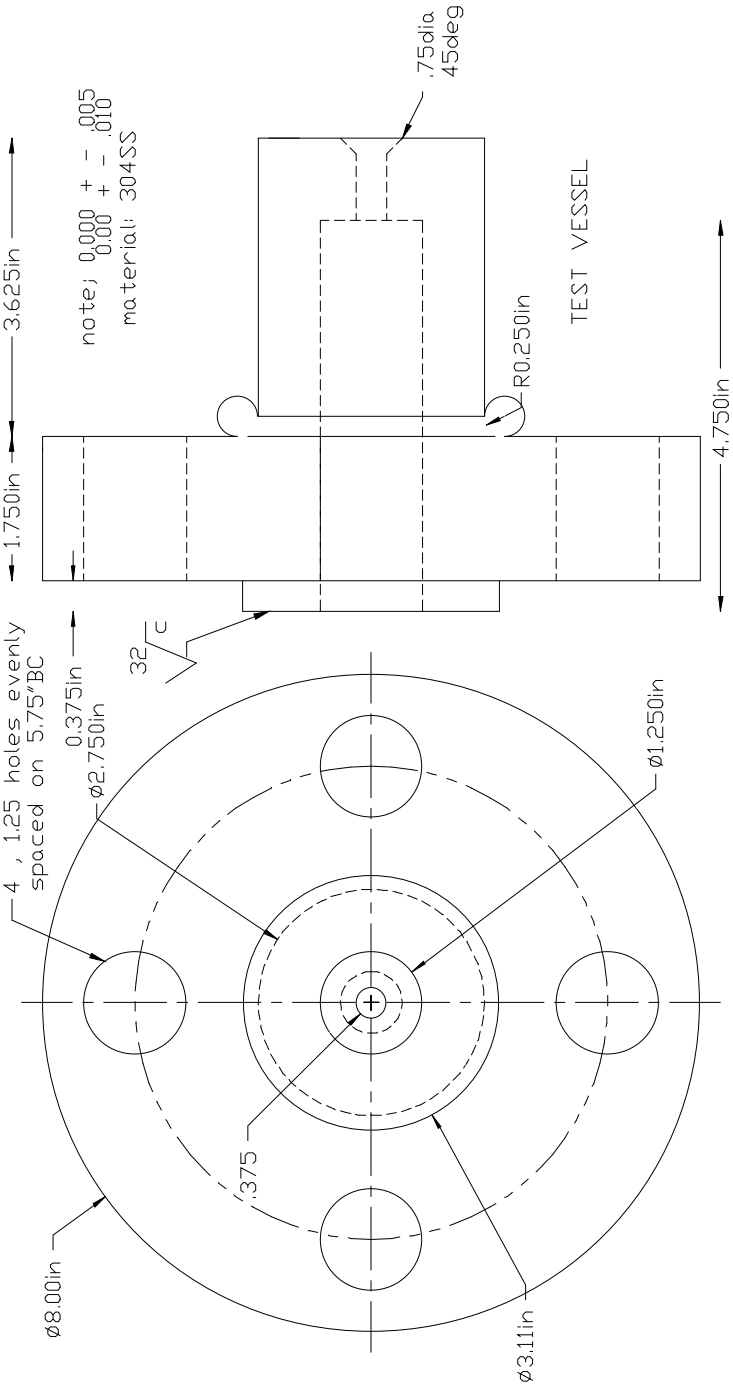

Figure A-1. Design drawing of single O-ring test vessel body.

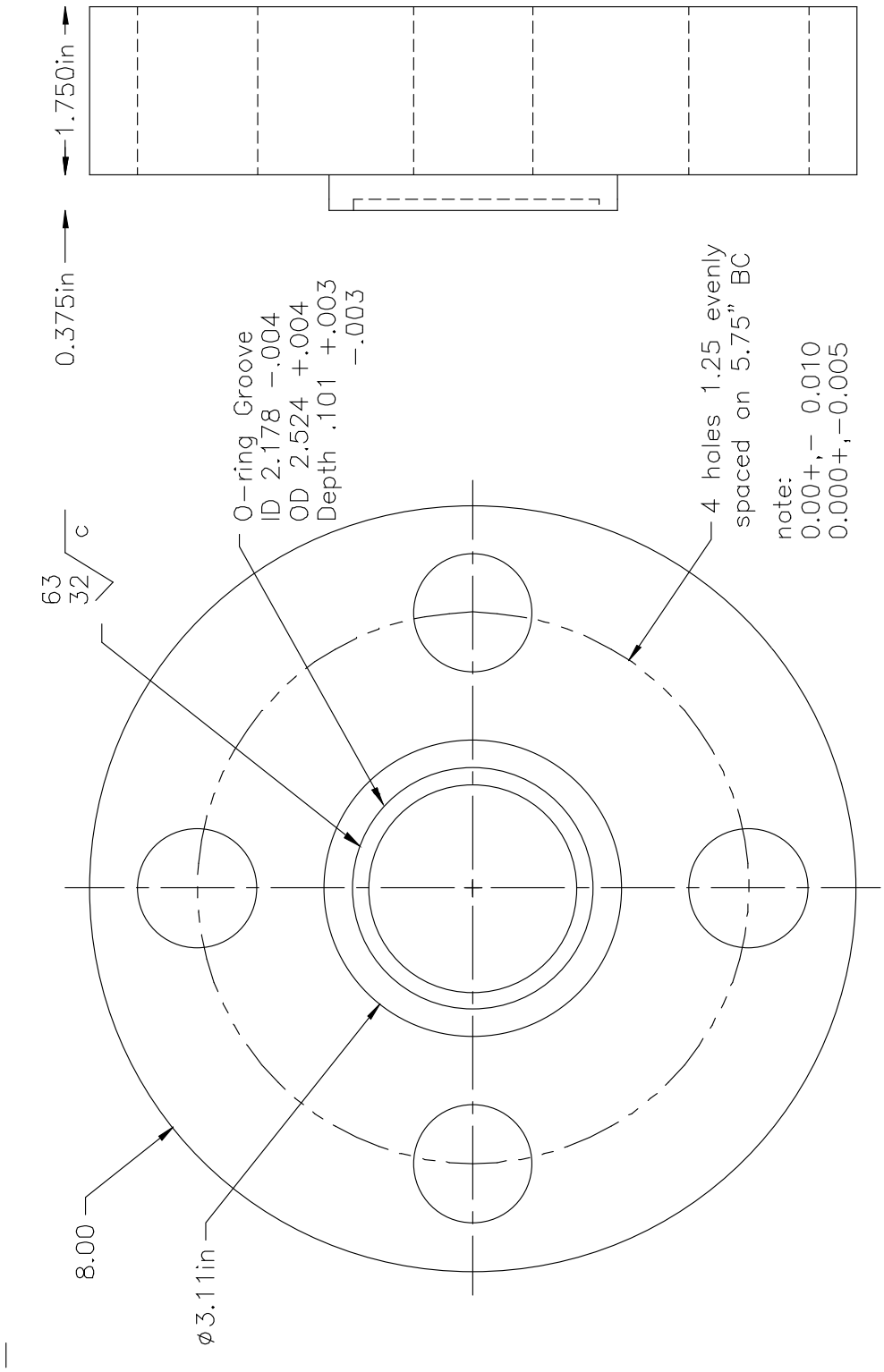

Figure A-2. Design drawing of removable flange for single metallic seal (vessel cap).

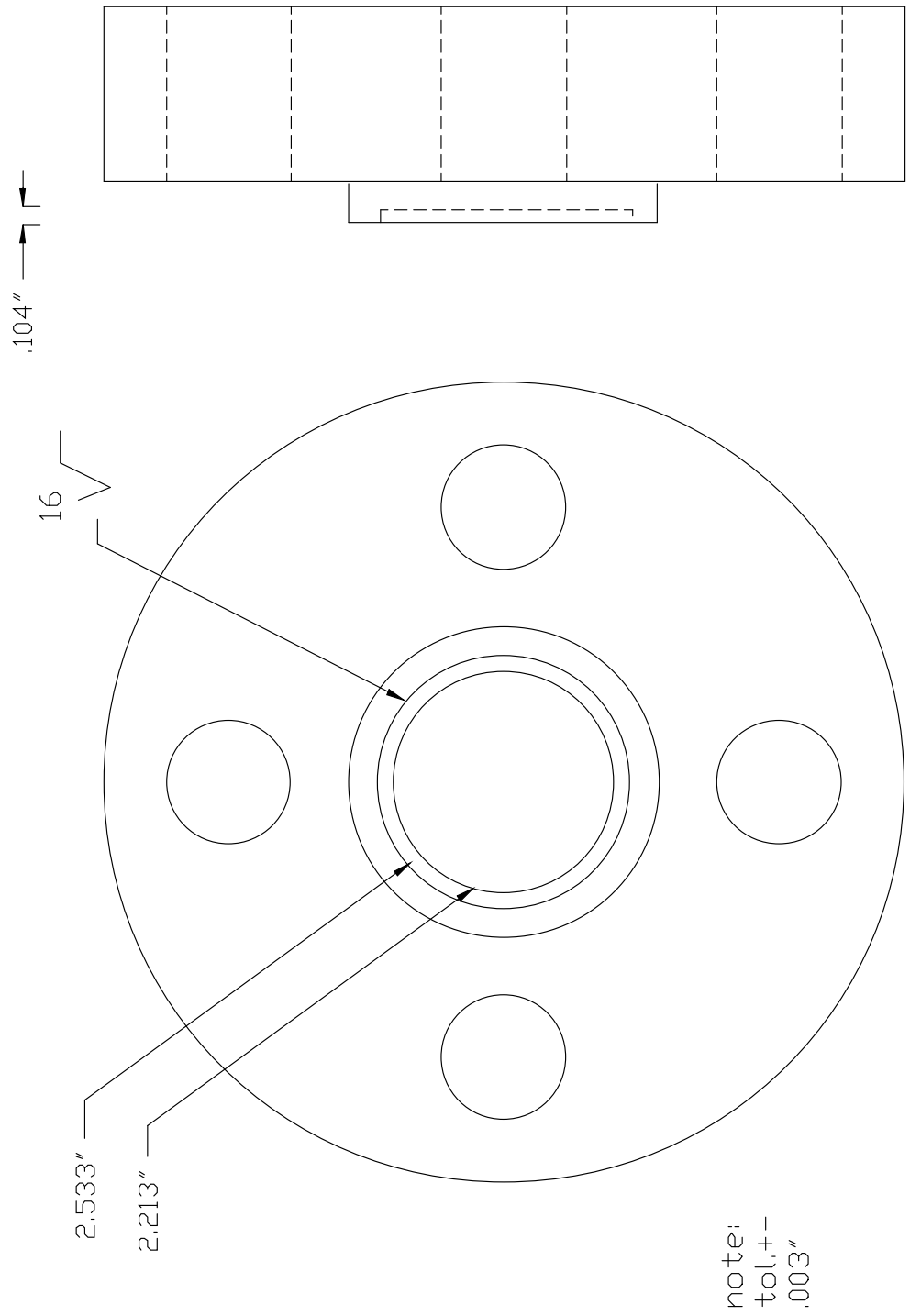

Figure A-3. Design drawing of removable flange for single polymeric seal (vessel cap).

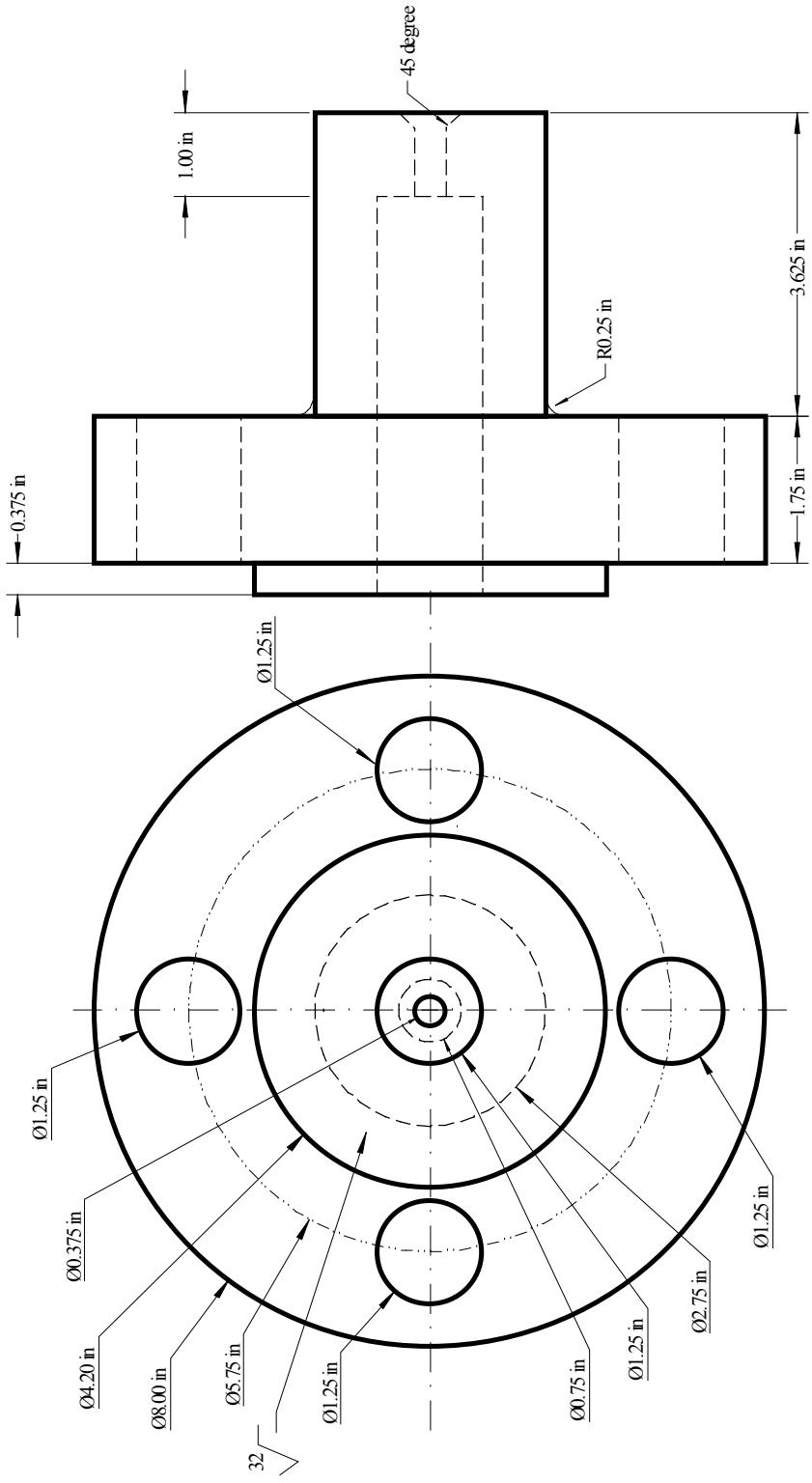

Figure A-4. Design drawing of double O-ring test vessel body.

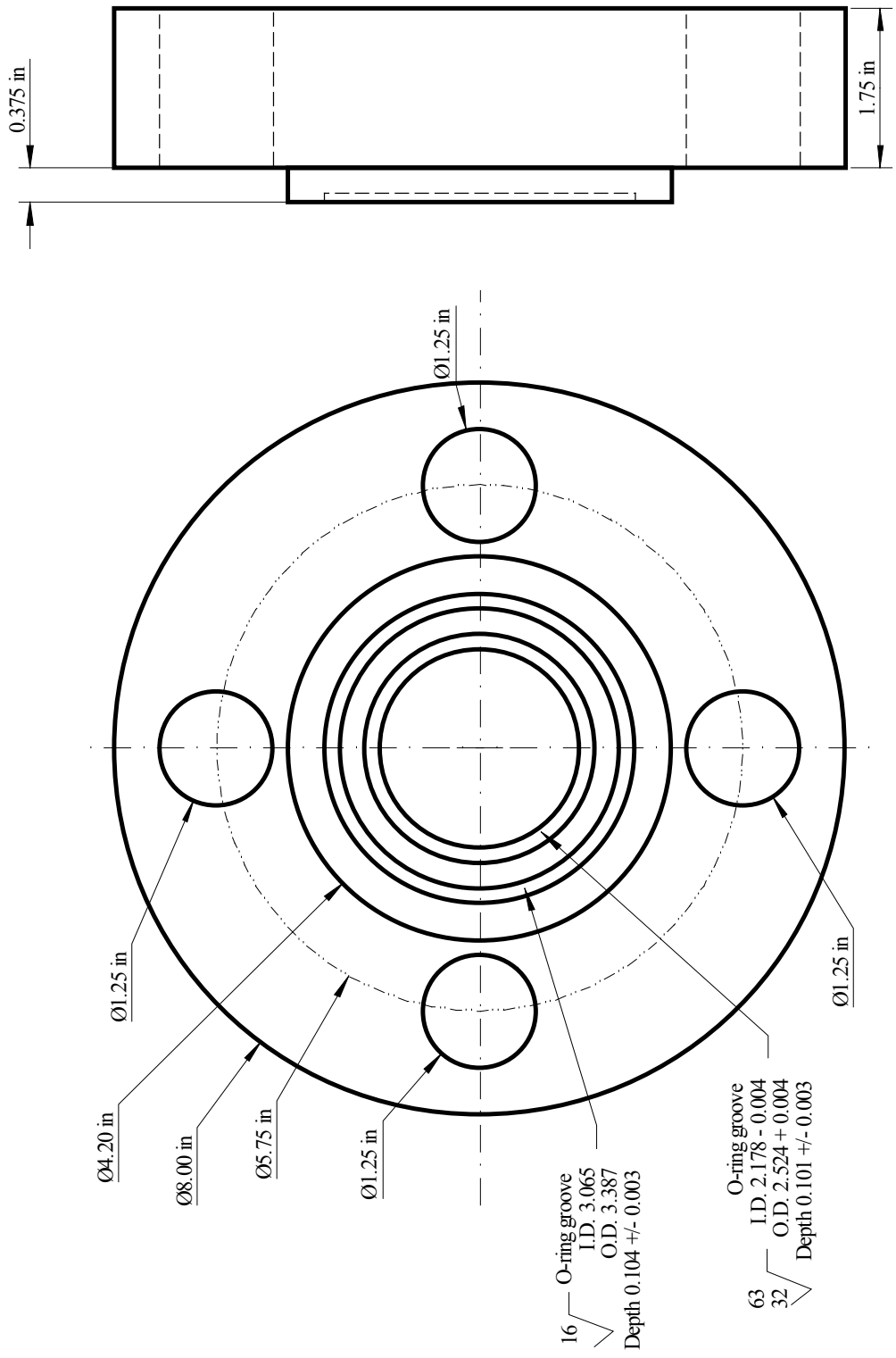

Figure A-5. Design drawing of removable flange for double O-ring (outer EPDM-inner metallic) seal (vessel cap).

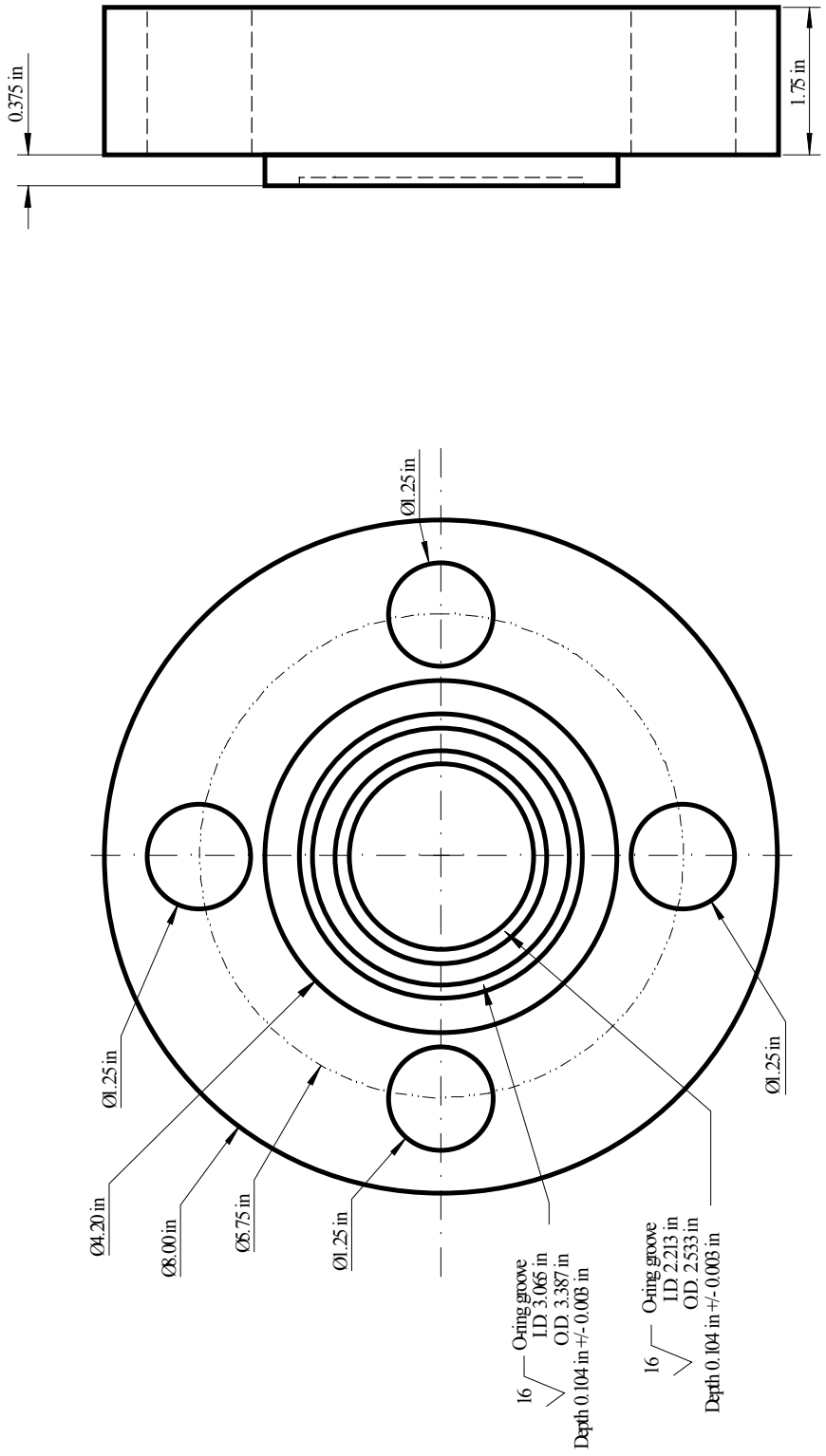

Figure A-6. Design drawing of removable flange for double O-ring (outer polymeric-inner polymeric) seal (vessel cap).

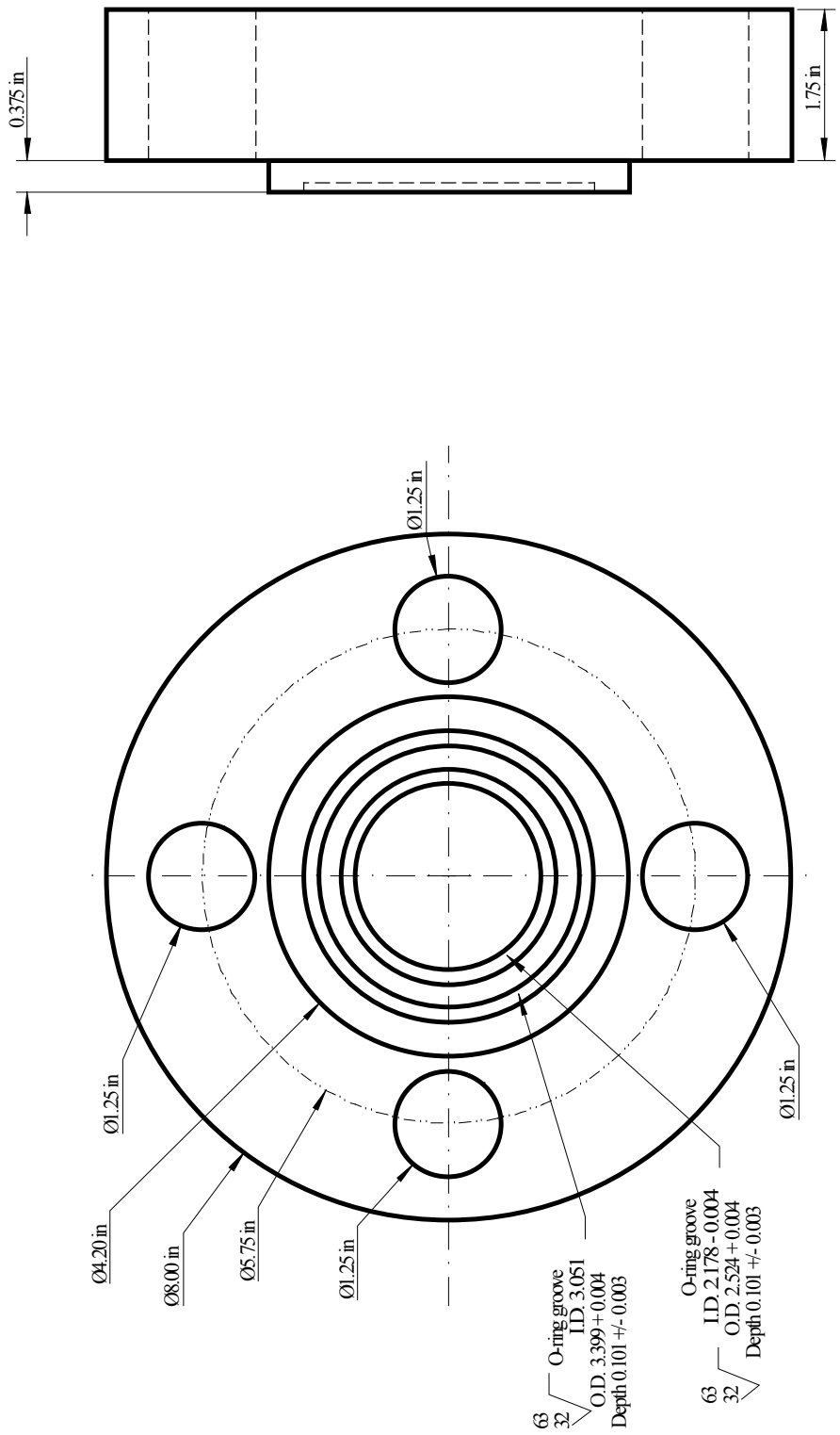

Figure A-7. Design drawing of removable flange for double O-ring (outer metallic-inner metallic) seal (vessel cap).

APPENDIX B VESSEL INTERNAL VOLUMES

Vessel internal volume (excluding the volume of the through hole for welding the tubing flush to the vessel interior) was measured at room temperature using an internal micrometer with a resolution of 0.005 mm (0.0002 in.). The inside diameter of the vessel was the averaged value from measurements made at several (at least five) depth locations of the vessel cavity using an electronic digital bore gauge with a resolution of 0.002 mm (0.0001 in.).

Table B-1. Measured internal volumes of pressure vessels at room temperature

Vessel #	Internal volume (m^3)
Vessel #1	9.56×10^{-5}
Vessel #2	9.52×10^{-5}
Vessel #3	9.56×10^{-5}
Vessel #3 (refurbished)	9.53×10^{-5}
Vessel #4	9.55×10^{-5}
Vessel #5	9.53×10^{-5}
Vessel #6*	9.46×10^{-5}
Vessel #7	9.57×10^{-5}
Vessel #8*	9.55×10^{-5}
Vessel #9	9.53×10^{-5}
Vessel #10	9.54×10^{-5}
Vessel #11	9.54×10^{-5}
Vessel #12	9.57×10^{-5}
Vessel #13	9.66×10^{-5}
Vessel #14	No vessel body; only cap
Vessel #15	No vessel body; only cap
Vessel #16	9.72×10^{-5}
Vessel #17	9.60×10^{-5}
Vessel #18	9.75×10^{-5}
Vessel #19	9.63×10^{-5}

*post-test measurements

APPENDIX C UNCERTAINTY ESTIMATE OF MEASUREMENTS

C.1 Uncertainty Estimate in Thermocouple Measurements

The uncertainty budget associated with the thermocouple measurements is summarized in Table C-1.

Table C-1. Summary of standard uncertainty components in thermocouple measurements

Standard uncertainty component	Source of uncertainty	Value of standard uncertainty	Source and comments
u_{TC}	Type-K thermocouple	0.64 °C	The thermocouples have a limit of error of 2.2 °C (from manufacturer specifications). An assumed rectangular probability distribution (ISO, 1993) results in 2.2 °C × 0.29 = 0.64 °C.
u_{ADC}	Analog to digital conversion	0.04 °C	The K-type thermocouples have an output range of ± 50 mV; 100 mV/2^{16} (16-bit) = 0.00153 mV, which corresponds to 0.04 °C using an approximate sensitivity of 40 μV/°C.
u_{CJ}	Cold-junction compensation	1 °C	Software cold-junction compensation using 25 °C as reference temperature.
Combined standard uncertainty (u_c)		$u_c = \sqrt{u_{TC}^2 + u_{ADC}^2 + u_{CJ}^2} = 1.2$ °C	
Expanded uncertainty U (with coverage factor k = 2)		$U = k\,u_C = 2.4$ °C	

C.2 Uncertainty Estimate in Pressure Transducer Measurements

The measurement uncertainty of the pressure transducer was estimated based on the specifications of the transducer provided by the manufacturer (see Table C-2). The uncertainty budget is listed in Table C-3.

Table C-2. Manufacturer's specifications of the pressure transducer

Excitation	24 VDC to 32 VDC
Input range	(0 to 500) psia ; (0 to 34.02) bar
Output range	(0 to 5) VDC ± 0.03 VDC
Linearity	0.05 % FSO (full scale output)
Hysteresis	0.05 % FSO
Repeatability	± 0.05 % FSO
Thermal zero drift	0.001 % FSO/°F
Operating temperature range	– 46 °C to 121 °C

Table C-3. Summary of standard uncertainty components in pressure measurements

Standard uncertainty component	Source of uncertainty	Value of standard uncertainty	Source and comments
u_P	Transducer output	0.0087 V	A rectangular probability distribution was assumed (ISO, 1993), resulting 0.29 × 0.03 V = 0.0087 V.
u_L	Linearity	0.0025 V	0.05 % × 5 V
u_H	Hysteresis	0.0025 V	0.05 % × 5 V
u_R	Repeatability	0.0025 V	0.05 % × 5 V
u_T	Thermal zero drift	9×10^{-4} V	18 °F × 0.001 % × 5 V/°F§
u_{ADC}	Analog to digital conversion	7.63×10^{-5} V	5 V/2^{16} (16-bit)

§ Since the pressure transducer was mounted outside the furnace, the temperature of the transducer was close to room temperature, and a 10 °C (18 °F) rise from room temperature was assumed to be the worst case.

The combined standard uncertainty (u_c)

$$u_c = \sqrt{u_P^2 + u_L^2 + u_H^2 + u_L^2 + u_T^2 + u_{ADC}^2}$$

Then u_c = 0.00976 V. Based on the calibration data of the pressure transducer provided by the manufacturer, P (bar) = –0.0147 + 6.8835 × output (V), the combined standard uncertainty, u_c = 0.00976 V, corresponds to u_c = 0.0525 bar. The expanded uncertainty U of the pressure transducer with a coverage factor k of 2 is $U = k \times u_c$ = 0.11 bar.

APPENDIX D VESSEL VOLUME EXPANSION AND LEAK RATE ESTIMATION

D.1 Vessel Volume Estimation due to Thermal Expansion

The total measurement system is idealized and treated as two systems, the pressure vessel (inside the electric furnace) and the rest (outside the furnace) which contains tubing, connections, the pressure transducer, and two valves. The pressure vessel is designated as System 1 using subscript 1, and the rest System 2 using subscript 2.

Figure D-1 shows the initial state of the two systems. They are at the same initial temperature T_o and pressure P_o. The initial amount of substance in System 1 is N_{1o}, and System 2, N_{2o}. The initial volume of the pressure vessel is V_{1o}, and the rest is V_{2o}. N is the total amount of substance in the two systems. Figure D-1 also shows the final state of the two systems. If there is no leak in the total system, then

$$N_1 + N_2 = N_{1o} + N_{2o} = N$$

Using the ideal gas law,

$$\frac{PV_1}{RT_1} + \frac{PV_2}{RT_2} = \frac{P_o(V_{1o} + V_{2o})}{RT_o}$$

It is assumed that during the thermal exposure the heat loss to the surrounding from System 2 is sufficient enough to keep System 2 at its initial temperature T_o. This assumption is reasonable since the tubing system remains cold to touch during the thermal exposure experiments. With $T_2 = T_o$ and $V_2 = V_{2o}$ (no volumetric thermal expansion in System 2), then the above equation can be written as

$$\frac{PV_1}{T_1} + \frac{PV_{2o}}{T_o} = \frac{P_o(V_{1o} + V_{2o})}{T_o}$$

Note that due to volumetric thermal expansion in System 1 during the thermal exposure, $V_1 \neq V_{1o}$. The final vessel volume V_1 can be expressed in terms of P as

$$V_1 = \frac{P_o T_1 (V_{1o} + V_{2o})}{P T_o} - \frac{T_1 V_{2o}}{T_o}$$

Since leakage was not observed in Tests # Metallic-2 (Test #2), # Metallic-5 (Test #5), # Metallic-6 (Test #6), # Metallic-7 (Test #7), and # Metallic-12 (Test #14), the test parameters and the experimental results from these five thorough tests were used in the calculations of V_1. The time-averaged values of T_1 (average of the four thermocouple readings) and P over the constant heating period were used. A V_{2o} value of 7 mL was estimated based on the internal dimensions of all the piping and fittings. Table D-1 tabulates the calculated V_1 and the percent volume expansion, $(V_1\text{-}V_{1o}) \times 100/V_{1o}$. The volume expansion is less than 6 % at the maximum temperature (800 °C) used in this test series. Compared to Test # Metallic-2 (Test #2), the

calculated percent volume expansion from Test # Metallic-12 (Test #14) is a bit low. This could be due to the assumptions used in analysis and the difficulty in delineating exactly Systems 1 and 2 from test to test since the test fixture was placed inside the furnace at a slightly different location in each test.

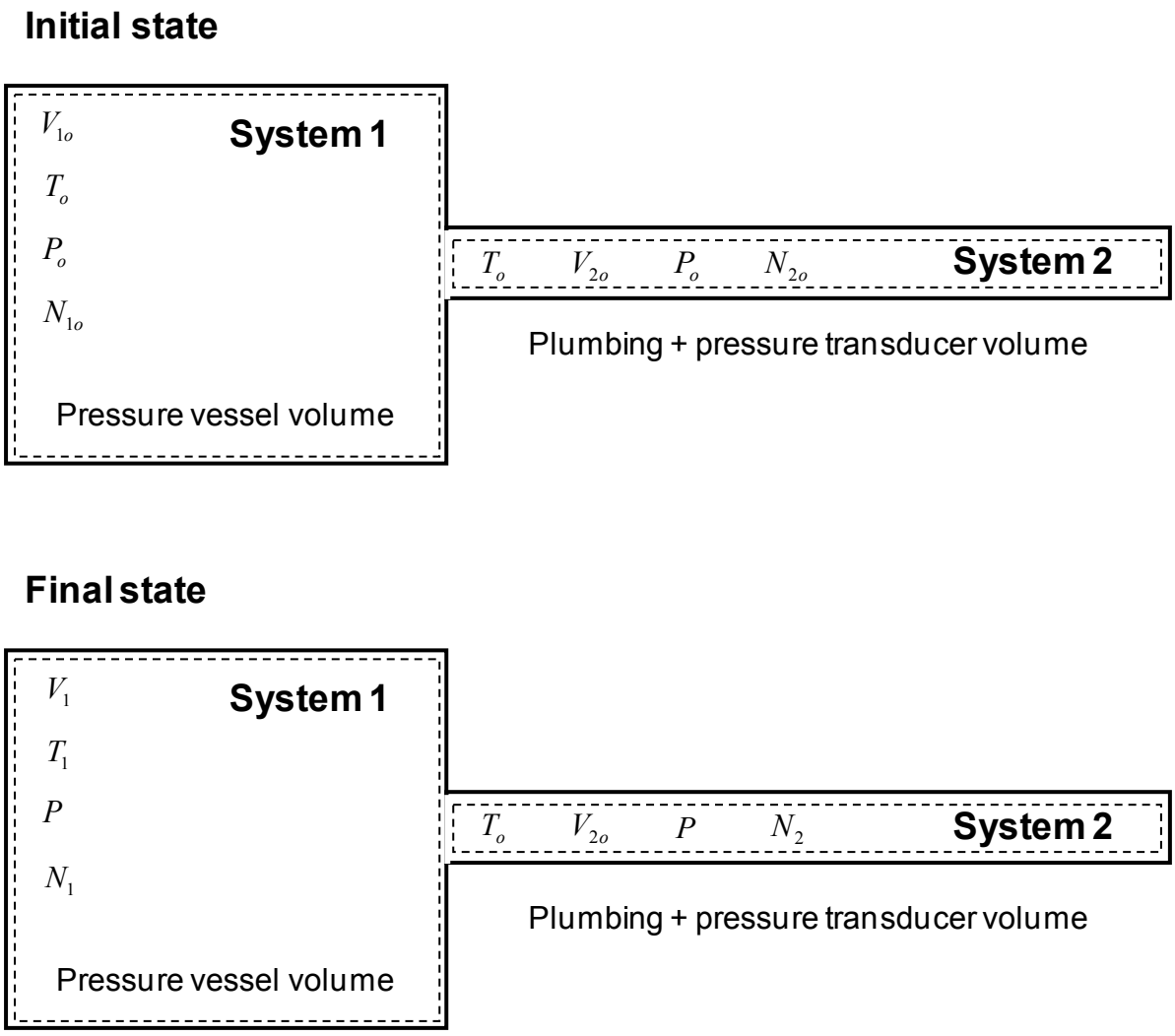

Figure D-1. Schematics showing the systems used in the thermodynamic analysis.

Table D-1. Calculations of vessel volume expansion at high temperatures

	T_0 (°C)	P_0 (bar)	V_{1o} (m^3)	T_1 (°C)	P (bar)	V_1 (m^3)	Volume expansion (%)
Test # Metallic-2	25	4.96	9.52×10^{-5}	802	14.55	1.01×10^{-4}	5.8
Test # Metallic-5	25	4.98	9.53×10^{-5}	425	10.34	9.91×10^{-5}	4.0
Test # Metallic-6	25	4.94	9.52×10^{-5}	425	10.20	9.97×10^{-5}	4.7
Test # Metallic-7	24	4.99	9.57×10^{-5}	426	10.39	9.97×10^{-5}	4.1
Test # Metallic-12	24	4.98	9.53×10^{-5}	801	14.79	9.92×10^{-5}	4.1

D.2 Isothermal Leakage Rate Estimation

If there is a leak after the final state is attained, then the leakage rate at the final-state temperature T_1 can be estimated by

$$-\frac{dN}{dt} = -\left(\frac{dN_1}{dt} + \frac{dN_2}{dt}\right) = -\frac{dP}{dt}\left(\frac{V_1}{RT_1} + \frac{V_{2o}}{RT_o}\right)$$

Since V_1/RT_1 is an order of magnitude larger than V_{2o}/RT_o, the above equation can be approximated by

$$-\frac{dN}{dt} \cong -\frac{dP}{dt}\left(\frac{V_1}{RT_1}\right)$$

Knowing the pressure-time history at the final-state temperature T_1 and the final-state volume V_1 due to thermal expansion, the leakage rate can be estimated using the above equation. In the formula described in ANSI N14.5-1997 and ISO 12807 for leakage rate estimation using pressure drop technique, no correction is made for the thermal expansion of vessel volume at high temperatures. For the conditions used in this test series, the thermal expansion of the vessel volume at the highest T_1 (800 °C) was estimated to be less than ≈ 6 % of the initial volume at room temperature, as described in Section D.1. In conforming to the ANSI and ISO practices and without the introduction of additional uncertainty associated with the estimation of V_1 at different values of T_1, V_1 is approximated in the above equation using V_{1o} with less than 6 % reduction in the leakage rate estimation.

$$-\frac{dN}{dt} \cong -\frac{dP}{dt}\left(\frac{V_{1o}}{RT_1}\right)$$

The time derivatives of vessel pressure (dP/dt) can be computed numerically from the pressure-time history curve using the scientific graphing package SigmaPlot® macro with a running average length of 1. Following ANSI N14.5-1997, the reference helium leakage rates $L_{R,He}$ (ref·cm^3/s) can be obtained by dividing $-dN/dt$ by 4.09 × 10^{-5} mol/cm^3, which is the amount of substance (ideal gas) contained in 1 × 10^{-6} m^3 (1 cm^3) at 1.01 × 10^5 Pa (1 atm) and 298 K (25 °C).

APPENDIX E O-RING MASS LOSS MEASUREMENTS

As an aside, mass loss measurements were also performed on the five polymeric O-rings used in Phase II to examine the extent of pyrolysis of the O-ring materials during thermal exposure. Table E-1 summarizes the test matrix.

To perform a mass loss measurement, an O-ring, used as-received, was placed in an acetone-cleaned square pan (10 cm × 10 cm × 3 cm) made of stainless steel (SS 304) sheet (with a thickness of 0.05 mm). The pan with the O-ring was weighed using a PioneerTM Ohaus PA214 electronic balance with a resolution of 0.0001 g and a maximum capacity of 210 g. The pan was then covered with a 0.05 mm stainless steel (SS 304) sheet, and placed in the preheated electric furnace, the same one used in Phase I, set at 316 °C (600 °F) for 8 h. This test temperature exceeds the maximum operating temperatures of all the O-ring materials. An exploratory test series was also performed using EPDM O-rings at a higher temperature of 450 °C (842 °F) for 8 h. After the thermal exposure, the covered pan with the O-ring was cooled to room temperature in the furnace overnight before being weighed without the cover. The mass loss was determined from the difference between the masses of the pan with the O-ring before and after the thermal exposure. A minimum of five repeated measurements for each polymeric material were performed. Digital photographs of the tested O-rings were also taken for examinations.

Table E-1. Test matrix for O-ring mass loss measurements

O-ring material	Number of tests	Test conditions
EPDM	7	316 °C (600 °F) for 8 h
Silicone	5	316 °C (600 °F) for 8 h
Butyl	5	316 °C (600 °F) for 8 h
Viton	5	316 °C (600 °F) for 8 h
PTFE	7	316 °C (600 °F) for 8 h
EPDM	4	450 °C (842 °F) for 8 h

Table E-2 summarizes the O-ring mass loss measurements at 316 °C (600 °F) for 8 h. The last column entries in the table were obtained by dividing the O-ring mass loss (column 6 in the table) by the original O-ring mass (column 4 in the table), expressed in percent. The entries with negative percent losses indicate the measured mass losses were negligible and that the differences in O-ring masses before and after thermal exposure could not be resolved within the uncertainty of the electronic balance used. Table E-3 summarizes the examinations of the O-rings after the thermal exposure. Figure E-1 shows sample photographs of the O-rings after thermal exposure. Note that only the fragmented EPDM and butyl O-rings are shown in the figure, and not every post-tested EPDM or butyl O-ring was found to be broken into pieces. O-rings made of materials other than EPDM and butyl remained intact after thermal exposure.

Table E-4 summarizes the EPDM O-ring mass loss measurements at 450 °C (842 °F) for 8 h.

After thermal exposure, the EPDM O-ring turned into powdery pieces (see Figure E-2). More than 60 % of the original O-ring mass was lost after thermal exposure at 450 °C (842 °F) for 8 h.

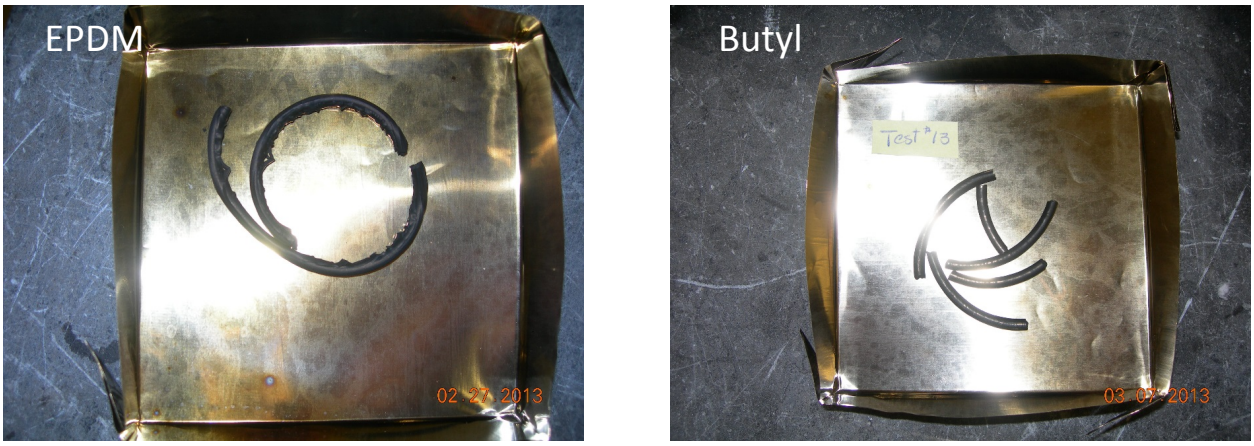

Figure E-1. Photographs showing EPDM and butyl O-rings after thermal exposure at 316 °C (600 °F) for 8 h.

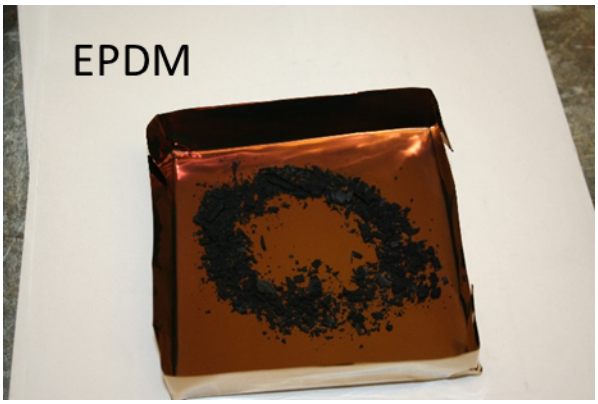

Figure E-2. Photograph showing an EPDM O-ring after thermal exposure at 450 °C (842 °F) for 8 h.

Table E-2. O-ring mass loss measurements at 316 °C (600 °F) for 8 h

O-ring material	Pan (g)	O-ring + Pan (g)	O-ring (g)	O-ring + Pan (after thermal exposure) (g)	O-ring mass loss (g)	% loss
EPDM	9.2259	11.3318	2.1059	11.2508	0.081	3.8
EPDM	9.4152	11.5303	2.1151	11.0647	0.4656	22.0
EPDM	9.5216	11.6260	2.1044	11.5542	0.0718	3.4
EPDM	9.2336	11.3193	2.0857	10.7297	0.5896	28.3
EPDM	9.5225	11.6188	2.0963	11.5499	0.0689	3.3
EPDM	9.4152	11.5213	2.1061	11.3265	0.1948	9.2
EPDM	9.4720	11.5744	2.1024	11.5164	0.058	2.8
Silicone	9.4559	11.8344	2.3785	11.7802	0.0542	2.3
Silicone	9.2265	11.6080	2.3815	11.5631	0.0449	1.9
Silicone	9.4213	11.8182	2.3969	11.7522	0.0660	2.8
Silicone	9.5315	11.9012	2.3697	11.8453	0.0559	2.4
Silicone	9.4739	11.8730	2.3991	11.8175	0.0555	2.3
Butyl	9.2263	11.5613	2.3350	10.9928	0.5685	24.3
Butyl	9.5208	11.8608	2.3400	11.6351	0.2257	9.6
Butyl	9.4155	11.7732	2.3577	11.6068	0.1664	7.1
Butyl	9.4727	11.7954	2.3227	11.5301	0.2653	11.4
Butyl	9.5218	11.8744	2.3526	11.6390	0.2354	10.0
Viton	9.4674	12.9175	3.4501	12.894	0.0235	0.7
Viton	9.4716	12.8799	3.4083	12.828	0.0519	1.5
Viton	9.2329	12.6557	3.4228	12.5874	0.0683	2.0
Viton	9.5219	12.9306	3.4087	12.902	0.0286	0.8
Viton	9.4552	12.8948	3.4396	12.8666	0.0282	0.8
PTFE	9.4153	13.4239	4.0086	13.4223	0.0016	0.04
PTFE	9.5215	13.5299	4.0084	13.5289	0.0010	0.02
PTFE	9.4553	13.4582	4.0029	13.4590	-0.0008	-0.020
PTFE	9.2253	13.2429	4.0176	13.2430	-1.00E-04	-0.002
PTFE	9.4731	13.4598	3.9867	13.4580	0.0018	0.045
PTFE	9.4514	13.3707	3.9193	13.3683	0.0024	0.061
PTFE	9.5221	13.5216	3.9995	13.5200	0.0016	0.040

Table E-3. O-ring examinations after thermal exposure at 316 °C (600 °F) for 8 h

O-ring material	Observations
EPDM	After thermal exposure, the color of the O-ring did not change; however, it became quite rigid and lost its elasticity. If compressed, the O-ring would crumble. In *some* tests, the O-rings were broken apart (in the pan) into chunks after thermal exposure*. When this happened, abnormally high mass losses were measured.
Silicone	After thermal exposure, the color of the O-ring did not change; the O-ring remained very elastic and intact.
Butyl	After thermal exposure, the color of the O-ring did not change; however, it became quite rigid and lost its elasticity. If compressed, the O-ring would crumble. In *some* tests, the O-rings were broken apart (in the pan) into chunks after thermal exposure*. When this occurred, abnormally high mass losses were measured.
Viton	After thermal exposure, the color of the O-ring did not change; the O-ring remained very elastic and intact.
PTFE	After thermal exposure, the color of the O-ring did not change; the O-ring retained the same hardness and remained intact.

*Since the pan was covered when it was being heated inside the electrical furnace, it was unclear whether the fragmentation of the O-ring occurred.

Table E-4. O-ring mass loss measurements at 450 °C (842 °F) for 8 h

O-ring material	Pan (g)	O-ring + Pan (g)	O-ring (g)	O-ring + Pan (after thermal exposure) (g)	O-ring mass loss (g)	% loss
EPDM	8.9926	11.0971	2.1045	9.7920	1.3051	62.01
EPDM	8.9948	11.1007	2.1059	9.7887	1.3120	62.30
EPDM	8.9952	11.1018	2.1066	9.7887	1.3131	62.33
EPDM	8.9944	11.0838	2.0894	9.7880	1.2958	62.02

Within the resolution of the electronic balance, PTFE O-rings were found to have negligible mass losses. Silicone O-rings were found to have mass losses ranging from 1.9 % to 2.8 % with an arithmetic mean of 2.3 % and a standard deviation of 0.3 %. For Viton O-rings, the lowest and highest measured mass losses were 0.7 % and 2 % respectively, with an arithmetic mean of 1.2 % and a standard deviation of 0.6 %. The mass loss results from EPDM and butyl O-rings were scattered due to three outliers in the EPDM measurements and one in the butyl's. For EPDM O-rings, the lowest and highest measured mass losses were 2.8 % and 28.3 % respectively, with an arithmetic mean of 10.4 % and a standard deviation of 10.5 %. For butyl O-rings, the lowest and highest measured mass losses were 7.1 % and 24.3 % respectively, with an arithmetic mean of 12.5 % and a standard deviation of 6.8 %. The examination of the EPDM and butyl O-rings after thermal exposure revealed that some of the O-rings were broken into several segments in the covered pan during thermal exposure. When the test O-ring fragmented during thermal exposure, abnormally high mass losses (outliers) were recorded. Since all the O-rings used in the experiments came from the same batches (lots), the reason why few EPDM and butyl O-rings fragmented and the majority did not during the thermal exposure remains unclear.

APPENDIX F LEAK RATE MEASUREMENTS WITHOUT O-RING

As an aside in Phase II, several helium leak rate measurements were conducted at room temperature using Vessel #3 without an O-ring and different torques to tighten the bolts that hold the vessel flanges together. The torques[21] used were 414 N m (305 lb ft, recommended for the metallic O-rings), 203 N m (150 lb ft), and 136 N m (100 lb ft, the lowest setting for the torque wrench used). Figure F-1 shows the measurement results. The vessel pressure started to decrease and leakage occurred immediately. The instantaneous leakage rate, which is proportional to the instantaneous slope of the pressure-time curve, is inversely proportional to the torque used; the higher the torque, the slower the leak.

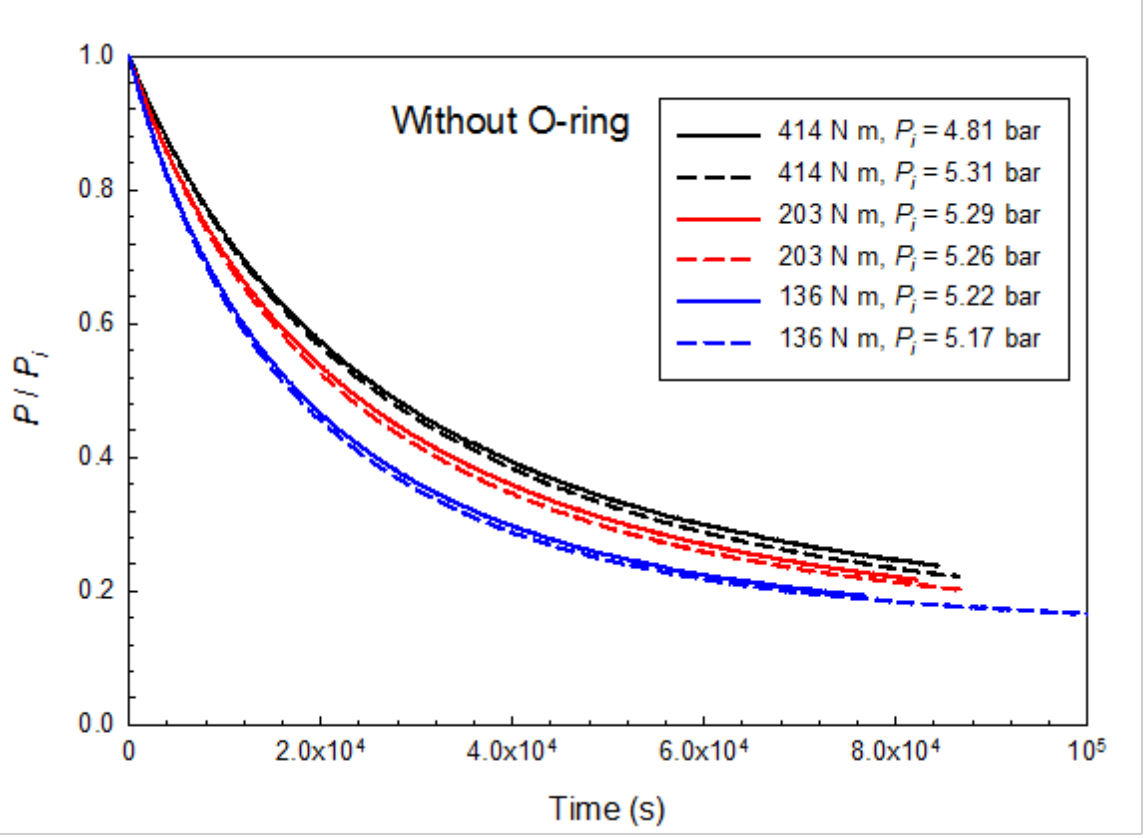

Figure F-1. Temporal variation of normalized vessel pressure at 24 °C without O-ring at different torques used to tighten the vessel flanges.

[21] The vessel could not be pressurized if the bolts were tightened by hand.

NRC FORM 335
(12-2010)
NRCMD 3.7

U.S. NUCLEAR REGULATORY COMMISSION

BIBLIOGRAPHIC DATA SHEET

(See instructions on the reverse)

1 REPORT NUMBER
(Assigned by NRC, Add Vol., Supp., Rev., and Addendum Numbers, if any.)
NUREG/CR-7115 Rev. 1

2 TITLE AND SUBTITLE
Performance of Metal and Polymeric O-Ring Seals in Beyond-Design-Basis Temperature Excursions – Revision 1

3 DATE REPORT PUBLISHED

MONTH	YEAR
November	2015

4 FIN OR GRANT NUMBER
N6550 and V6327

5 AUTHOR(S)
Jiann C. Yang, Edward J. Hnetkovsky, Doris Rinehart, and Marco Fernandez

6 TYPE OF REPORT
Technical Report

7. PERIOD COVERED (Inclusive Dates)
Aug/2009 to Aug/2015

8 PERFORMING ORGANIZATION - NAME AND ADDRESS (If NRC, provide Division, Office or Region, U. S. Nuclear Regulatory Commission, and mailing address, if contractor, provide name and mailing address.)
National Institute of Standards and Technology
Building and Fire Research Laboratory
Gaithersburg, Maryland 20899-8663

9 SPONSORING ORGANIZATION - NAME AND ADDRESS (If NRC, type "Same as above", if contractor, provide NRC Division, Office or Region, U S Nuclear Regulatory Commission, and mailing address.)
Division of Risk Analysis
Office of Nuclear Regulatory Research
U.S. Nuclear Regulatory Commission
Washington, DC 20555-0001

10 SUPPLEMENTARY NOTES
NRC Project Manager: Felix Gonzalez

11. ABSTRACT (200 words or less)
This report documents the beyond-design-basis thermal exposure test results of the performance of metallic and polymeric seals typically used in spent fuel transportation packages. The overall objective of the project is to provide test data and insights to the performance of these O-ring seals (metallic or polymeric) when exposed to beyond-design-basis temperature conditions that could result due to a severe fire. Tests were conducted using a small-scale test package (pressure vessel) made of stainless steel SS 304 filled with helium initially pressurized at either 5 bar or 2 bar at room temperature. The test package was then exposed in an electric furnace to temperatures equal to or over the specified maximum operating temperatures of these seals (up to 900 □C) for a pre-determined period (typically 8 h to 9 h). The pressure drop technique was used to determine if leakage occurred during thermal exposure. There are three test phases, Phases I, II, and III, in the study. The revision contains test results from Phases II and III. In Phase I, one metallic and two polymeric (ethylene-propylene compound (EPDM) and Teflon (PTFE) seals were used. A total of fifteen tests, twelve used metallic seals, two used EPDM, and one used Teflon, were performed. In Phase II, additional test data on EDPM, PTFE O-rings, Butyl, Viton, and silicone were obtained. In Phase III, the test series involved the use of a similar test package, but with a double O-ring configuration with an inner metallic O-ring and an outer polymeric (EPDM) or no outer O-ring.

12 KEY WORDS/DESCRIPTORS (List words or phrases that will assist researchers in locating the report.)
Beyond-design-basis testing
Seal performance
Thermal

13 AVAILABILITY STATEMENT
unlimited

14 SECURITY CLASSIFICATION
(This Page)
unclassified
(This Report)
unclassified

15 NUMBER OF PAGES

16 PRICE

Federal Recycling Program

UNITED STATES
NUCLEAR REGULATORY COMMISSION
WASHINGTON, DC 20555-0001

OFFICIAL BUSINESS